Endoplasmic reticulum exit of glycosylphosphatidylinositol-anchored proteins in the yeast 'Saccharomyces Cerevisiae'

Castillon, Guillaume Alain

UNIVERSITÉ DE GENÈVE FACULTÉ DES SCIENCES

Section de chimie et biochimie
Département de biochimie Professeur Howard Riezman

Endoplasmic Reticulum Exit of Glycosylphosphatidylinositol-Anchored Proteins in the Yeast *Saccharomyces Cerevisiae*

THÈSE

présentée à la Faculté des sciences de l'Université de Genève pour obtenir le grade de Docteur ès sciences, mention biochimique

par

Guillaume Alain CASTILLON

de

Saint-Michel d'Euzet (France)

Thèse N°4031

GENÈVE
Repromail
2008

UNIVERSITÉ DE GENÈVE FACULTÉ DES SCIENCES

Section de chimie et biochimie
Département de biochimie Professeur Howard Riezman

Endoplasmic Reticulum Exit of Glycosylphosphatidylinositol-Anchored Proteins in the Yeast *Saccharomyces Cerevisiae*

THÈSE

présentée à la Faculté des sciences de l'Université de Genève pour obtenir le grade de Docteur ès sciences, mention biochimique

par

Guillaume Alain CASTILLON

de

Saint-Michel d'Euzet (France)

Thèse N°4031

GENÈVE
Repromail
2008

UNIVERSITÉ
DE GENÈVE

FACULTÉ DES SCIENCES

Doctorat ès sciences
mention biochimie

Thèse de *Monsieur Guillaume Alain CASTILLON*

intitulée :

" Endoplasmic Reticulum Exit of Glycosylphosphatidylinositol-Anchored Protein in the Yeast *Saccharomyces Cerevisiae* "

La Faculté des sciences, sur le préavis de Messieurs H. RIEZMAN, professeur ordinaire et directeur de thèse (Département de biochimie), J. GRUENBERG, professeur ordinaire (Département de biochimie) et A. CONZELMANN, professeur (Université de Fribourg, Département de biochimie, Fribourg, Suisse) autorise l'impression de la présente thèse, sans exprimer d'opinion sur les propositions qui y sont énoncées.

Genève, le 31 octobre 2008

Thèse - 4031-

Le Doyen Jean-Marc TRISCONE

N.B.- La thèse doit porter la déclaration précédente et remplir les conditions énumérées dans les "Informations relatives aux thèses de doctorat à l'Université de Genève".

Nombre d'exemplaires à livrer par colis séparé à la Faculté : - 4 -

Remerciements (acknowledgements):

Cette thèse n'aurait pu aboutir sans la présence de mon précieux jury de thèse composé de Andreas Conzelmann, de Jean Gruenberg et de Howard Riezman. Merci encore d'avoir accepté de faire partie de mon jury de thèse.

Merci encore à Howard Riezman de m'avoir accueilli dans son laboratoire. Merci aussi aux actuels et anciens membres du laboratoire pour leur précieuse aide : Reika Watanabe, Béatrice Vallée, Joanna Kaminska, Kouichi Funato, Harald Pichler, Yukiko Shimada, Cleiton De Souza, Debdyuti Mukhopadhyay, Manuel Muniz, Auxi Aguilera-Romero, Pierre Morsomme, Natsuko Yahara, Morihisa Fujita, Yves Bourbonnais, Yong Mei, Xueli Guan, Tanya Ivanova, Gisèle Dewhurst, Isabelle Riezman, Brigitte Bernadet, Sophie Friant, Sharon Epstein, Marcy Taylor, Tatjana Schwabe, Kyohei Umebayashi, Ursula Loizides-Mangold, Thomas Hannich.

Merci aux membres du département et aux membres du secrétariat.

Je voudrais présenter mes remerciements aux personnes avec qui j'ai travaillé dans le passé, et qui ont fortement contribué à ma formation : John Cooper, Rick Heil-Chapdelaine, Rosine Haguenauer-Tsapis, Danièle Urban-Grimal, Naima Belgareh, Dorothy Schafer, Gareth Griffiths, Jacomine Krinjse-Locker, Martin Wear, Wei-Lih Lee, Alissa Weaver, Sophie Dupré, Jean Marc Galan, Michael Young, Kyoungtae Kim...

Merci à Reika et Anna, à mes parents Guy et Danielle, à ma sœur Carole, à mes grands-parents, à David et à tous mes amis.

The Plan

Le résumé

Les protéines à ancrage glycosyl phosphatidyl inositol (GPI) sont des protéines, qui après attachement au GPI dans le réticulum endoplasmique (RE), sont exportées à la surface de la cellule. Exposées au milieu extracellulaire, elles assurent diverses fonctions comme l'interaction cellule-cellule, l'adhésion cellulaire ou la transduction du signal dans les cellules eucaryotes supérieures. Dans la levure *Saccharomyces cerevisiae*, les protéines à ancrage GPI participent essentiellement à la synthèse de la paroi extracellulaire, qui protège la cellule contre de nombreux stress extérieurs.

Durant ce travail de thèse, nous nous sommes intéressés à la sortie du RE des protéines à ancrage GPI. La formation de vésicules destinées au transport de protéines du RE à l'appareil de Golgi est assurée par l'assemblage du manteau COPII. Après échange du GDP par du GTP, la Ras GTPase Sar1p recrute le complexe Sec23p/Sec24p et les protéines à charger. Ensuite s'associe le complexe Sec13p/Sec31p, ce qui finalise l'assemblage du manteau COPII, et ainsi, une vésicule dérivée du RE est formée. Il a été montré qu'il existe en fait deux populations de vésicules à manteau COPII : Une population transportant la protéine transmembranaire Gap1p et une population transportant la protéine à ancrage GPI Gas1p. Ce résultat suggère qu'il existe deux mécanismes d'incorporation des cargos et de bourgeonnement des vésicules à partir du RE.

Dans un premier temps, nous avons recherché à identifier les signaux essentiels à l'événement de triage des protéines lors de la sortie du RE. Ainsi nous avons pu observer que l'ancrage GPI est un pré-requis à l'export de Gas1p. Cependant la fusion de l'ancre GPI à la protéine soluble α-factor, ne permettait pas à α-factor de sortir du RE dans les vésicules dédiées aux protéines à ancrage GPI. Cependant dans le mutant *erv29Δ*, Erv29p étant le récepteur de sortie du RE de α-factor, α-factor était incorporé dans une nouvelle population de vésicules à la sortie du RE. Il était connu que α-factor interagissait avec Erv29p par ce que l'on appelle un signal de sortie de RE. L'ancre GPI est également un signal de sortie de RE, et potentiellement un signal de triage, cependant ce signal est récessif comparé au signal contenu dans α-factor.

Dans un deuxième temps nous avons travaillé sur les mécanismes de triage des protéines à la sortie du RE. Pour cela nous avons développé de nouveaux outils, qui nous ont permis de visualiser par microscopie à fluorescence l'événement de sortie du RE. Nous avons ainsi fusionné la protéine à ancrage GPI Cwp2p avec la protéine fluorescente Venus, et la protéine transmembranaire Hxt1p avec la protéine fluorescente CFP. En utilisant un mutant thermosensible *sec31-1* à 37°C, nous pouvons provoquer l'accumulation de ces molécules dans des sites spécialisés pour le bourgeonnement de vésicules à la surface du RE, appelés sites de sortie du RE (ERES : ER exit sites en anglais). En effet dans le mutant *sec31-1* les cargos sont concentrés dans les vésicules en formation, mais le manque de Sec31p empêche l'assemblage final du manteau COPII. Dans un tel contexte nous avons pu voir que Cwp2p et

Hxt1p sont concentrés dans des ERES différents. Des expériences supplémentaires suggèrent que la concentration de Hxt1p dans les ERES est dépendante des composants COPII, Sec12p et Sec16p et du récepteur de sortie du RE Erv14p. Plus surprenant la concentration de Cwp2p dans des domaines spécifiques à la surface du RE est indépendante du manteau COPII. Plus tard nous avons pu observer que la concentration des protéines à ancrage GPI nécessite l'enzyme Bst1p, qui dé-acétyle le groupe inositol de l'ancre GPI. Cette étape est un pré-requis au remodelage des lipides de l'ancre GPI. La protéine de la famille p24, Emp24p a été pressentie comme le récepteur de sortie de RE des protéines à ancrage GPI. En effet dans le mutant *emp24Δ* on peut observer un défaut de maturation de la protéine à ancrage GPI Gas1p, ce qui est très souvent le reflet d'un défaut de transport entre le RE et le Golgi. De plus, Emp24p est capable d'interagir physiquement avec Gas1p. Nous avons voulu tester si Emp24p était impliquée dans la concentration des protéines à ancrage GPI. Dans le mutant *sec31-1emp24Δ,* Cwp2p est toujours capable de s'accumuler à des sites précis de la surface du RE, suggérant qu'Emp24p ne participe pas à la concentration de Cwp2p mais à l'incorporation de protéines à ancrage GPI concentrées dans les vésicules à manteau COPII.

Après avoir vérifié qu'Emp24p et les enzymes impliquées dans le remodelage participent génétiquement à la même fonction, nous avons regardé la localisation d'Emp24p. De manière très surprenante, Emp24p ne colocalise que partiellement avec les protéines à ancrage GPI dans le mutant *sec31-1*. Ce résultat exclut donc qu'Emp24p soit le récepteur spécifique pour la sortie du RE des protéines à ancrage GPI, ou alors, le mode d'action d'Emp24p en tant que récepteur est très atypique. Néanmoins la localisation d'Emp24p est fortement affectée dans les mutants pour le remodelage lipidique de l'ancre GPI, suggérant qu'Emp24p fonctionne en aval du remodelage lipidique. Des études supplémentaires devront être fournies afin de comprendre la fonction moléculaire accomplie par Emp24p.

Une autre remarquable observation est que les protéines à ancrage GPI ne nécessitent pas la Ras GTPase Sar1p lors de la formation des vésicules à manteau COPII. Dans ce contexte il serait légitime d'imaginer que les deux populations de vésicules à manteau COPII diffèrent par la composition du manteau COPII lui-même et possiblement par le mode de recrutement des cargos. Cette différence est probablement suffisante pour générer le triage des cargos lors du bourgeonnement des vésicules à partir du RE.

En utilisant la réversibilité du phénotype de *sec31-1* après rétablissement de la température permissive, il est possible de synchroniser la sécrétion des cargos accumulés. Présentant différentes cinétiques de motilité les protéines à ancrage GPI et la protéine transmembranaire Hxt1p suivent des routes parallèles jusqu'à la surface de la cellule. Outre le fait que le triage des cargos à la sortie du RE peut être important pour la localisation différentielle de certains cargos, il est vraisemblable que la mise en place du mécanisme alternatif de formation de vésicules à manteau COPII pour les protéines à ancrage GPI soit un pré-requis au transport vésiculaire des céramides.

I-Introduction

I.A-GPI-anchored proteins

10 to 20% of secretory proteins are modified after their synthesis and translocation into the endoplasmic reticulum (ER) at their C-termini by glycosylphosphatidylinositol (GPI). Addition of GPI allows anchoring to the inner leaflet of the ER membrane and therefore after trafficking through the secretory pathway, the GPI-anchored proteins are exposed extracellularly. In mammalian cells, GPI-anchored proteins are important for cell adhesion, cell-cell interaction, signal transduction and host defence (Ikezawa, 2002; Kinoshita et al., 1995). In the yeast *Saccharomyces cerevisiae*, most of the 60 predicted GPI-anchored proteins are involved in cell wall biogenesis and assembly (Kapteyn et al., 1999).

Synthesis of the GPI in the ER is the result of the sequential action of at least 10 enzymes comprising more than 20 gene products (Orlean and Menon, 2007; Pittet and Conzelmann, 2007). Biosynthesis of GPI is essential for embryonic development in mammals (Nozaki et al., 1999), for growth in yeast (Leidich et al., 1994) and for certain life cycle stages of the African sleeping sickness parasite *Trypanosoma brucei*(Nagamune et al., 2000).

I.A.1-Structure of GPI-anchored proteins

The core backbone structure, EtNP-6Manα1-2Manα1-6Manα1-4GlcNα1-6*myo*Inositol-phospholipid (where EtNP is ethanolamine phosphate ; Man is mannose ; and GlcN is glucosamine), is common to various eukaryotic GPI-anchored proteins, such as yeast (*Saccharomyces cerevisiae*), protozoan parasites (*Trypanosoma brucei* and *Plasmodium falciparum*), and plant (*Pyrus communis*) (Ferguson et al., 1999; Ikezawa, 2002; Orlean and Menon, 2007; Oxley and Bacic, 1999; Pittet and Conzelmann, 2007). However some differences in mannose and ethanolamine phosphate branching can be observed between

GPI-anchored proteins and between organisms (Orlean and Menon, 2007; Taron et al., 2004). (Fig. 1).

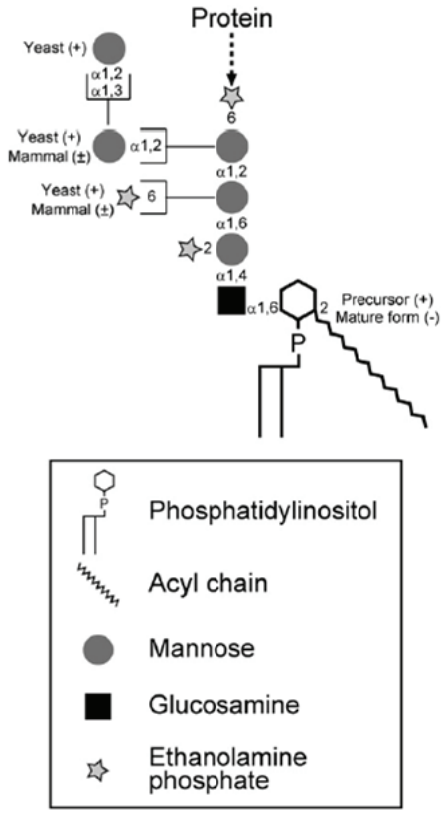

Fig.1. Structure of GPI core portion in yeast and mammal. From (Fujita and Jigami, 2008).

I.A.2-Biosynthesis of the GPI precursor

More than 20 gene products are directly required for the synthesis of the GPI precursor and its transfer to protein. Most of these proteins are polytopic membrane proteins found in the membrane of the ER (Benachour et al., 1999; Canivenc-Gansel et al., 1998; Grimme et al., 2001; Sutterlin et al., 1997b; Taron et al., 2004). An overview of the biosynthetic pathway is illustrated in Fig. 2, and the proteins associated with each step are listed in table 1. After synthesis of the GPI precursor, the GPI transamidase catalyses the endoproteolytic cleavage of the C-terminal GPI attachment signal of the future GPI-anchored protein and the attachment of the GPI-anchor to the newly generated C-terminus (Benghezal et al., 1996; Fraering et al., 2001; Hamburger et al., 1995; Hong et al., 2003; Ohishi et al., 2001).

Fig. 2. The main pathway of GPI biosynthesis in yeast. From (Pittet and Conzelmann, 2007)

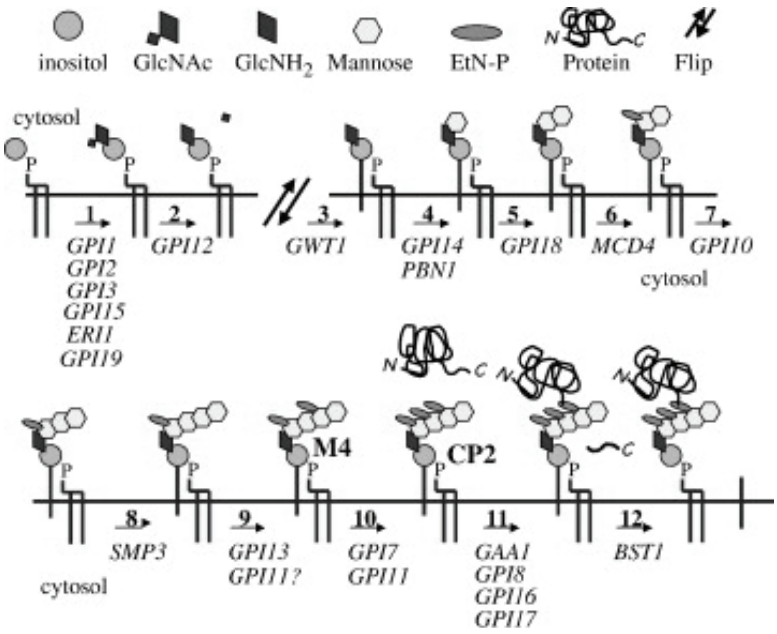

Table 1. Protein machinery for GPI anchoring in yeast and mammals. From (Orlean and Menon, 2007).

Reaction	Mammalian protein	Yeast protein
GlcNAc-PI synthesis	PIG-A	Gpi3p
	PIG-G	Gpi2p
	PIG-H	Gpi15p
	PIG-P	Gpi19p
	PIG-Q	Gpi1p
	PIG-Y	Eri1p
	DPM2	-
GlcNAc-PI de-*N*-acetylation	PIG-L	Gpi12p
GPI flipping	Not identified	Arv1p?
Inositol acylation	PIG-W	Gwt1p
α 1,4 mannosyltransfer	PIG-M	Gpi14p
	PIG-X	Pbn1p?
Etn-P transfer to Man-1	PIG-N	Mcd4p
α 1,6 mannosyltransfer	PIG-V	Gpi18p
α 1,2 mannosyltransfer	PIG-B	Gpi10p
Etn-P transfer to Man-3	PIG-O	Gpi13p
	PIG-F	Gpi11p?
α 1,2 mannosyltransfer	hSmp3	Smp3p
Etn-P transfer to Man-2	hGpi7	Gpi7p
	PIG-F	Gpi11p?
GPI transamidase	PIG-K	Gpi8p
	GAA1	Gaa1p
	PIG-S	Gpi17p
	PIG-T	Gpi16p
	PIG-U	Gab1p
Inositol deacylation	PGAP1	Bst1p
***sn*-2 deacylation**	PERLD1/PGAP3	Per1p
***sn*-2 C_{26} acylation**		Gup1p
***sn*-2 acylation**	PGAP2	Cwh43p?

I.A.3-Lipid remodeling of GPI-anchored proteins

I.A.3.1-Lipid moieties of the GPI anchor

The lipid moieties of the phosphatidylinositol (PI) of the GPI precursor consist of unsaturated fatty acyl chains at the sn-2 position. In yeast the PI contains commonly C16:0/C18:1, and in mammalian cells C18:0/C20:4 (Maeda et al., 2007; Sipos et al., 1997). Later, during the process called remodeling, the unsaturated fatty acyl chains at the sn-2 position are replaced by C26:0 in yeast, or C18:0 in mammalian cells. Eventually in yeast the GPI can be remodeled into C18:0 phytosphingosine (PHS) and C26:0 or PHS and monohydroxylated C26:0 (Bosson et al., 2006; Maeda et al., 2007; Reggiori et al., 1997; Sipos et al., 1997) (Fig. 3).

Fig. 3. Lipid moieties of GPI anchor in yeast and mammalian cells. From (Fujita and Jigami, 2008).

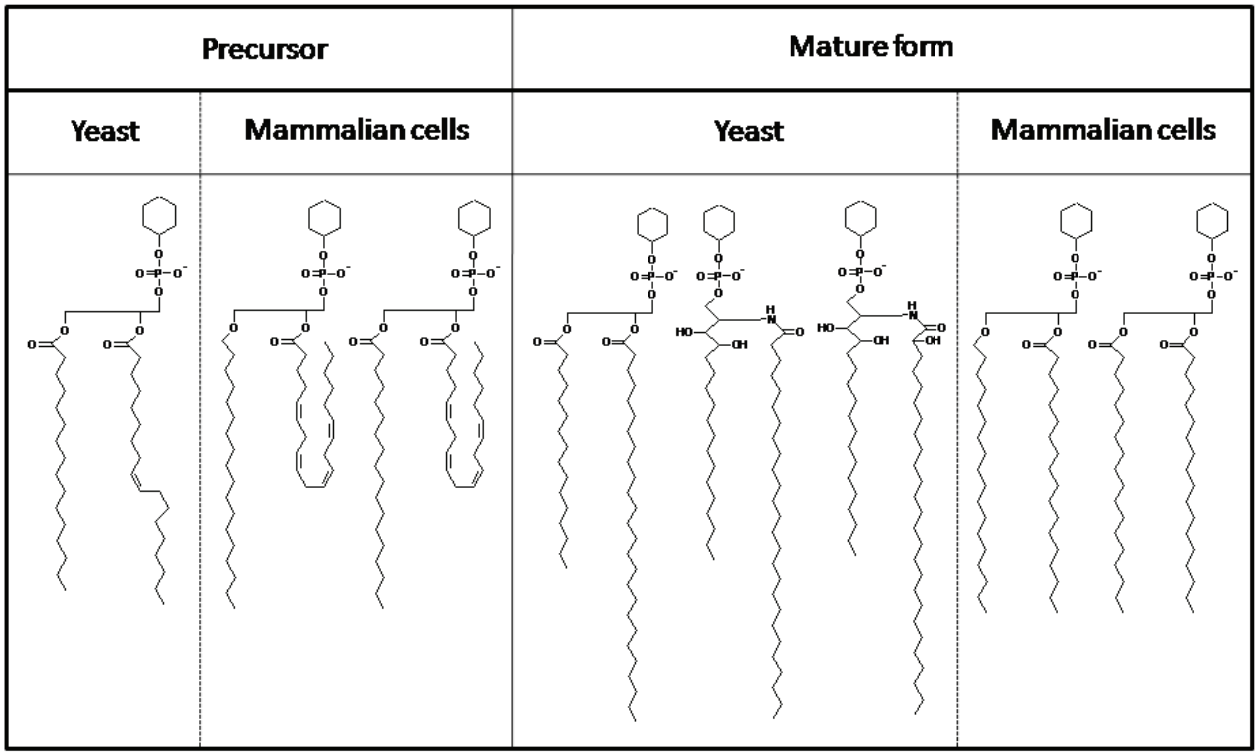

I.A.3.2-Remodeling

As mentioned above, the lipid remodeling process ensures the exchange of the lipid moieties of GPI (Fig. 4). This process takes place after the deacylation of PI in the ER by the yeast protein Bst1p or the mammalian protein PGAP1 (Chen et al., 1998; Fujita et al., 2006a; Tanaka et al., 2004). In human erythrocytes, the PI deacylation and subsequently the remodeling process do not occur (Tanaka et al., 2004). In yeast the remodeling process takes place in the ER lumen, whereas in mammals it occurs in the Golgi apparatus (Fujita et al., 2006a; Maeda et al., 2007; Sipos et al., 1997). After the deacylation, the acyl chain at the sn-2 position of the PI is removed by the yeast protein Per1p or the mammalian homologue PGAP3/PERLD1 to form lyso-PI (Chen et al., 1998; Maeda et al., 2007; Sipos et al., 1997). Then C26:0 in yeast or C18:0 in mammalian cells is added to lyso-PI by yeast Gup1p or PGAP2 in mammals (Bosson et al., 2006; Maeda et al., 2007; Tashima et al., 2006). In yeast the diacylglycerol of the GPI can be further modified into ceramide (Reggiori et al., 1997; Sipos et al., 1997). Even though the precise mechanism has not been elucidated yet, it is

Fig. 4. Lipid remodeling of GPI-anchored proteins in yeast and mammalian cells. From (Fujita and Jigami, 2008).

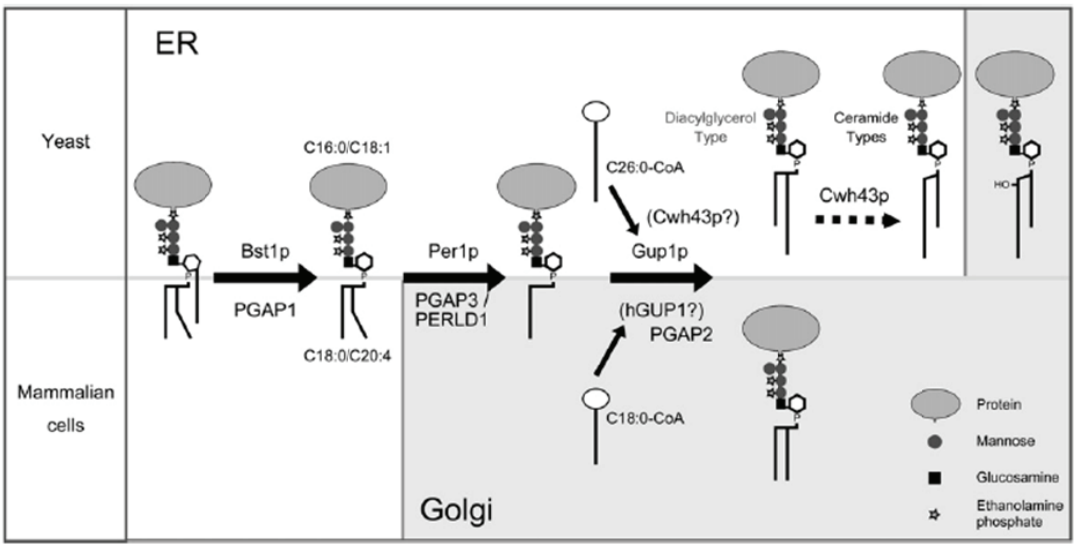

believed that Cwh43p is responsible for such conversion (Ghugtyal et al., 2007; Umemura et al., 2007).

I.A.3.3-Lipid association of GPI-anchored proteins

After remodeling, GPI anchoring confers a specific association with detergent-resistant membranes (DRMs) (Brown and Rose, 1992; Simons and Ikonen, 1997). Still under debate, the DRM association may be the consequence of the GPI-anchored protein association with specialized membrane domains known as “raft” microdomains. Raft microdomains have been described to be membranes enriched in sterols and sphingolipids (Simons and Ikonen, 1997). In yeast, GPI-anchored proteins are associated with DRMs from the ER and later in the secretory pathway, whereas in mammalian cells this association starts in the Golgi (Bagnat et al., 2000; Brown and London, 1998). The ER membrane association of yeast GPI-anchored proteins is weakened in mutants for the synthesis of ceramides (Barz and Walter, 1999; Sutterlin et al., 1997a; Watanabe et al., 2002), and GPI-anchored proteins are not associated with DRMs in yeast and mammalian remodelling mutants (Fujita et al., 2006a; Fujita et al., 2006b; Umemura et al., 2007). Failure of GPI-anchored proteins to be found in microdomains in yeast results in an ER-to-Golgi transport delay of GPI-anchored proteins. This was not observed in mammalian cells (Yasuda et al., 2001). Likely ceramides are building blocks of the ER microdomains in yeast. We would expect an important function of sterols with regard to GPI-anchored proteins membrane association and therefore on GPI-anchored protein secretion. However ergosterol is not required for ER-to-Golgi transport of GPI-anchored proteins in yeast (Heese-Peck et al., 2002). This suggests that the presence of sterols within the microdomains containing ceramides and GPI-anchored proteins is dispensable for stable GPI association.

Later along secretory pathway, the microdomains in which ceramides are replaced by complex sphingolipids, require ergosterol in yeast. Upon pheromone induction, GFP-GPI localized to the mating tip in yeast (Bagnat and Simons, 2002a; Bagnat and Simons, 2002b; Valdez-Taubas and Pelham, 2003). Disturbance of ergosterol or sphingolipid synthesis induces the relocalization of GFP-GPI to the cell cortex. In mammalian cells, the DRM association of GPI-anchored proteins occurs in the Golgi apparatus in connection with the GPI remodelling by the sequential action of PGAP3/PERLD1 and PGAP2. Even though not sufficient, association of GPI-anchored proteins with lipid rafts is essential for apical sorting in several epithelial cell lines and to the axonal region of neuronal cells (Benting et al., 1999; Brown et al., 1989; Lisanti et al., 1989; Lisanti et al., 1990; Paladino et al., 2004). Treatment with an inhibitor of the ceramide synthase, fumonisin B1, disturbs the apical transport of GPI-anchored proteins but does not affect transmembrane protein transport (Lipardi et al., 2000).

I.B-ER-to-Golgi transport

The transport of proteins along the secretory pathway starts from the endoplasmic reticulum (ER). After translation and translocation into the ER, secretory proteins undergo folding and post-translational modifications. Afterwards they are concentrated into transport vesicles coated by the COPII complex. The COPII vesicles ensure the transport of secretory proteins from the ER to the Golgi apparatus or the ER-Golgi intermediate compartment (ERGIC)(Sato, 2004).

I.B.1-COPII coat assembly

The assembly of the COPII coat occurs on specialized regions of the ER surface called ER exit sites (ERES) (Bannykh et al., 1996; Orci et al., 1991). The assembly of the COPII coat is initiated by the activation of the small Ras-like GTPase Sar1p (Nakano and Muramatsu, 1989) (Fig. 5). The conversion of GDP to GTP is mediated by the guanine exchange factor Sec12p. Sec12p is strictly localized to the ER (Barlowe and Schekman, 1993; Nakano et al., 1988). Upon activation Sar1p is anchored into the ER membrane and therefore recruits the heterodimer Sec23p-Sec24p (Bi et al., 2002; Huang et al., 2001). The Sec23p/Sec24p/Sar1p complex binds to cargo molecules to form the pre-budding complex (Kuehn et al., 1998). The pre-budding complex then recruits the heterotetramer complex Sec13p-Sec31p (Lederkremer et al., 2001). Sec13p-Sec31p assemble in order to deform the ER membrane and cage the nascent ER-derived vesicles (Stagg et al., 2008) (Fig.6). The fission of the COPII coated vesicle from the ER membrane has been suggested to be triggered by the GTP hydrolysis by Sar1p (Bielli et al., 2005). Two additional proteins are known to participate to the COPII coat assembly. Sec16p is a peripheral protein

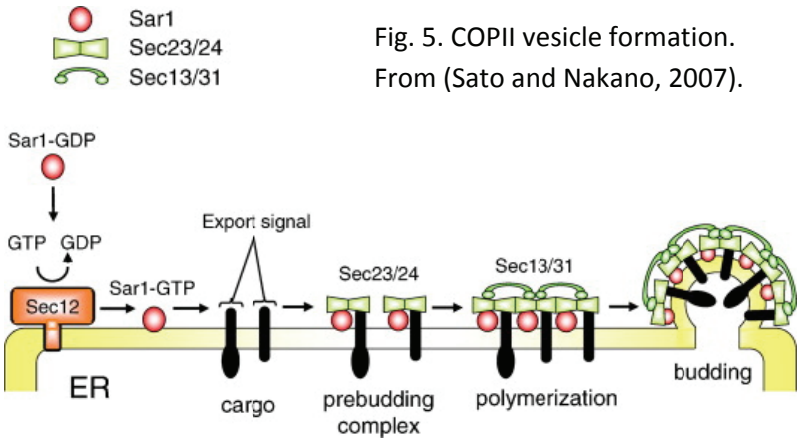

Fig. 5. COPII vesicle formation. From (Sato and Nakano, 2007).

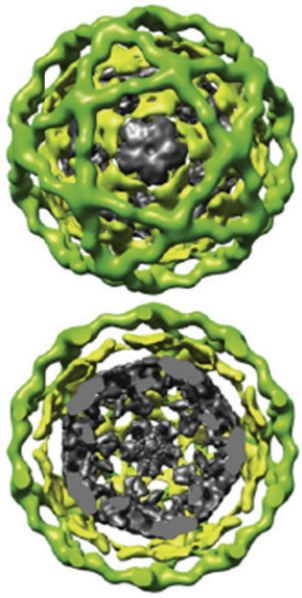

Fig. 6. Structure of the COPII coat. Sec13p-Sec31p (green). Sec23p-Sec24p (yellow). Nonspecifically bound proteins (gray). From (Stagg et al., 2008).

associated to the ER involved in the organization of the ERES (Espenshade et al., 1995; Gimeno et al., 1996; Matsuoka et al., 1998; Supek et al., 2002). Sed4p is an integral membrane protein located at the ER membrane, and its cytoplasmic domain shares homology with Sec12p (Gimeno et al., 1995; Saito-Nakano and Nakano, 2000). However no GEF activity has been found for Sed4p. Sec16p and Sed4p interact directly (Gimeno et al., 1995), but still their precise functions remain unclear.

I.B.2-Cargo selection

Most membrane and soluble cargo proteins are concentrated into COPII vesicles. The selective concentration and loading of cargoes is ensured by export signals. The export signals or ER exit signals allow either the direct interaction with the COPII coat or the interaction with an adaptor protein, which itself can bind to COPII.

I.B.2.1-Concentration of transmembrane proteins

Different ER exit signals have been identified on various transmembrane cargo proteins. The di-acidic motif DxD found at the cytoplasmic C-terminus of the transmembrane protein Gap1p drives the direct interaction with COPII (Malkus et al., 2002). Other motifs such as di-hydrophobic motifs (FF, YY, LL or FY) or tyrosine containing motif, which ensure efficient ER exit, have been identified (Dominguez et al., 1998; Kappeler et al., 1997; Otte and Barlowe, 2002; Sato and Nakano, 2002). In order to be efficiently packaged into COPII coated vesicles, yeast SNAREs display special ER exit signal such as YxxxNPF and LxxME on Sed5p and LxxLE motif on Bet1p (Mossessova et al., 2003).

I.B.2.2-Cargo-specific adaptor proteins

In yeast, several adaptors/receptors for ER exit have been identified (Table 2). Exclusively luminal soluble cargo proteins cannot bind to COPII directly and therefore need the contribution of an adaptor protein or ER exit receptor for efficient ER exit. In the case of the yeast soluble α-factor, recruitment to COPII vesicles is possible through the interaction with the transmembrane protein Erv29p (Belden and Barlowe, 2001b). In the pro-region of the α-factor, the Ile-Leu-Val (ILV) motif mediates the binding with Erv29p. Erv29p is required for the efficient export of carboxypeptidase Y. Erv14p is able to link the transmembrane proteins Axl2p and Sma2p to the COPII coat (Nakanishi et al., 2007; Powers and Barlowe, 2002). The *Drosophila melanogaster* homolog of Erv14p, *cornichon*, is involved in ER export of the growth factor Gurken (Bokel et al., 2006). Moreover during sporulation, Erv14p and Erv15p are essential for ER exit of several cargo proteins (Nakanishi et al., 2007).

Table. 2. Confirmed and putative cargo receptors

Receptor	Cargo	Species	Ref
Erv29p	gpαF and CPY	*S. cerevisiae*	(Belden and Barlowe, 2001b; Otte and Barlowe, 2004)
Erv26p	p-ALP	*S. cerevisiae*	(Bue et al., 2006)
Erv14p	Axl2p and Sma2p	*S. cerevisiae*	(Nakanishi et al., 2007; Powers and Barlowe, 2002)
Vma21p	Vo of the vacuolar H^+-ATPase	*S. cerevisiae*	(Malkus et al., 2004)
Cornichon	Gurken	*D. melanogaster*	(Bokel et al., 2006)
Emp24p-Erv25p	Gas1p, Yps1p and Suc2p	*S. cerevisiae*	(Muniz et al., 2000)
Emp46p-Emp47p	Glycoproteins	*S. cerevisiae*	(Sato and Nakano, 2003)
Erv41p-Erv46p	None identified	*S. cerevisiae* and *M. musculus*	(Otte and Barlowe, 2002; Welsh et al., 2006)
LMAN1-MCFD2	FV and FVIII; catC and catZ	*M. musculus* and *H. sapiens*	(Zhang et al., 2005; Zhang et al., 2006)
BAP31	MHC class I	*M. musculus* and *H. sapiens*	(Ladasky et al., 2006)

Erv26p is specifically involved in ER export of the precursor form of the vacuolar alkaline phosphatase (pro-ALP) (Bue et al., 2006). Emp46p and Emp47p are yeast homologous proteins containing a lectin-like carbohydrate-recognition domain (CRD). Cells mutant for Emp46p, Emp47p, or both, display a glycoprotein secretion defect (Sato and Nakano, 2003; Satoh et al., 2006). Additionally, the Erv41p-Erv46p transmembrane-protein complex is potentially involved as an ER exit receptor (Otte and Barlowe, 2002; Welsh et al., 2006).

I.B.2.3-Emp24p-Erv25p

Being exclusively luminal GPI-anchored proteins must interact with the prebudding complex via the interaction with a cargo receptor. In yeast, the member of the p24 family Emp24p has been proposed to be an ER exit receptor for GPI-anchored proteins in association with Erv25p, Erp1p and Erp2p other members of the p24 family. Emp24p and Erv25p have been found in COPII vesicles, and cycle between ER and Golgi (Belden and Barlowe, 1996). Erv25p and Emp24p are single transmembrane proteins with a short 10 amino-acid C-terminus exposed at the cytoplasmic side (Belden and Barlowe, 1996). The C-terminal di-aromatic motifs YF and FF of Erv25p and Emp24p bind to Sec23p-Sec24p and Sec13p-Sec31p (Belden and Barlowe, 2001a). The FF motif of Emp24p can additionally bind to Sar1p (Belden and Barlowe, 2001a). Moreover the C-termini of Emp24p and Erv25p can bind to COPI, Erv25p displaying a higher affinity for COPI (Belden and Barlowe, 2001a). Gas1p maturation is delayed in *emp24Δ* and in *erv25Δ* cells (Muniz et al., 2000). Emp24p and Erv25p depend upon each other in order to form a stable protein complex efficient for GPI-anchored protein ER exit (Belden and Barlowe, 1996). Furthermore, it has been observed that Emp24p can be crosslinked with Gas1p but not with the transmembrane protein Gap1p upon ER exit (Muniz et al., 2000). The mammalian homolog of Emp24p named p23 is required for efficient

transport of GPI-anchored proteins from the ER to the Golgi compartment, but no evidence for a direct interaction with GPI-anchored proteins was found (Takida et al., 2008). Emp24p and Erv25p have been shown to facilitate the COPI coated vesicle formation through the ArfGAP Glo3p (Aguilera-Romero et al., 2008). This could be linked to the fact that ER-to-Golgi transport of GPI-anchored proteins is specifically defective in the mutant (*ret1-1*) for the α-subunit of the COPI coatmer(Sutterlin et al., 1997a). *EMP24, ERV25* and *BST1* were originally identified as synthetic survival mutants with *SEC13* (Elrod-Erickson and Kaiser, 1996). The reason for this genetic interaction remains still unclear but suggests that a decrease in GPI-anchored proteins ER export permits formation of COPII vesicles in the absence of Sec13p. One hypothesis, which has to be proven, would be that GPI-anchored proteins are able to be incorporated into alternative COPII coated vesicles where the Sec13p requirement is not strict. Then by preventing a fraction of GPI-anchored proteins to enter these alternative ER-derived vesicles, enough non-GPI-anchored cargo proteins could use this pathway and their ER exports ensure cell survival. Alternatively, it could be that the altered composition of the ER membrane due to the lack of GPI-anchored protein exit may make it easier to deform the ER membrane, rendering Sec13p dispensible.

I.B.2.4-Cargo recognition by Sec24p

In order to be efficiently exported from the ER a variety of proteins has to bind to COPII. Sec24p is believed to interact directly with transmembrane cargo proteins. There are at least three independent signal-binding sites on Sec24p, termed “A-site”, “B-site” and “C-site”. The YxxxNPF motif on the SNARE Sed5p binds to the “A-site”, whereas the SNARE Sec22p binds to the “C-site”. The “B-site” recognizes multiple motifs, such as the di-acidic motif DxD and the Lxx(L/M)E motif of the SNAREs Bet1p and Sed5p (Miller et al., 2003; Mossessova et al.,

2003). Moreover two non-essential Sec24p paralogs have been identified in yeast: Sfb2p (formerly named Iss1p), and Sfb3p/Lst1p (Miller et al., 2003). The ER exit of the GPI-anchored protein Gas1p and the transmembrane protein Pma1p is defective in *sfb3Δ* cells (Peng et al., 2000). The different paralogs of Sec24p might expand the capacity of the COPII coat to capture various cargo proteins. In mammalian cells, four isoforms of Sec24 have been identified.

I.B.3-Sorting upon ER exit

In yeast, the GPI-anchored protein Gas1p and the transmembrane protein Gap1p exit ER in different ER-derived vesicle populations(Muniz et al., 2001). Regarding vesicular traffic, proteins are sorted and packaged into vesicles that bud from a donor membrane. The vesicles are transported and tethered to the acceptor membrane prior to SNARE complex formation and subsequent membrane fusion. The tethering events require the function of a distinct Rab GTPase. The specificity of membrane targeting is driven by combined actions of Rabs, tethering factors and SNARES. Because they are spatially and temporally separated, budding and targeting/fusion steps are considered to be independent. It has been shown that the mutant for the tethering factor Uso1p not only prevents tethering of ER derived vesicles, but displays a sorting defect in which GPI-anchored proteins and non-GPI-anchored proteins are found in the same ER-derived vesicle population (Morsomme and Riezman, 2002). In the same study, it has been found that the small Rab-GTPase Ypt1p and the tethering factors Sec34p/35p are also necessary for sorting upon ER exit. This sorting defect appears to occur during the budding event, suggesting that Ypt1p and the tethering complex is required for sorting during budding at the level of ER. Additionally, it has been reported that mutants in the v-SNAREs Bos1p, Sec22p and Bet1p produce *in vitro* ER-derived vesicles

unable to fuse to the Golgi and in which Gas1p and Gap1p are not sorted (Morsomme et al., 2003).

In mammalian cells, sorting between GPI-anchored proteins and others cargo proteins upon ER exit has not been observed. Indeed upon 15°C block, the GPI fused with GFP and VSVG are found co-localized in ERGIC compartment (Stephens and Pepperkok, 2004). It appears that sorting occurs at the trans-Golgi network level. Rafts might largely contribute to this event (Benting et al., 1999; Campana et al., 2007; Paladino et al., 2007; Schuck and Simons, 2004). It is interesting to make the parallel between the place of sorting and the localization of the GPI remodelling enzymes. In yeast, remodelling and sorting occurs at the level of ER, whereas in mammalian cells remodelling and sorting take place in the Golgi apparatus.

II-Thesis project

The purpose of this thesis work was to study the ER exit of GPI-anchored proteins. How are GPI-anchored proteins incorporated into COPII coated vesicles and sorted from other cargo proteins? What is the molecular mechanism behind the sorting upon ER exit?

In the first part, we investigated whether the GPI anchor is an ER exit signal and whether it is required for sorting. In the second part, we developed tools that allowed us to follow ER exit and sorting of GPI-anchored proteins *in vivo*. The use of these new tools provided us with some leads on cargo concentration into ER-derived vesicles and on the sorting mechanism.

In the third part, we have focused our investigation on the molecular function of Emp24p and on remodeling. In the last part, I have put together various experimental results in which we looked at the Sar1p requirement for ER exit of GPI-anchored proteins and the function of the SNAREs, particularly Bos1p, in protein sorting. Finally, we followed the secretion of cargo proteins after ER exit.

III-Results

III.A- The presence of an ER exit signal determines the protein sorting upon ER exit in yeast.(Watanabe et al., 2008)

In this work, we determined that the GPI anchor can be considered as an ER exit signal. Indeed replacement of the GPI anchor attachment site of Gas1p by an artificial transmembrane domain leads to the reduction of the budding efficiency. The soluble cargo, α-factor, fused with a GPI-anchor is sorted similarly to endogenous α-factor, because it can still interact with its ER exit receptor Erv29p. In *erv29Δ* cells, α-factor ER exit is strongly decreased, and α-factor is no longer incorporated into Gap1p-containing vesicles. We concluded that if the GPI anchor is a sorting determinant, then it is not dominant over the proteinaceous sorting signal contained in α-factor.

BJ www.biochemj.org

BJ Cell

Biochem. J. (2008) **414**, 237–245 (Printed in Great Britain) doi:10.1042/BJ20080715

The presence of an ER exit signal determines the protein sorting upon ER exit in yeast

Reika WATANABE[1], Guillaume A. CASTILLON[1], Anja MEURY and Howard RIEZMAN[2]

Department of Biochemistry, University of Geneva, Sciences II, 30 quai Ernest Ansermet, CH-1211 Geneva, Switzerland

In yeast, there are at least two vesicle populations upon ER (endoplasmic reticulum) exit, one containing Gap1p (general amino-acid permease) and a glycosylated α-factor, gpαF (glycosylated proα-factor), and the other containing GPI (glycosylphosphatidylinositol)-anchored proteins, Gas1p (glycophospholipid-anchored surface protein) and Yps1p. We attempted to identify sorting determinants for this protein sorting event in the ER. We found that mutant Gas1 proteins that lack a GPI anchor and/or S/T region (serine- and threonine-rich region), two common characteristic features conserved among yeast GPI-anchored proteins, were still sorted away from Gap1p-containing vesicles. Furthermore, a mutant glycosylated α-factor, gpαGPI, which contains both the GPI anchor and S/T region from Gas1p, still entered Gap1p-containing vesicles, demonstrating that these conserved characteristics do not prevent proteins from entering Gap1p-containing vesicles. gpαF showed severely reduced budding efficiency in the absence of its ER exit receptor Erv29p, and this residual budding product no longer entered Gap1p-containing vesicles. These results suggest that the interaction of gpαF with Erv29p is essential for sorting into Gap1p-containing vesicles. We compared the detergent solubility of Gas1p and the gpαGPI in the ER with that in ER-derived vesicles. Both GPI-anchored proteins similarly partitioned into the DRM (detergent-resistant membrane) in the ER. Based on the fact that they entered different ER-derived vesicles, we conclude that DRM partitioning of GPI-anchored proteins is not the dominant determinant of protein sorting upon ER exit. Interestingly, upon incorporation into the ER-derived vesicles, gpαGPI was no longer detergent-insoluble, in contrast with the persistent detergent insolubility of Gas1p in the ER-derived vesicles. We present different explanations for the different behaviours of GPI-anchored proteins in distinct ER-derived vesicle populations.

Key words: bulk flow, detergent-resistant membrane (DRM), endoplasmic reticulum (ER) exit receptor, ER exit signal, ER-to-Golgi transport, glycosylphosphatidylinositol-anchored protein.

INTRODUCTION

Proteins of the eukaryotic secretory pathway are synthesized and inserted into the ER (endoplasmic reticulum) where they receive co- and post-translational modifications important for their function and structure. The ER exit process of the proteins is mediated by the sequential recruitment of COPII (coat protein complex II) components to the ER membrane, leading to the formation of COPII-coated vesicles, which carry proteins and lipid from the ER to the Golgi structure [1]. Historically, two models exist to explain how cargo proteins are packaged into COPII-coated vesicles: a bulk flow model and a signal-mediated export model. In the bulk flow model, any protein that is soluble or free to move in the membrane is incorporated into vesicles and transported towards the Golgi compartment. ER-resident proteins are localized to the ER by retention or retrieval from the Golgi. This model is consistent with results showing that two highly abundant secretory proteins, amylase and chymotrypsinogen, are not concentrated when they are packaged into COPII vesicles in mammalian pancreatic cells but rather at a later stage, presumably due to reduction of the volume of the recently budded compartment from recycling of membrane components back to the ER [2]. In the signal-mediated export model, proteins that leave the ER contain specific ER exit signals and are selectively transported out of the ER. Recently, several classes of ER exit signals have been identified for transmembrane and luminal proteins in yeast [3–5]. Proteins carrying ER exit signals bind to COPII components directly or indirectly via receptors, and are concentrated into vesicles upon ER exit [3,6]. Among them, the Gap1p (general amino-acid permease) is a transmembrane protein enriched approximately 3-fold in COPII vesicles relative to membrane phospholipids. The di-acidic sequence in the C-terminal cytoplasmic domain is essential for this concentrative sorting [7]. A soluble secretory protein, gpαF (glycosylated proα-factor), is enriched 20-fold in vesicles [7] and contains a hydrophobic signal within the proregion that is essential and sufficient to direct its export via the transmembrane receptor protein Erv29p [8,9]. Importantly, ER exit of gpαF is not absolutely dependent on Erv29p [8] and bulk flow movements of those precursor proteins from the ER could explain the reduced transport rate in the absence of those potential receptors [7].

GPI (glycosylphosphatidylinositol)-anchored proteins are localized on the surface of eukaryotic cells via a glycolipid anchor. In the lumen of the ER, a preassembled GPI anchor is transferred *en bloc* to the newly generated C-terminus of the precursor protein after cleavage of the GPI-attachment signal [10]. GPI-attachment is indispensable for further transport to the Golgi apparatus [11–13]. Efficient transport of the GPI-anchored proteins requires Emp24p/p24 protein members, which have been proposed to fulfil a receptor function for ER exit [14,15]. We have shown that GPI-anchored proteins are transported from the ER to the Golgi apparatus in distinct vesicles from Gap1p and gpαF in yeast

Abbreviations used: ALP, alkaline phosphatase; COPII, coat protein complex II; DRM, detergent-resistant membrane; ER, endoplasmic reticulum; Gap1p, general amino-acid permease; Gas1p, glycophospholipid-anchored surface protein; gpαF, glycosylated proα-factor; GPI, glycosylphosphatidylinositol; GST, glutathione transferase; HA, haemagglutinin; ORF, open reading frame; SD, synthetic dropout; S/T region, serine- and threonine-rich region; TMD, transmembrane domain.

[1] These authors contributed equally to this work.

[2] To whom correspondence should be addressed (email Howard.Riezman@biochem.unige.ch).

Table 1 Strains used in the present study

Strain	Genotype	Source/reference
RH2043	*Matα sec18 pep4Δ::URA3 his4 leu2 ura3 bar1*	Lab strain
RH5646	*Matα gas1Δ::ADE2 gap1Δ::LEU2 ade2 leu2 lys2 ura3*	Lab strain
RH2874	*Matα leu2 lys2 trp1 ura3 bar1*	Lab strain
RH6159	*Matα mfα1Δ::natMX leu2 lys2 trp1 ura3 bar1*	Lab strain
RH6153	*Matα erv29Δ::kanMX leu2 lys2 trp1 ura3 bar1*	The present study
RH5240	*Matα sec18 gas1Δ::ADE2 gap1Δ::LEU2 ade2 leu2 lys2 ura3*	The present study
RH4913	*Matα sec18 ade2 his4 leu2 lys2 ura3 bar1*	Lab strain

Table 2 Plasmids used in the present study

Plasmid	Description	Source/reference
pPL269	Own promotor Gap1p-HA (GAP1::FLU1) in YCp405 (CEN, LYS2)	[49]
pGAS1(URA3)	Own promotor Gas1p in YEplac195 (2 μm, URA3)	The present study
pGAS1(TRP1)	Own promotor Gas1p in YEplac112 (2 μm, TRP1)	The present study
pGAS1TMD	Own promotor Gas1p (ΔAla^{529}–Val^{559}) + L^{19}RRSS in pSEY8 (2 μm, URA3)	The present study
pGAS1(−S/T)	Own promotor Gas1p (ΔSer^{490}–Ser^{525}, K526S) in YEplac195 (2 μm, URA3)	The present study
pGAS1(−S/T)TMD	ADH (alcohol dehydrogenase) promotor Gas1p (ΔSer^{489}–Val^{559}) + L^{19}RRSS in pCM189 (CEN, URA3)	The present study
pTD52	Triosephosphate isomerase promotor Prepro α + Gas1p (Ser^{497}–Val^{559}) in pYX112 (CEN, URA3)	[42]
pGSTTMD	ADH promotor Invertase (Met^{1}–Ser^{20}) + GST + L^{19}RRSS in pCM189 (CEN, URA3)	The present study

[16]. The sorting, but not budding efficiency, of GPI-anchored proteins depends on the Rab GTPase Ypt1p, tethering factors Uso1p and the COG (conserved oligomeric Golgi) complex, and SNARE (soluble *N*-ethylmaleimide-sensitive factor-attachment protein receptor) molecules [17,18]. In addition to these protein factors, sphingolipid/sterol-enriched DRMs (detergent-resistant membranes) may also function in sorting of GPI-anchored proteins, since GPI-anchored proteins are partitioned into these membrane domains in the ER [19]. This idea is also supported by the fact that ongoing sphingolipid synthesis is specifically required for efficient ER-to-Golgi-transport of GPI-anchored proteins [20–22]. Besides GPI-anchored proteins, various plasma-membrane-localized transporters, such as Pma1p, Tat2p, Fur4p and Can1p, are incorporated into DRM along the secretory pathway, and disturbance of DRM affects the targeting and/or stability of the proteins in the plasma membrane [23–31].

In the present study, we attempted to identify the sorting determinants in the ER protein sorting between GPI-anchored proteins and other secretory proteins using several mutant proteins. We also examined the significance of DRM partitioning of those proteins for the choice of the vesicles upon ER exit. As a result, we found that protein–protein interactions via ER exit signals, but not DRM partitioning in the ER, determine the sorting into distinct vesicle populations upon ER exit.

EXPERIMENTAL

Yeast strains and plasmids

Yeast strains and plasmids used in the present study are listed in Tables 1 and 2. ORFs (open reading frames) of *MFα1* and *ERV29* were replaced by NatMX [32] or KanMX [33] disruption cassettes respectively to produce RH6159 (*mfα1Δ*) and RH6153 (*erv29Δ*), in the RH2874 background. They were selected with clonNAT (Werner BioAgents) and G418-containing YPUAD [1 % (w/v) yeast extract, 2 % (w/v) peptone, 2 % (w/v) glucose and 40 mg/l each of uracil and adenine] plates respectively, and disruption was verified by PCR. For construction of plasmids carrying wild-type *GAS1* (glycophospholipid-anchored surface protein), we amplified *GAS1* from the yeast genome by PCR. A 2.4 kbp PCR fragment was ligated into YEplac195 or YEplac112 using SphI and SacI sites. For the plasmid containing *GAS1TMD* (where TMD is transmembrane domain), four independent steps of PCR reactions were done. First, the DNA fragment coding for L^{19}R^{2}S^{2} and fragments of the *GAS1* 3′-region, both containing short flanking homologous sequences, were amplified. After mixing these PCR products, another round of PCR was performed to obtain the fused fragment. A fragment containing the 5′-region and part of the *GAS1* ORF (M1-N528) was also amplified by PCR. These PCR fragments were mixed and finally a fused fragment containing *GAS1TMD* was obtained by PCR and ligated into pSEY8 using BamHI at both ends of the fragment. For construction of the plasmid containing *GAS1(S/T)*, where S/T is a serine- and threonine-rich region, a 4.5 kbp SphI and SacI fragment from pGsm [34] was ligated into YEplac195. For the plasmid containing *GAS1(S/T)TMD*, we amplified part of the *GAS1* ORF (M1-E488) fused with a sequence coding for L^{19}RRSS. A 1.6 kbp PCR fragment was ligated into pCM189 [35] using PmeI and NotI sites. For the plasmid containing *GSTTMD*, we amplified GST (glutathione transferase) fused with a sequence coding for the signal sequence of *SUC2* (M1-S20) and a sequence coding for L^{19}R^{2}S^{2}. A 0.8 kbp PCR fragment was ligated into pCM189 [35] using PmeI and NotI sites.

In vitro ER-budding assay and vesicle immunoisolation

In vitro ER-budding assay and vesicle immunoisolation are performed as described in [14,16]. Briefly, cells were grown in SUD medium [0.16 % yeast nitrogen base without amino acids and without $(NH_4)_2SO_4$, 2 % glucose and 0.1 % urea] at 24 °C and then grown overnight in SD (synthetic dropout) YE medium (0.67 % yeast nitrogen base without amino acids, 2 % glucose and 0.2 % yeast extract) at 24 °C. Cells were harvested at 5×10^6 cells/ml, and pulse-labelled for 4 min with [^{35}S]methionine and cysteine EasyTag (NEG772; Amersham) in SD medium at 24 °C. Semi-intact cells were prepared as described in [36] with few modifications. Cells were treated with 10 mM MESNA (sodium 2-mercaptoethanesulfonic acid) instead of DTT (dithiothreitol) and lyticase to digest the cell wall. By a gentle freeze–thaw cycle, we obtained transport-competent semi-intact cells. The cytosol was prepared from the strain RH2043 (*sec18*) as described previously [37].

The *in vitro* ER-budding assay was performed in the presence of 2.5×10^8 semi-intact cells, cytosol, an ATP regeneration system, GTP, GDP-mannose, recombinant Sar1p (1 μM), protease inhibitor mix (leupeptin, pepstatin and antipain) for 1 h at 30 °C. ER-budding assays were performed using the cytosol prepared from *sec18* cells, which are defective in the fusion of ER-derived vesicles with the Golgi apparatus to preferentially analyse the primary ER-derived vesicles. Vesicle fractions were

isolated by flotation of Nycodenz layers [38] and processed for immunoprecipitation. Rabbit polyclonal antibodies against Gas1p, Gap1p, α-factor and goat polyclonal anti-GST (GE Healthcare) and Protein A–Sepharose Fast Flow (GE Healthcare) were used for immunoprecipitation. The samples were separated by SDS/PAGE and quantified using a cyclone phosphoimager (Packard). Vesicle immunoisolation using the mouse anti-HA (haemagglutinin) antibody (Roche) and Protein G–Sepharose 4 Fast Flow (GE Healthcare) was performed as described previously [16]. Pellet (P) corresponds to immunoisolated vesicles and supernatant (S) corresponds to the vesicle fraction that was not precipitated. Individual fractions were processed for immunoprecipitation and analysed as above. To quantify the percentage of proteins in Gap1p-containing vesicles, we divided the percentage of individual proteins found in the pellet fraction by the percentage of immunoisolated Gap1p. This process enables comparisons of several independent experiments in which immunoisolation efficiency of Gap1p-containing vesicles can vary.

Fractionation of the DRM fraction

The preparation of a DRM fraction of newly synthesized proteins in the ER was basically performed as described in [19]. The *sec18* mutant cells expressing cargo proteins were pulse-labelled for 6 min with [^{35}S]methionine and [^{35}S]cysteine EasyTag (NEG772) at the non-permissive temperature, 30 °C. The labelling reaction was stopped by the addition of 20 mM NaN_3. The cells were lysed in TNE buffer (50 mM Tris/HCl, pH 7.4, 500 mM NaCl, 5 mM EDTA, 1 mM protease inhibitor mix and 1 mM PMSF) by glass beads. The supernatant was collected and centrifuged at 500 ***g*** for 5 min to remove unbroken cells and large debris. The cleared lysate was incubated for 30 min on ice with 1 % (w/v) Triton X-100. OptiPrep solution (Axis-Shield, Oslo, Norway) was added to reach 40 % OptiPrep. A 750 μl portion of this fraction was overlaid with 1.2 ml of 30 % OptiPrep in TXNE (0.1 % Triton X-100 in TNE) and 200 μl of TXNE. The samples were centrifuged at 55 000 rev./min for 2 h in a TLS55 rotor (Beckman), and six fractions were collected from the top. Each fraction was solubilized and analysed by immunoprecipitation [22].

For isolation of a DRM fraction from ER-derived vesicles, the *in vitro* ER-budding reaction was performed using 5×10^8 semi-intact cells as described above. Nycodenz-purified vesicle fractions were treated with 1 % (w/v) Triton X-100 in TNE at 4 °C for 30 min. The pellet (P) and supernatant (S) fractions were obtained by ultracentrifugation at 65 000 rev./min for 1 h in a TLA-100.3 rotor (Beckman) at 4 °C. Both fractions were solubilized and analysed by immunoprecipitation.

RESULTS

Removal of potential signals from Gas1p

To investigate the mechanism of sorting of GPI-anchored proteins into distinct vesicles upon ER exit, we searched for common characteristic motifs conserved among yeast GPI-anchored proteins. Most, if not all, yeast GPI-anchored proteins share two characteristic features: the GPI anchor and an S/T region. The GPI anchor is covalently attached to a newly generated C-terminal residue (ω site) after cleavage of the GPI-attachment signal in the ER. The S/T region upstream of the ω site [39] is a site for O-mannosylation [34,40], which begins in the ER in yeast [41].

To investigate the role of the GPI anchor and the S/T region of Gas1p in ER budding efficiency and sorting, we used three Gas1p mutant constructs: Gas1TMD, which contains an artificial TMD consisting of 19 leucine residues and two arginine and serine residues instead of a GPI anchor; Gas1(−S/T), which lacks the S/T region, Gas1(−S/T)TMD, which lacks the S/T region and contains an artificial TMD (Figure 1). We measured budding and sorting of these mutant proteins in *gas1Δ* cells using an *in vitro* assay that reconstitutes ER-derived vesicle formation. Pulse-labelled semi-intact cells were incubated with exogenous cytosol, Sar1p, GTP and an ATP-regeneration system. ER-derived vesicles were separated from the starting membranes by centrifugation and further purified by Nycodenz flotation. All mutant Gas1 proteins budded from the ER in a cytosol-dependent manner (Figure 2A). Gas1TMD and Gas1(−S/T)TMD showed reduced budding efficiency (60 % of wild-type Gas1p) (Figure 2B). This fits with the results of the *in vivo* pulse–chase experiments that show significant delayed appearance of the Golgi form of Gas1TMD compared with wild-type Gas1p (results not shown). In contrast, Gas1(−S/T) budded with an efficiency similar to wild-type Gas1p (Figure 2B). From these results, it is possible that the GPI anchor, but not the S/T region, facilitates budding from the ER or that the artificial TMD inhibits budding.

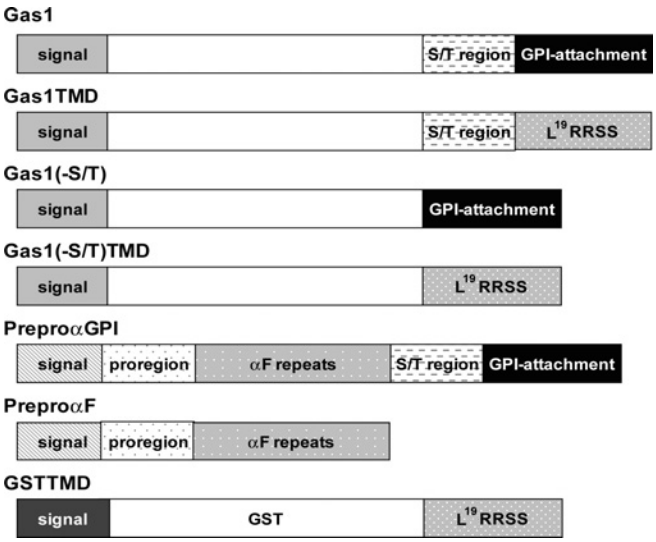

Figure 1 Schematic representation of wild-type and mutant proteins used in the present study

Signal, various N-terminal signal peptides (derived from *GAS1*, *MFα1* or *SUC2*); GPI-attachment, GPI-attachment signal; L^{19}RRSS, artificial TMD consisting of 19 leucine, followed by two arginine and two serine residues; αF repeats, α-factor repeats. This Figure is not drawn to scale.

Next, we analysed protein segregation upon incorporation into ER-derived vesicles by immunoisolation of Gap1p–HA-containing vesicles. Consistent with our previous results [16], only 24 % of Gas1p was precipitated with 77 % of Gap1p–HA (Figure 2C), showing that Gap1p and Gas1p are mainly incorporated into distinct ER-derived vesicles. To our surprise, all mutant proteins behaved similarly to wild-type Gas1p (Figures 2C and 2D), indicating that neither the GPI anchor nor the S/T region is essential for keeping Gas1p out of the Gap1p-containing vesicles.

Addition of potential signals to prepro α-factor

We next addressed whether the GPI anchor and S/T region can function to prevent entry into Gap1p-containing vesicles. We used prepro αGPI, a chimaeric protein of prepro α-factor fused with the C-terminus of Gas1p, including the S/T region and GPI-attachment signal (Figure 1) [42]. Endogenous prepro α-factor

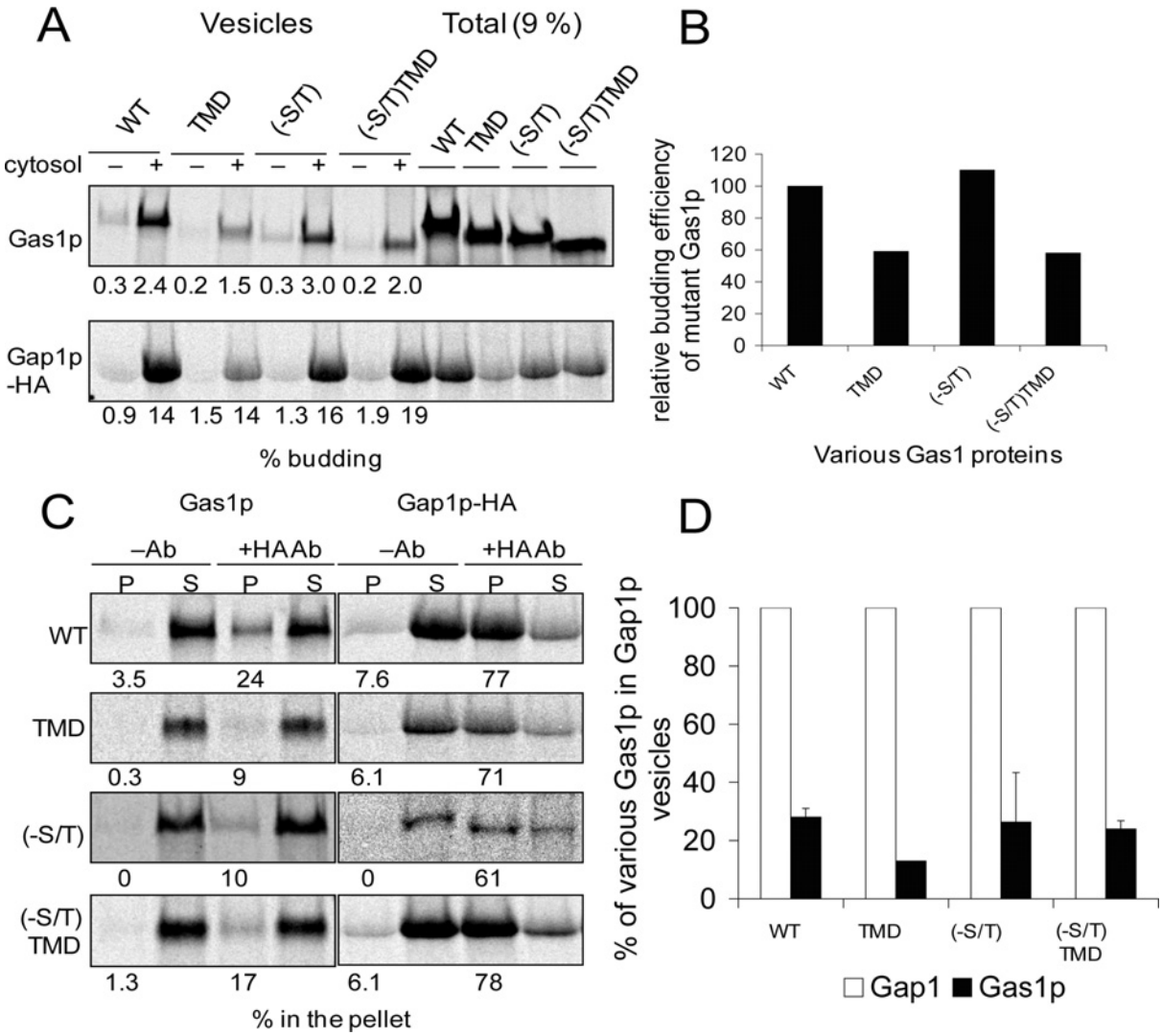

Figure 2 All Gas1 mutant proteins bud from the ER in a cytosol-dependent manner and are sorted from Gap1p

(**A**) *In vitro* budding assay using semi-intact cells derived from RH5646 (*gas1Δ*) cells expressing either wild-type or mutant Gas1p together with HA-tagged Gap1p was performed done in the presence or absence of cytosol prepared from *sec18* cells. The numbers correspond to budding efficiency. Budding efficiencies were calculated as the percentage of the total input that was recovered in the purified vesicles for each individual protein. 'Total' indicates immunoprecipitate from 9 % of total input. A representative result is shown. (**B**) After normalization using Gap1p budding efficiency in each strain, the budding efficiency of mutant Gas1 proteins was compared with that of wild-type Gas1p (set as 100). A representative result of two to three experiments is shown. (**C**) Vesicles generated in (**A**) were immunoisolated with or without monoclonal anti-HA antibody. The pellets (P) fraction corresponds to immunoisolated vesicles and the supernatant (S) fraction corresponds to the vesicle fraction that was not precipitated. The numbers correspond to the percentage found in the pellets. A representative result is shown. (**D**) To quantify the percentage of proteins in Gap1p-containing vesicles, the percentage of individual proteins found in the pellet fraction was divided by the percentage of immunoisolated Gap1p. The bars represent the means for several independent experiments.

is processed to gpαF in the ER where its ER exit signal is recognized by a transmembrane receptor, Erv29p [8,9]. Prepro αGPI is processed into a glycosylated and GPI-anchored protein (gpαGPI) in the ER [42]. gpαGPI (Figure 3A) and endogenous gpαF (Figure 4A) were incorporated into vesicles in a cytosol-dependent manner *in vitro*. The budding of gpαGPI was Erv29p-dependent (Figures 3A and 3B). We noticed that in comparison with gpαF, the dependence of gpαGPI on Erv29p was less tight (Figure 3B). This might be because gpαGPI contains a GPI anchor and thus is membrane-anchored, compared with gpαF which is a soluble luminal protein. Since gpαF forms dimers [8,43], we also measured gpαGPI budding in *mfα1Δ* cells, which express very little gpαF. In *mfα1Δ* cells, gpαGPI was incorporated more efficiently into vesicles than in wild-type cells; in contrast, Gas1p and Gap1p budded with similar efficiency as in wild-type cells (Figures 3A and 3B). This is probably due to the increased availability of Erv29p in the absence of endogenous gpαF. Next, we measured the sorting of gpαGPI into ER-derived vesicles. In wild-type and *mfα1Δ* cells, a substantial amount of gpαGPI was precipitated with Gap1p-containing vesicles, similar to gpαF (Figures 3C and 3D). These results demonstrate that it is possible for a GPI-anchored protein to enter the same vesicles as Gap1p. Therefore the S/T region and the GPI anchor of Gas1p are not dominant sorting signals to prevent entry into Gap1p-containing vesicles.

Removal of a receptor of the signal-mediated pathway

If these two regions are neither necessary nor sufficient for segregation of GPI-anchored protein from Gap1p-containing

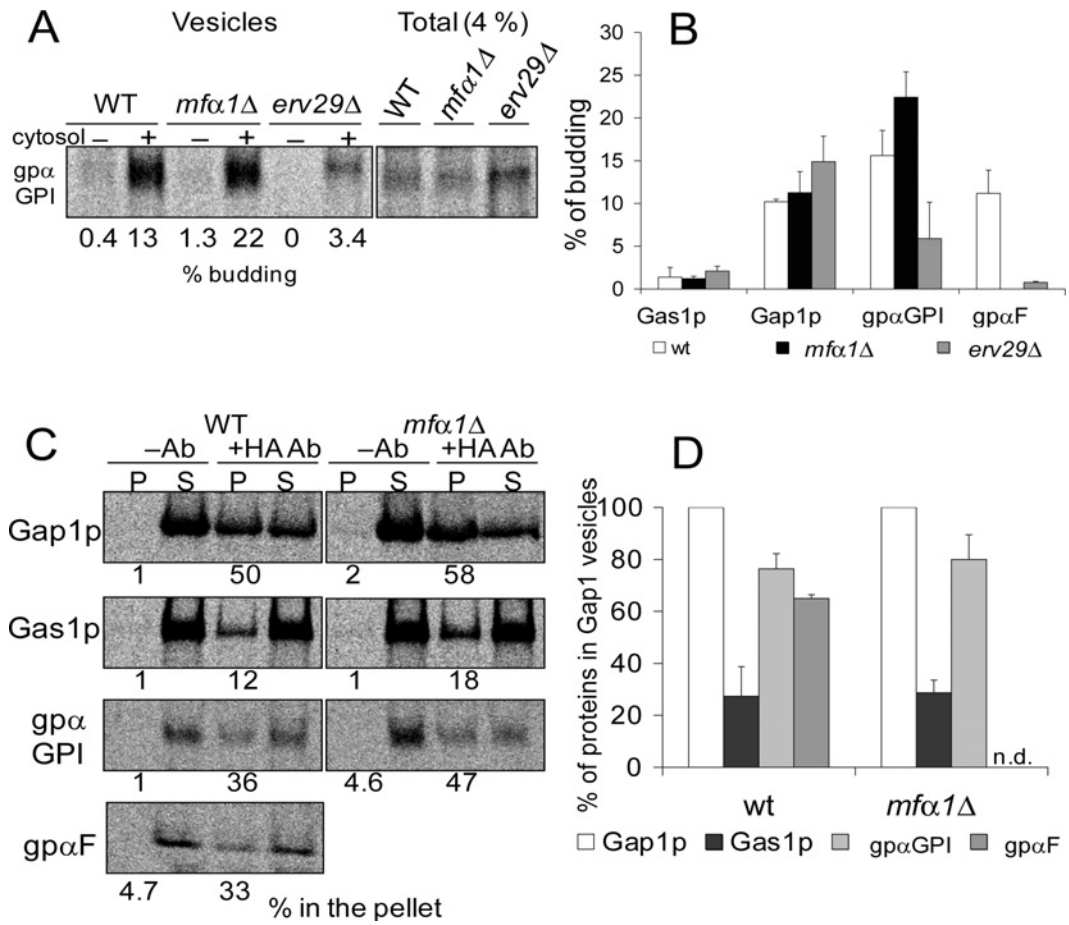

Figure 3 gpαGPI buds from the ER in a cytosol-dependent manner and is sorted into Gap1p-containing vesicles

(**A**) *In vitro* budding assay using semi-intact cells derived from RH2874 (WT), RH6159 (*mfα1Δ*) and RH6153 (*erv29Δ*) cells expressing preproαGPI together with wild-type Gas1p and HA-tagged Gap1p was done in the presence or absence of *sec18* cytosol. The samples were analysed as in Figure 2. 'Total' indicates immunoprecipitate from 4 % of total input. (**B**) A comparison of the budding efficiency of each cargo protein in wild-type, *mfα1Δ* and *erv29Δ* cells; $n = 2$. (**C**) Vesicles generated in (**A**) were immunoisolated with or without monoclonal anti-HA antibody. (**D**) Quantification was carried out as in Figure 2; $n = 3$.

vesicles upon ER exit, then how is cargo selection achieved? The simplest explanation is that GPI-anchored proteins may not be actively kept out of Gap1p-containing vesicles. Instead, Gap1 and gpαF, which contain ER exit signals [7,9], are actively sorted into a specialized population of ER-derived vesicles. To test this idea, we studied gpαF, which is found in Gap1p vesicles in wild-type cells (Figure 4). Instead of eliminating its ER exit signal, which could cause misfolding of gpαF, we tested its sorting in the absence of its ER exit receptor Erv29p as an endogenous bulk flow marker, reported in [7]. In our *in vitro* budding assay, strong reduction of budding of gpαF but not Gap1p and Gas1p in *erv29Δ* cells was observed (Figures 3B and 4A) as reported [8]. A 22-fold increased signal of labelled gpαF accumulated during the 4 min pulse labelling in semi-intact cells derived from *erv29Δ* cells compared with wild-type cells (Figure 4A, 'Total'), suggesting accumulation of gpαF *in vivo* in *erv29Δ* cells [8]. Even though the budding efficiency of gpαF in *erv29Δ* cells was low, it was cytosol dependent. In contrast with wild-type cells (Figure 3), most of the vesicular gpαF in *erv29Δ* cells was not incorporated into Gap1p vesicles (Figures 4B and 4C), behaving like Gas1p. These results support the hypothesis that proteins with a functional ER exit signal are actively incorporated into the signal-mediated vesicles, which are separate from other ER-derived vesicles.

Naive protein

If our hypothesis is correct, exogenous protein without any secretory information should be sorted away from Gap1p-vesicles. We used GST fused N-terminally with a cleavable signal peptide and C-terminally membrane-anchored with an artificial TMD (L^{19}RRSS) (Figure 1). GST should not contain any secretory information since it is a cytoplasmic protein and has no consensus motifs for *N*-glycosylation. *In vitro*, GSTTMD budded in a cytosol-dependent manner (Figure 5A). Only a small fraction of GSTTMD was isolated with Gap1p-containing vesicles (Figures 5B and 5C). Importantly, Gas1p, Gap1p and GSTTMD showed similar kinetics of *in vitro* budding (Figures 5D and 5E). This rules out the possibility that Gas1p and GSTTMD are packaged into different vesicles to Gap1p due to temporal causes. The result confirms that proteins without ER exit signals are not packaged into signal-mediated ER-derived vesicles.

Detergent insolubility of GPI-anchored proteins in the ER and ER-derived vesicle fractions

GPI-anchored proteins are known to be incorporated into DRM fractions in the ER in yeast [19]. In order to examine the correlation between partitioning into the DRM fraction and protein sorting in the ER, we examined detergent insolubility of Gas1TMD

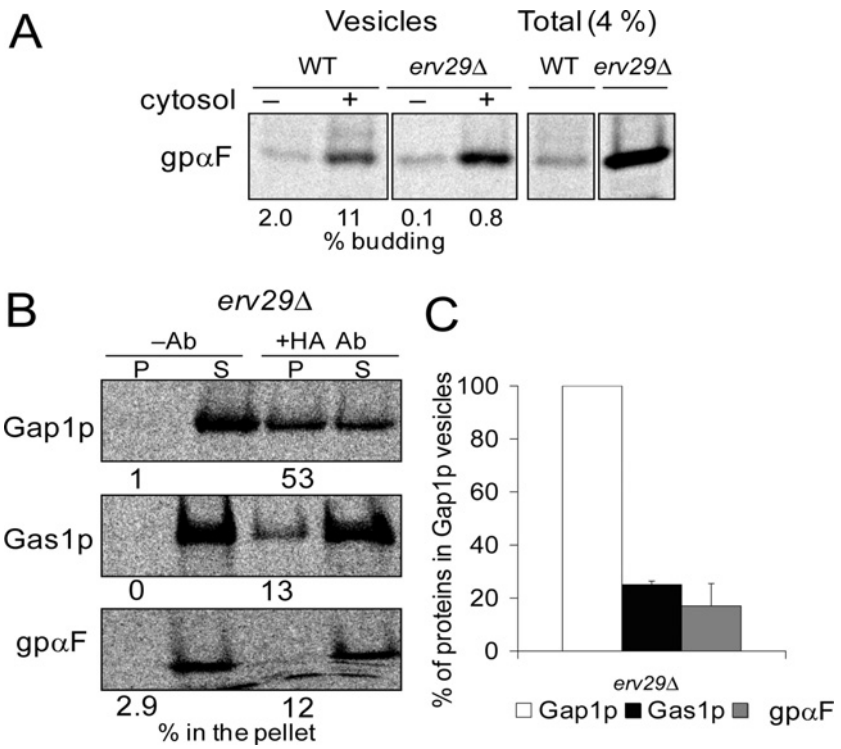

Figure 4 In the absence of Erv29p, gpαF is no longer incorporated into Gap1p-containing vesicles

(**A**) *In vitro* budding assay using semi-intact cells derived from RH2874 (WT) and RH6153 (*erv29Δ*) cells expressing wild-type Gas1p and HA-tagged Gap1p was performed in the presence or absence of *sec18* cytosol. The samples were analysed as in Figure 2. Total fraction corresponds to 4% of input. (**B**) Vesicles generated from *erv29Δ* cells were immunoisolated with or without monoclonal anti-HA antibody. (**C**) Quantification was carried out as in Figure 2; $n = 3$.

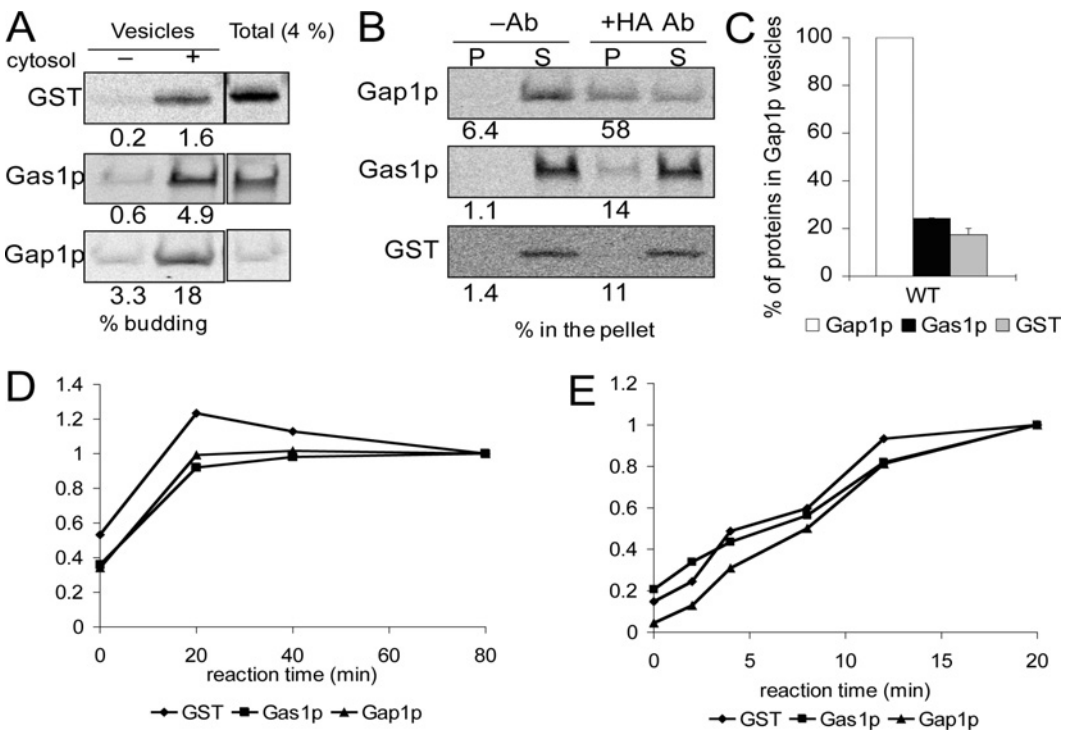

Figure 5 An exogenous naive protein is sorted away from Gap1p-containing vesicles

(**A**) *In vitro* budding assay using semi-intact cells derived from RH2874 (WT) cells expressing GSTTMD together with wild-type Gas1p and HA-tagged Gap1p was performed in the presence or absence of *sec18* cytosol. The samples were analysed as in Figure 2. (**B**) Vesicles generated in (**A**) were immunoisolated with or without monoclonal anti-HA antibody. (**C**) Quantification was carried out as in Figure 2; $n = 2$. (**D**, **E**) Kinetics of *in vitro* budding of GSTTMD, Gas1p and Gap1p. *In vitro* budding assay was performed as in (**A**) for the indicated time at 30 °C. Budding efficiencies of the cargo proteins at each time point were plotted as a fraction of that found at the end of the time period.

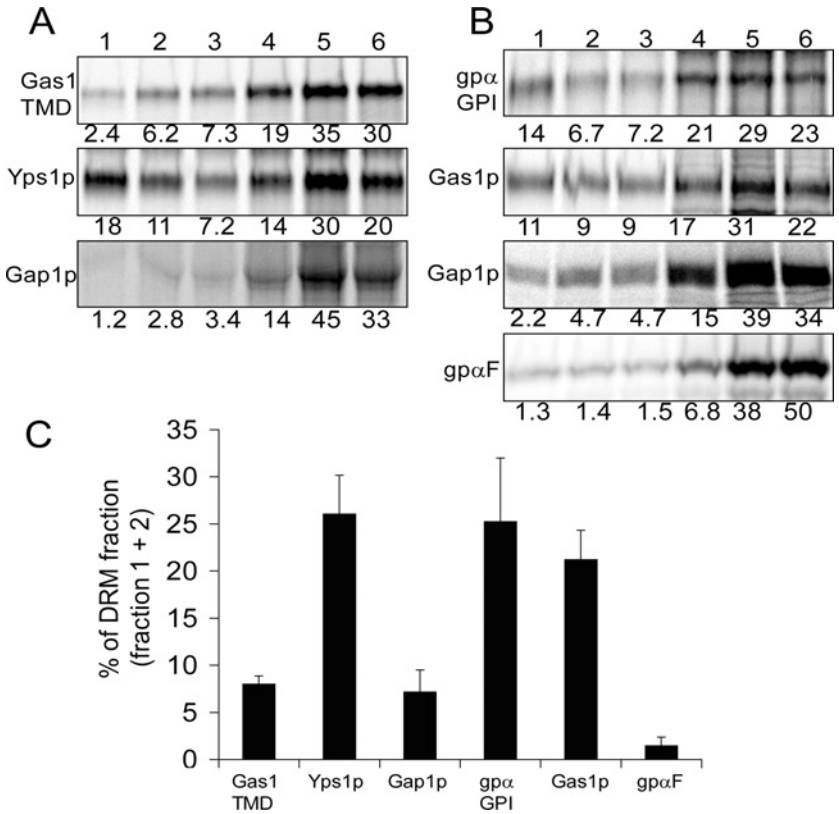

Figure 6 The GPI anchor is a determinant for DRM partitioning of proteins

DRM isolation was performed using pulse-labelled RH5240 (*gas1Δ, sec18*) cells expressing Gas1TMD together with HA-tagged Gap1p (**A**) and pulse-labelled RH4913 (*sec18*) cells expressing prepro αGPI together with HA-tagged Gap1p (**B**). Fractions 1–6 were collected from the top of OptiPrep gradients and analysed by immunoprecipitation. Total recovery, fractions 1–6, was set to 100 %. Numbers represent percentage of recovery in each fraction. (**C**) Bars for each protein represent the means for percentage recovered in the DRM fraction (fraction 1 plus 2) of several independent experiments; $n = 2–5$.

and gpαGPI in the ER using previously described techniques [19]. To detect newly synthesized proteins in the ER, we used *sec18* cells, which show a block in all ER-to-Golgi transport, pulse-labelled with [^{35}S]methionine and [^{35}S]cysteine. The total protein extract was treated with 1 % Triton X-100 at 4 °C for 30 min. The detergent-treated protein fraction was subjected to flotation in an OptiPrep gradient by ultracentrifugation. The DRM fraction floats into the upper two fractions [19]. Concerning the two endogenous GPI-anchored proteins, Yps1p and Gas1p, more than 20 % of the pulse-labelled proteins are partitioned into DRM (Figure 6) as reported previously [19]. Similar to endogenous GPI-anchored proteins, 20.7 % of gpαGPI was partitioned into the DRM fraction in contrast with 2.7 % of endogenous gpαF (Figures 6B and 6C). In contrast, a significantly lower amount of Gas1TMD (8.6 %) was partitioned into the DRM fraction similar to transmembrane proteins, Gap1p (4–7 %) (Figures 6A and 6C). These results demonstrate that a GPI anchor determines partitioning into the DRM fraction in the ER. Based on the sorting results described above (Figures 2 and 3), it seems that DRM partition in the ER does not show any correlation with protein sorting upon ER exit, at least concerning these mutant proteins. Next we examined the detergent insolubility of GPI-anchored proteins in *in vitro* produced ER-derived vesicles (Figure 7). Because of the low signal intensity in the vesicle fractions, we incubated the vesicle fraction with cold Triton X-100 and separated the extracts by ultracentrifugation into supernatant and pellet fractions, the latter corresponding to the DRM fraction. Interestingly, in the vesicle fraction, gpαGPI was no longer partitioned into the DRM fraction in contrast with Gas1p, which was still partitioned into the DRM fraction to a similar level as in the ER (Figures 6 and 7). We obtained the same results in *mfα1Δ* cells (Figure 7, *mfα1Δ*), excluding the possibility that interaction with endogenous gpαF in the vesicle fraction is the reason for the loss of the insolubility of gpαGPI in the vesicle fraction. These results show the remarkably different status of two GPI-anchored proteins incorporated into the distinct vesicle populations.

DISCUSSION

We previously reported that Gap1p and gpαF are incorporated into the same vesicle populations and two GPI-anchored proteins are found in a different vesicle population upon ER exit [16]. In the present study, we found that the efficient incorporation of gpαF into Gap1p-containing vesicles requires its ER exit receptor Erv29p. Another protein incorporated into the same vesicle population is pro-ALP (alkaline phosphatase) [16]. Recently, Erv26p has been identified as its ER exit receptor [44]. Therefore we might predict that incorporation of pro-ALP into Gap1p-vesicles also requires Erv26p. Importantly, ER exit of gpαF and pro-ALP is not absolutely dependent on Erv29p and Erv26p respectively [8,44], and bulk flow movements of those precursor proteins from the ER would explain the reduced transport rate in the absence of those potential receptors [7]. It has been reported that α-factor production is absolutely essential for mating of Mat α cells [45]. The fact that Mat α *erv29Δ* cells have only a small

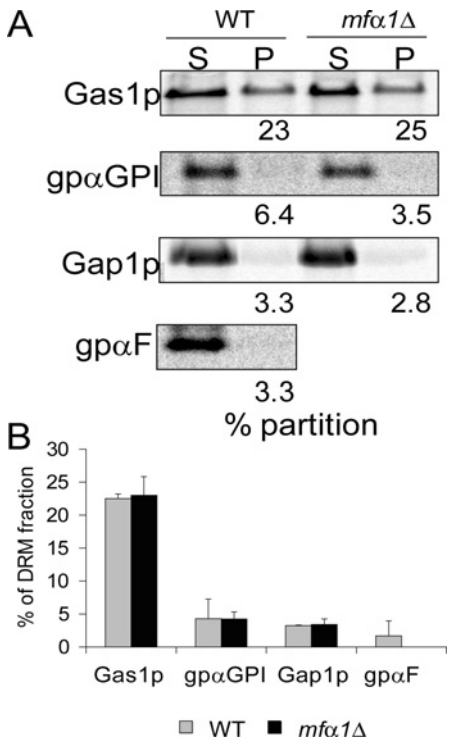

Figure 7 DRM partitioning of gpαGPI is greatly reduced after incorporation into vesicles

(**A**) DRM isolation was performed using an *in vitro* produced ER-derived vesicle fraction derived from RH2874 (WT) and RH6159 (*mfα1Δ*) cells expressing preproαGPI together with wild-type Gas1p and HA-tagged Gap1p in the presence of *sec18* cytosol. The Nycodenz floated vesicle fractions were treated with 1% Triton X-100 and separated by ultracentrifugation. The 'S' corresponds to detergent-solubilized supernatant fraction and 'P' corresponds to detergent-resistant pelletable fraction. % partition, percentage of protein partitioned in the pellets. (**B**) Bars correspond to the percentage of proteins detected in the pellet fraction; $n = 2$.

effect in a quantitative mating test (results not shown) provides *in vivo* evidence that an alternative to receptor-mediated ER exit exists and is functional in yeast. In the present study, we provide biochemical evidence that most of the cargo proteins transported by bulk flow movements, such as gpαF in *erv29Δ* and GSTTMD, are incorporated into vesicle populations different from the signal- and receptor-mediated pathway upon ER exit.

The fact that gpαGPI enters Gap1p-containing vesicles (Figure 3) demonstrates that the proteinaceous signal of gpαF is dominant over a GPI anchor, even though the GPI anchor might have some role in protein exit and sorting from the ER. Both in yeast and mammalian cells, Emp24p/p24 family proteins are required for efficient transport of GPI-anchored proteins from the ER [14,15]. Several lines of evidence suggest that there is a specific mechanism for efficient transport of GPI-anchored proteins from the ER. The transmembrane version of Gas1 proteins showed lower budding efficiency than the GPI-anchored version of Gas1 proteins (Figures 2A and 2B). The gpαGPI protein in the absence of Erv29p budded more efficiently (3.4% in Figure 3A) than the naive transmembrane protein, GSTTMD (1.6% in Figure 5A) or than gpαF in the absence of Erv29p. At present, we cannot test whether or not endogenous GPI-anchored proteins are incorporated into the same vesicle population as various Gas1p mutant proteins or signal-less proteins such as GSTTMD, because GPI-anchored proteins do not contain a cytoplasmic domain, which would permit their specific immunoisolation.

In yeast, GPI-anchored proteins are known to be incorporated into DRM in the ER [19]. We found that Gas1p and gpαGPI are incorporated into the DRM fraction in the ER to a similar extent. The fact that these two proteins enter different vesicle populations in the ER demonstrates that DRM association is not a dominant determinant in the choice of ER-derived vesicles. Interestingly, after incorporation into ER-derived vesicles, gpαGPI no longer partitioned into the DRM fraction in contrast with persistent partition of Gas1p into the DRM in the vesicle fraction. These results demonstrate the different status of the two GPI-anchored proteins in the different vesicle populations. We can put forward several interpretations, which are not mutually exclusive. The efficient budding of gpαGPI upon incorporation into the vesicle fraction depends on Erv29p (Figures 3A and 3B). The tight interaction with Erv29p, which has four TMDs [46], might prevent DRM partitioning of gpαGPI in the vesicle fraction. Alternatively, non-GPI-anchored precursors of gpαGPI, before GPI anchoring in the ER, are exclusively incorporated into the vesicle fraction. We believe that this is unlikely because it was shown that GPI attachment is required for efficient transport and secretion of gpαGPI [42]. Finally, one could think that this difference reflects a distinct lipid and protein environment in different ER-derived vesicle populations. Recently, it has been shown that biosynthesis of GPI-anchored proteins is required for efficient transport of DRM-associated proteins, such as Tat2p and Fur4p from the ER [47] and lipid components of DRM, such as ceramide and ergosterol from the ER in yeast [48]. Together with the present results, we can speculate that a class of ER-derived vesicles carrying endogenous GPI-anchored proteins might contain specific lipids together with proteins that have higher affinity for these lipids. In contrast, signal-mediated Gap1p-containing vesicles might contain a much lower amount of those specific lipids. Further analysis of protein and lipid composition of the different vesicle populations is required to address this hypothesis.

We thank Jan Massner for the initial stage of this study, T.L. Doering, M. Vai, P.O. Ljungdahl and R. Schekman for providing antibody, plasmids and strains and Gisèle Dewhurst, Isabelle Riezman and Brigitte Bernadets for technical help. We thank past and present members of the Riezman laboratory for comments and discussions. This work was supported by the Human Frontiers Science Program through a long-term fellowship (to R.W.) and a research grant (to H.R.) and the Swiss National Science Foundation through a Marie Heim-Vögtlin fellowship (to R.W.) and a research grant (to H.R.).

REFERENCES

1 Lee, M. C., Miller, E. A., Goldberg, J., Orci, L. and Schekman, R. (2004) Bi-directional protein transport between the ER and Golgi. Annu. Rev. Cell Dev. Biol. **20**, 87–123
2 Martinez-Menarguez, J. A., Geuze, H. J., Slot, J. W. and Klumperman, J. (1999) Vesicular tubular clusters between the ER and Golgi mediate concentration of soluble secretory proteins by exclusion from COPI-coated vesicles. Cell **98**, 81–90
3 Barlowe, C. (2003) Signals for COPII-dependent export from the ER: what's the ticket out? Trends Cell Biol. **13**, 295–300
4 Farhan, H., Reiterer, V., Korkhov, V. M., Schmid, J. A., Freissmuth, M. and Sitte, H. H. (2007) Concentrative export from the endoplasmic reticulum of the gamma-aminobutyric acid transporter 1 requires binding to SEC24D. J. Biol. Chem. **282**, 7679–7689
5 Fernandez-Sanchez, E., Diez-Guerra, F. J., Cubelos, B., Gimenez, C. and Zafra, F. (2008) Mechanisms of endoplasmic reticulum export of glycine transporter-1 (GLYT1). Biochem. J. **409**, 669–681
6 Bonifacino, J. S. and Glick, B. S. (2004) The mechanisms of vesicle budding and fusion. Cell **116**, 153–166
7 Malkus, P., Jiang, F. and Schekman, R. (2002) Concentrative sorting of secretory cargo proteins into COPII-coated vesicles. J. Cell Biol. **159**, 915–921
8 Belden, W. J. and Barlowe, C. (2001) Role of Erv29p in collecting soluble secretory proteins into ER-derived transport vesicles. Science **294**, 1528–1531
9 Otte, S. and Barlowe, C. (2004) Sorting signals can direct receptor-mediated export of soluble proteins into COPII vesicles. Nat. Cell Biol. **6**, 1189–1194

10 Kinoshita, T. and Inoue, N. (2000) Dissecting and manipulating the pathway for glycosylphosphatidylinositol-anchor biosynthesis. Curr. Opin. Chem. Biol. **4**, 632–638
11 Field, M. C., Moran, P., Li, W., Keller, G. A. and Caras, I. W. (1994) Retention and degradation of proteins containing an uncleaved glycosylphosphatidylinositol signal. J. Biol. Chem. **269**, 10830–10837
12 Doering, T. L. and Schekman, R. (1996) GPI anchor attachment is required for Gas1p transport from the endoplasmic reticulum in COPII vesicles. EMBO J. **15**, 182–191
13 McDowell, M. A., Ransom, D. M. and Bangs, J. D. (1998) Glycosylphosphatidylinositol-dependent secretory transport in *Trypanosoma brucei*. Biochem. J. **335**, 681–689
14 Muniz, M., Nuoffer, C., Hauri, H. P. and Riezman, H. (2000) The Emp24 complex recruits a specific cargo molecule into endoplasmic reticulum-derived vesicles. J. Cell Biol. **148**, 925–930
15 Takida, S., Maeda, Y. and Kinoshita, T. (2008) Mammalian GPI-anchored proteins require p24 proteins for their efficient transport from the ER to the plasma membrane. Biochem. J. **409**, 555–562
16 Muniz, M., Morsomme, P. and Riezman, H. (2001) Protein sorting upon exit from the endoplasmic reticulum. Cell **104**, 313–320
17 Morsomme, P. and Riezman, H. (2002) The Rab GTPase Ypt1p and tethering factors couple protein sorting at the ER to vesicle targeting to the Golgi apparatus. Dev. Cell **2**, 307–317
18 Morsomme, P., Prescianotto-Baschong, C. and Riezman, H. (2003) The ER v-SNAREs are required for GPI-anchored protein sorting from other secretory proteins upon exit from the ER. J. Cell Biol. **162**, 403–412
19 Bagnat, M., Keranen, S., Shevchenko, A. and Simons, K. (2000) Lipid rafts function in biosynthetic delivery of proteins to the cell surface in yeast. Proc. Natl. Acad. Sci. U.S.A. **97**, 3254–3259
20 Horvath, A., Sutterlin, C., Manning-Krieg, U., Movva, N. R. and Riezman, H. (1994) Ceramide synthesis enhances transport of GPI-anchored proteins to the Golgi apparatus in yeast. EMBO J. **13**, 3687–3695
21 Sutterlin, C., Doering, T. L., Schimmoller, F., Schroder, S. and Riezman, H. (1997) Specific requirements for the ER to Golgi transport of GPI-anchored proteins in yeast. J. Cell Sci. **110**, 2703–2714
22 Watanabe, R., Funato, K., Venkataraman, K., Futerman, A. H. and Riezman, H. (2002) Sphingolipids are required for the stable membrane association of glycosylphosphatidylinositol-anchored proteins in yeast. J. Biol. Chem. **277**, 49538–49544
23 Bagnat, M., Chang, A. and Simons, K. (2001) Plasma membrane proton ATPase Pma1p requires raft association for surface delivery in yeast. Mol. Biol. Cell **12**, 4129–4138
24 Eisenkolb, M., Zenzmaier, C., Leitner, E. and Schneiter, R. (2002) A specific structural requirement for ergosterol in long-chain fatty acid synthesis mutants important for maintaining raft domains in yeast. Mol. Biol. Cell **13**, 4414–4428
25 Umebayashi, K. and Nakano, A. (2003) Ergosterol is required for targeting of tryptophan permease to the yeast plasma membrane. J. Cell Biol. **161**, 1117–1131
26 Hearn, J. D., Lester, R. L. and Dickson, R. C. (2003) The uracil transporter Fur4p associates with lipid rafts. J. Biol. Chem. **278**, 3679–3686
27 Dupre, S. and Haguenauer-Tsapis, R. (2003) Raft partitioning of the yeast uracil permease during trafficking along the endocytic pathway. Traffic **4**, 83–96
28 Malinska, K., Malinsky, J., Opekarova, M. and Tanner, W. (2004) Distribution of Can1p into stable domains reflects lateral protein segregation within the plasma membrane of living *S. cerevisiae* cells. J. Cell Sci. **117**, 6031–6041
29 Malinska, K., Malinsky, J., Opekarova, M. and Tanner, W. (2003) Visualization of protein compartmentation within the plasma membrane of living yeast cells. Mol. Biol. Cell **14**, 4427–4436
30 Opekarova, M., Malinska, K., Novakova, L. and Tanner, W. (2005) Differential effect of phosphatidylethanolamine depletion on raft proteins: further evidence for diversity of rafts in *Saccharomyces cerevisiae*. Biochim. Biophys. Acta **1711**, 87–95
31 Gaigg, B., Toulmay, A. and Schneiter, R. (2006) Very long-chain fatty acid-containing lipids rather than sphingolipids *per se* are required for raft association and stable surface transport of newly synthesized plasma membrane ATPase in yeast. J. Biol. Chem. **281**, 34135–34145
32 Goldstein, A. L. and McCusker, J. H. (1999) Three new dominant drug resistance cassettes for gene disruption in *Saccharomyces cerevisiae*. Yeast **15**, 1541–1553
33 Wach, A., Brachat, A., Pohlmann, R. and Philippsen, P. (1994) New heterologous modules for classical or PCR-based gene disruptions in *Saccharomyces cerevisiae*. Yeast **10**, 1793–1808
34 Gatti, E., Popolo, L., Vai, M., Rota, N. and Alberghina, L. (1994) O-linked oligosaccharides in yeast glycosyl phosphatidylinositol-anchored protein gp115 are clustered in a serine-rich region not essential for its function. J. Biol. Chem. **269**, 19695–19700
35 Gari, E., Piedrafita, L., Aldea, M. and Herrero, E. (1997) A set of vectors with a tetracycline-regulatable promoter system for modulated gene expression in *Saccharomyces cerevisiae*. Yeast **13**, 837–848
36 Baker, D., Hicke, L., Rexach, M., Schleyer, M. and Schekman, R. (1988) Reconstitution of SEC gene product-dependent intercompartmental protein transport. Cell **54**, 335–344
37 Salama, N. R., Yeung, T. and Schekman, R. W. (1993) The Sec13p complex and reconstitution of vesicle budding from the ER with purified cytosolic proteins. EMBO J. **12**, 4073–4082
38 Barlowe, C., Orci, L., Yeung, T., Hosobuchi, M., Hamamoto, S., Salama, N., Rexach, M. F., Ravazzola, M., Amherdt, M. and Schekman, R. (1994) COPII: a membrane coat formed by Sec proteins that drive vesicle budding from the endoplasmic reticulum. Cell **77**, 895–907
39 Caro, L. H., Tettelin, H., Vossen, J. H., Ram, A. F., van den Ende, H. and Klis, F. M. (1997) *In silicio* identification of glycosyl-phosphatidylinositol-anchored plasma-membrane and cell wall proteins of *Saccharomyces cerevisiae*. Yeast **13**, 1477–1489
40 Gentzsch, M. and Tanner, W. (1997) Protein-O-glycosylation in yeast: protein-specific mannosyltransferases. Glycobiology **7**, 481–486
41 Strahl-Bolsinger, S., Gentzsch, M. and Tanner, W. (1999) Protein O-mannosylation. Biochim. Biophys. Acta **1426**, 297–307
42 Doering, T. L. and Schekman, R. (1997) Glycosyl-phosphatidylinositol anchor attachment in a yeast *in vitro* system. Biochem. J. **328**, 669–675
43 Kuehn, M. J., Herrmann, J. M. and Schekman, R. (1998) COPII–cargo interactions direct protein sorting into ER-derived transport vesicles. Nature **391**, 187–190
44 Bue, C. A., Bentivoglio, C. M. and Barlowe, C. (2006) Erv26p directs pro-alkaline phosphatase into endoplasmic reticulum-derived coat protein complex II transport vesicles. Mol. Biol. Cell **17**, 4780–4789
45 Kurjan, J. (1985) Alpha-factor structural gene mutations in *Saccharomyces cerevisiae*: effects on alpha-factor production and mating. Mol. Cell. Biol. **5**, 787–796
46 Foley, D. A., Sharpe, H. J. and Otte, S. (2007) Membrane topology of the endoplasmic reticulum to Golgi transport factor Erv29p. Mol. Membr. Biol. **24**, 259–268
47 Okamoto, M., Yoko-o, T., Umemura, M., Nakayama, K. and Jigami, Y. (2006) Glycosylphosphatidylinositol-anchored proteins are required for the transport of detergent-resistant microdomain-associated membrane proteins Tat2p and Fur4p. J. Biol. Chem. **281**, 4013–4023
48 Kajiwara, K., Watanabe, R., Pichler, H., Ihara, K., Murakami, S., Riezman, H. and Funato, K. (2008) Yeast ARV1 is required for efficient delivery of an early GPI intermediate to the first mannosyltransferase during GPI assembly and controls lipid flow from the ER. Mol. Biol. Cell **19**, 2069–2082
49 Ljungdahl, P. O., Gimeno, C. J., Styles, C. A. and Fink, G. R. (1992) SHR3: a novel component of the secretory pathway specifically required for localization of amino acid permeases in yeast. Cell **71**, 463–478

Received 4 April 2008/6 May 2008; accepted 7 May 2008
Published as BJ Immediate Publication 7 May 2008, doi:10.1042/BJ20080715

III.B- Concentration of GPI-anchored proteins upon ER exit in yeast.

Traffic,submitted

In this work, we looked at the mechanism of concentration of cargo proteins in ER exit sites. In the COPII temperature sensitive allele *sec31-1*, the GPI-anchored protein Cwp2p and the transmembrane protein Hxt1p accumulate in different ER exit sites (ERES). ERES incorporation of Hxt1p depends on the COPII components Sec12p and Sec16p and the ER exit receptor Erv14p. Concentration of Cwp2p prior to budding depends on the inositol deacylase Bst1p. This suggests that remodeling and incorporation of GPI-anchored proteins into ceramide-enriched microdomains might be a prerequisite for GPI-anchored protein concentration. The hypothetical ER exit receptor of GPI-anchored proteins, Emp24p, is not required for concentration of Cwp2p in the ER. However Emp24p is essential for budding of concentrated GPI-anchored proteins, perhaps by linking them to the COPII coat.

Concentration of GPI-anchored proteins upon ER exit in Yeast.

Guillaume A. Castillon, Reika Watanabe, Marcia Taylor, Tatjana M. E. Schwabe and Howard Riezman*

Department of Biochemistry, University of Geneva, Sciences II

30 quai Ernest Ansermet, CH-1211 Geneva, Switzerland.

*Correspondence: Howard.Riezman@biochem.unige.ch Tel. 0041223796469

Running Head: GPI-anchored proteins ER exit in yeast

Key-words: GPI-anchored proteins, ER exit site, Emp24p, Erv14p, COPII, Hxt1p.

Number of characters: 69633

Abstract
Previous biochemical work has revealed two parallel routes of exit from the endoplasmic reticulum in the yeast *S. cerevisiae*, one seemingly specific for GPI-anchored proteins. Using the COPII mutant *sec31-1*, we visualized ER exit sites (ERES) and identified three distinct ERES populations *in vivo.* One contains glycosylated pro-α-factor, the second contains the GPI-anchored proteins Cwp2p, Ccw14p and Tos6p, and the third is enriched with the hexose transporter, Hxt1p. Concentration of GPI-anchored proteins into ERES requires anchor remodeling and incorporation into ERES of Hxt1p requires the Cornichon homologue, Erv14p and the COPII components Sec12p and Sec16p. The p24 family member, Emp24p, is not involved in GPI-anchored protein concentration into ERES, but in the attachment of concentrated GPI-anchored proteins to COPII. Upon budding, Cwp2p and Hxt1p leave the ER into separated vesicles which move with different speeds.

Introduction

Secretory proteins are synthesized and inserted into the endoplasmic reticulum (ER) from where they are transported to their final destinations via the Golgi apparatus. ER to Golgi transport of proteins and lipids is ensured by the assembly of coat protein complex components (COPII) on the ER membrane leading to formation of COPII-coated vesicles (1). GPI-anchored proteins are luminal secretory proteins attached to the inner leaflet of the membrane via a glycosylphosphatidylinositol (GPI) anchor. After the synthesis via the enzymatic reactions of more than 20 gene products, GPI is attached to the C-terminus of newly synthesized GPI-anchored proteins within the ER (2, 3). Then the GPI-anchored proteins are remodeled; the primary lipid moiety of the anchor consisting of diacylglycerol after synthesis is replaced in the ER by either a diacylglycerol with a C26 in the sn2 positon or more frequently by ceramide consisting of C18:0 phytosphingosine and a C26:0 fatty acid in yeast (2, 3). The remodeling confers to GPI-anchored proteins the property to associate with detergent-resistant membranes (DRM), which is postulated to reflect the enrichment of GPI-anchored proteins into specialized membrane domains. Any defect in the enonced steps induces a delay in GPI-anchored protein maturation, likely by preventing efficient ER exit (4-6). In mammalian cells, the remodeling event occurs in the Golgi compartment resulting in alkyl-acylglycerol or diacylglycerol with a saturated stearic acid in sn-2 position (7). In mammalian cells, GPI-anchored proteins associate with microdomains in the Golgi and not in the ER in contrast to yeast. Therefore remodeling of GPI-anchored proteins does not affect their transport from the ER to the Golgi in mammalian cells (8).

In yeast, GPI-anchored proteins are transported from the ER to the Golgi apparatus in distinct vesicles from other secretory proteins (9). One ER-derived vesicle population contains the glycosylated proα-factor (gpαF), the general amino acid permease, Gap1p, and alkaline phosphatase. The other vesicle population contains at least two GPI-anchored proteins, Gas1p and Yps1p. However, this data has been principally generated by biochemical means using cell fractionation techniques *in vitro*. Moreover, little is known about the mechanisms responsible for cargo sorting into different vesicles. The presence of an hydrophobic ER exit signal on gpαF appears essential for gpαF to enter into Gap1p-containing vesicles and artificially GPI-anchored gpαF is still sorted into Gap1p-containing vesicles, suggesting that the ER exit signal is the determinant for protein sorting (10). In mammalian cells, such sorting has been observed upon Golgi exit. Earlier events were visualized after a 15°C block and VSVG and GFP-GPI colocalized at the ERGIC(11), a compartment without a clear equivalent in yeast.

In the present study, we have developed new tools that allow us to investigate early steps of the secretory pathway by live fluorescent imaging techniques. In combination with the use of a thermosensitive allele of the COPII component Sec31p, we identified three different types of ER exit sites (ERES), which differ by the type of cargo they concentrate and export out of the ER. One ERES population concentrates the soluble glycosylated pro-α-factor. Another ERES population carries Hxt1p, for which we have not yet identified additional cargo proteins. The third ERES population ensures the ER export of the GPI-anchored proteins Cwp2p, Ccw14p and Tos6p. Furthermore, we revealed some possible components of the concentration mechanism into ERES including the inositol deacylase Bst1p, the COPII components Sec12p and Sec16p and the Cornichon homologue Erv14p. Indeed, GPI-anchored protein incorporation into ERES specifically requires Bst1p in contrast to transmembrane proteins, whose ERES entry is generally Sec12p/Sec16/Erv14p-dependent. Futhermore, we investigated the implication of the potential GPI-anchored protein ER exit receptor Emp24p for concentration into ERES.

Results

At 37°C in *sec31-1* cells, the GPI-anchored protein Cwp2p and the hexose transporter Hxt1p localize to ER exit sites (ERES).

In *S. cerevisiae*, hexoses are transported by facilitated diffusion via 20 different hexose transporters, members of the major facilitator superfamily (12). The presence of ER exit signals in the C-termini of other permeases, such as the di-acidic motif found in Gap1p and Can1p, appears to be crucial for their efficient ER exit (13, 14). We noticed a potential di-aromatic (FY) ER exit signal in the C-terminus of the hexose transporter Hxt1p. In order to prevent any disturbance of Hxt1p ER exit, we fused the CFP variant Cerulean or the YFP variant Venus to the N-terminus of Hxt1p. These fluorescent fusions are seen at the cell surface and in the vacuole in WT cells (Fig. 1A), similar to the endogenous protein (15). Cwp2p has previously been described as a cell wall GPI-anchored protein (16). Cwp2p fused with Venus or Cerulean (CFP) after its signal sequence localizes to the cell surface in WT cells (Fig. 1A). From our biochemical experiments we postulated that cargo protein sorting upon ER exit would occur before the vesicle scission event. Sec31p is part of the COPII coat, and assembles with Sec13p onto the pre-budding complex formed by Sar1p, Sec23p and Sec24p, in order to cage nascent ER-derived vesicles (17-20). After one hour at 37°C, a temperature at which the thermosensitive *sec31-1* cells display a strong ER exit block without strongly compromising growth, CFP-Hxt1p and Cwp2-CFP were found in dot-like structures (Fig. 1C, 1E, S1B-C). In *sec31-1* at 37°C, cargo proteins appear in dots, presumably concentrated and loaded by the pre-budding complex, but unable to bud from the ER. Interestingly the localization of the COPII component Sec13p does not appear to be disturbed in *sec31-1* at 37°C, compared to WT cells (Fig. 1B). To further characterize these dots, we investigated whether CFP-Hxt1p and Cwp2-Venus colocalized with Sec13-GFP, which would be consistent with their localization in ER exit sites (ERES) (21, 22). Since the CFP-Hxt1p and Cwp2-CFP signals leak into the GFP channel (Fig. S1A-C), we visualized the co-localization with Sec13-GFP by acquiring fluorescence in the CFP and the YFP channels. Moreover, even though the dots can be visualized on raw images we deconvoluted the images and enhanced the contrast in order to highlight the dots, when co-localization was required during the study. After deconvolution, 82% of the Cwp2-CFP dots and 86% of the CFP-Hxt1p co-localized with Sec13-GFP in *sec31-1* at 37°C (Fig. 1C-F). Similar results were obtained with Hxt1p fused C-terminally with CFP (data not shown).

Next, we determined if the *sec31-1* phenotype is reversible. After the shift to 37°C, the cultures were incubated at 24°C. After 20 minutes, more than 50% of the dots no longer colocalized with Sec13-GFP suggesting that under these conditions the cargo proteins were able to exit ER (Fig. 1G-H). The observed dots did not result from endocytosis, since they colocalized minimally with FM4-64 at 37°C (5% for Cwp2-Venus, 20% for CFP-Hxt1p) or 20 minutes after reestablishment of the permissive temperature (10% for Cwp2-Venus, 30% for CFP-Hxt1p) (data not shown). We have determined that the dot-like structures observed for fluorescent Hxt1p and Cwp2 were not the result of protein aggregation. Analysis of the aggregation state of CFP-Hxt1p and Cwp2-Venus by Blue-Native PAGE shows the same pattern in WT and *sec31-1* cells at 37°C (data not shown).

In *sec31-1* at 37°C, Cwp2p and Hxt1p are sorted into different ERES.

Next, we quantified the co-localization of Cwp2-Venus and CFP-Hxt1p at ERES in *sec31-1* at 37°C (Fig. 2). Cwp2-Venus dots and CFP-Hxt1p dots co-localized only minimally (23%±12%) (Fig. 2A-B). As a control, we confirmed that two different fluorescent versions of the same cargo protein co-localized substantially. In *sec31-1* cells at 37°C, Cwp2-CFP and Cwp2-Venus co-localized (82%±4%) (Fig. 2C-D) and CFP-Hxt1p and Venus-Hxt1p co-localized (75%±9%) (Fig. 2E-F). It is possible that ERES are highly mobile *in vivo* and this could cause an underestimation of the co-localization due to movement between acquisition in the first channel and acquisition in the second channel. We quantified the co-localization of CFP-Hxt1p and Cwp2-Venus in 4% paraformaldehyde fixed cells (Fig. S2A). Again the two cargo proteins co-localized only minimally (22%±8%) (Fig. S2B). We have previously shown that Gap1p and Gas1p are mis-sorted upon ER exit in the v-SNARE mutant *bos1-1* (23). We assayed the localization of CFP-Hxt1p and Cwp2-Venus in *bos1-1* at 37°C. Both cargoes accumulate in dot-like structures (Fig. S2C). Cwp2-Venus and CFP-Hxt1p strongly co-localized in *bos1-1* at 37°C (Fig. S2D). But the morphology suggests that the cargoes accumulate in structures different that ERES. Taken together, these results show that Hxt1p and Cwp2p are sorted into distinct ERES upon ER exit.

The hexose transporter Hxt1p is sorted into a third population of ER-derived Vesicles.

Next, we examined biochemically whether fluorescently tagged Cwp2p and Hxt1p enter into different ER-derived vesicles. Using an *in vitro* budding assay which reconstitutes ER-derived vesicle formation using exogenous cytosol and pulse-labeled semi-intact cells (9), we determined that the ER budding of Venus-Hxt1p and Cwp2-Venus was cytosol-dependent even though it was rather inefficient compared to Gap1p (Fig. 3A-B). In order to disprove that the ER-derived vesicles produced in this assay result from ER fragmentation, we quantified the amount of an ER resident protein, Sec61p, found in the vesicle fraction (Fig. 3C). Clearly, the cargo proteins are incorporated into the ER-derived vesicles in a selective and concentrative manner. We next examined whether Hxt1p and Cwp2p were incorporated into distinct vesicle populations. Using the *in vitro* ER-derived vesicles from cells expressing CFP-Hxt1p and Cwp2-Venus, we precipitated the majority of CFP-Hxt1p-containing vesicles with a polyclonal anti-Venus antibody, which recognizes the different variants of GFP. Under these conditions only a small fraction of Cwp2-Venus was found in the pellet fraction (Fig. 3D, G). These results demonstrate that two cargo

proteins, which accumulated in different ERES, are indeed incorporated into different ER-derived vesicles *in vitro*. The fact that Cwp2p-Venus was not precipitated by Venus antibody also provides evidence for the intact nature of Cwp2p-Venus-containing vesicles because the lumenal Venus was not accessible to the antibody. In the same experiment, endogenous Gap1p was not co-precipitated with CFP-Hxt1p-containing vesicles, suggesting that the two proteins are not incorporated into the same ER-derived vesicles. We also confirmed that Cwp2-Venus was not incorporated into the Gap1p-HA-containing vesicles (Fig. 3E,H) as previously shown for other GPI-anchored proteins such as Gas1p and Yps1p (9), and Tos6p and Ccw14p (data not shown). Next, using cells expressing Gap1p-HA and Venus-Hxt1p, we confirmed that Gap1p and Hxt1p were indeed incorporated into the different ER-derived vesicles by vesicle immunoisolation using anti-HA antibody or anti-Venus antibody, (Fig. 3F,I). The GPI-anchored protein Gas1p was not precipitated by either antibody.

Altogether, these results suggest that at least three different populations of vesicles are generated upon ER budding. The first population of vesicles carries Gap1p, gpαF, and alkaline phosphatase (9, 10), all containing identified ER exit signals. The second population contains Hxt1p and the third population contains the GPI-anchored proteins Gas1p, Yps1p, and Cwp2p.

GPI-anchored proteins are concentrated into the same ERES *in vivo*.

Using our *in vitro* sorting assay, we repeatedly observed that GPI-anchored proteins such as Gas1p, Cwp2p (Fig. 3), Ccw14p and Tos6p (data not shown) were excluded from the Gap1p-containing vesicles and Hxt1p-containing vesicles. Because GPI-anchored proteins are exclusively luminal, we could not prove through immunoisolation that GPI-anchored proteins exit the ER in the same vesicle population. To address this point, we fused two other GPI-anchored proteins Ccw14p (YLR390W-A) and Tos6p (YNL300W) (24, 25) with Venus and co-expressed them with Cwp2-CFP in *sec31-1* at 37°C (Fig. 4A, C). In this manner, we could observe that Cwp2-CFP and Ccw14-Venus are found in the same ERES (92%±7%) (Fig. 4B) and Cwp2-CFP and Tos6-Venus co-localize at the ERES (83%±14%) (Fig. 4D). These results suggest that most, if not all, GPI-anchored proteins leave the ER in the same ER-derived vesicle population.

Cargo proteins incorporated into different ER-derived vesicles accumulate in different ERES.

Next we tried to examine whether Cwp2p or Hxt1p are found in the ERES corresponding to ER exit signal-dependent vesicles, such as Gap1p containing vesicles. We looked at gpαfactor, which is preferentially incorporated into Gap1p-containing vesicles (10), since Gap1-GFP failed to accumulate into ERES in *sec31-1* at 37°C(data not shown). In *sec31-1* cells at 37°C, a minority of Cwp2-CFP and ye-citrine-tagged gpαfactor (yECgpαF) co-localized (38%±15%) (Fig. 4E-F). Similarly, a minority of CFP-Hxt1p and yECgpαF co-localized (32%±15%) (Fig. 4G-H). These data show that the majority of yECgpαF was segregated from Cwp2p and Hxt1p containing ER exit sites *in vivo*.

In contrast to Hxt1p, Cwp2p does not require COPII for concentration.

Next we wanted to investigate the COPII requirement for the incorporation of cargoes into ERES. Sec12p is an ER-bound transmembrane GEF of Sar1p, involved in the initiation of the COPII coat assembly (26, 27). Sec16p has been described as the organizer of the ERES (28, 29). In *sec12-4* cells, the number of Sec13-GFP dots is strongly reduced at 37°C and in *sec16-2* cells, the distribution of Sec13-GFP is different than the one observed in WT cells at 37°C (Fig. 5B) (30). Indeed the size of the Sec13-GFP dots tends to be more heterogenous in *sec16-2* cells and the perinuclear ER localization of the Sec13-GFP dots is less obvious compared to WT cells. In contrast to *sec31-1*, in *sec12-4* and in *sec16-2* to a lower extent, CFP-Hxt1p cannot accumulate into dots (Fig. 5A, C-D). Surprisingly in these mutants the GPI-anchored protein Cwp2p is still present in dot-like strutures in similar proportion as seen in *sec31-1* (Fig. 5A, C-D). It appears that both cargoes require COPII coat to exit the ER, but Cwp2p does not require the early components of the COPII machinery in order to be concentrated. However since Sec13p localization is strongly affected in *sec12-4* and *sec16-2*, it is not clear whether the dot-like structures observed in these mutants can be assimilated to ERES. Among the *sec16-2* cells in which we could still observe dots of Hxt1p, we quantified the co-localization of CFP-Hxt1p and Cwp2-Venus. In these cells, more than 60% of the Hxt1p dots co-localized with Cwp2p dots (Fig. 5E-F). This result suggests that COPII or at least Sec16p is important for sorting upon cargo concentration.

Cwp2p requires remodeling to be concentrated into ERES.

Early during the GPI anchor synthesis, inositol is acylated by Gwt1p. After the transamidase attachs the GPI-anchor to the protein, Bst1p removes the acyl chain from the inositol, and the GPI-anchored proteins can be remodeled (5). In *bst1Δ* cells, GPI-anchored proteins are not remodeled, fail to associate with DRMs and their ER exit is delayed (5) (Fig. 6A-B). To examine concentration into ERES, we constructed the double mutant *bst1Δsec31-1*, and observed the capacity of Cwp2p to accumulate into dot-like structures. In the double mutant at 37°C, Cwp2p did not localize into dots in contrast to Hxt1p (Fig. 6A, C-D). From this result, we can hypothesize that remodeling and perhaps DRM association are required for concentration of GPI-anchored proteins into ERES.

ER export of Cwp2p and Hxt1p are defective in *emp24Δ* and *erv14Δ* cells respectively.

Next, we investigated the implication of potential ER exit receptors for incorporation into ERES. Emp24p is a member of the p24 family (31). The p24 proteins assemble into heteromeric complexes that continuously cycle between ER and Golgi (32-35). Transport of Gas1p is delayed in *emp24Δ* cells and budding of Gas1p is defective (36). Erv14p was identified on COPII-coated vesicles and cycles between ER and Golgi compartments (37, 38). It is also highly conserved throughout evolution. The

Drosophila melanogaster homologous protein, Cornichon, is required for efficient ER export of the growth factor α-like signaling molecule Gurken (39-41). The human homologue, CNIH4 plays a role in the transport of the transmembrane protein tsO45G to the cell surface by RNAi screening (42). In yeast, *erv14Δ* cells display ER retention of the transmembrane secretory proteins Axl2p and Sma2p (37, 43). In *emp24Δ* cells, Cwp2-Venus but not Venus-Hxt1p nor Gap1-GFP, accumulated in perinuclear ER. In *erv14Δ* cells, Venus-Hxt1p and Gap1-GFP were specifically retained in the ER (Fig. 7A, C). Using the *in vitro* budding assay, we observed that Cwp2-Venus budding was specifically reduced using *emp24Δ* spheroplasts, whereas its budding was unaffected in *erv14Δ* cells (Fig. 7D-E). On the other hand, Venus-Hxt1p and Gap1-GFP budding was strongly reduced in *erv14Δ* cells specifically. To better understand the specificity of Emp24p and Erv14p for cargo export from the ER, we looked at the localization of various cargo proteins in *emp24Δ* cells and *erv14Δ* cells. In *emp24Δ* cells, the GPI-anchored protein Ccw14p was retained in the ER (Fig. 7B-C). Hxt2p is a high affinity hexose transporter that shares 67% identity with Hxt1p, but does not exhibit any known ER exit signal within its C-terminus. Mid2p is a single transmembrane protein that senses cell wall integrity. ER exit of Hxt2p and Mid2p was defective in *erv14Δ* cells (Fig. 7B-C). Pma1p is a plasma membrane H^+-ATPase. Interestingly, Pma1p ER export did not depend on either Emp24p or Erv14p (Fig. 7B-C). With the exception of Pma1p, it appears that most transmembrane proteins depend on Erv14p for efficient ER export, whereas the ER exit of GPI-anchored proteins depends on Emp24p. As postulated by others, Emp24p and Erv14p might be ER exit receptors. They bind to cargoes and are found in COPII coated vesicles. Moreover absence of Emp24p or Erv14p does not affect Sec13-GFP localization (Fig. 8A). We constructed the double mutants *emp24Δsec31-1* and *erv14Δsec31-1*. Even though slightly affected, Cwp2-Venus was localized into dot-like structures in *erv14Δsec31-*1 at 37°C, whereas Hxt1p failed to concentrate in ERES (Fig. 8B-D). Surprisingly Cwp2-Venus was concentrated into dot-like structures in *emp24Δsec31-1* at 37°C (Fig. 8B-D). Altogether these results support the conclusion that Erv14p is the ER exit receptor for a certain number of transmembrane proteins. Concerning Emp24p, it appears that it is not essential for GPI-anchored protein concentration.

Cargo protein ER exit in *sec31-1* cells

As observed in figure 1G-H, around 80% of Cwp2-Venus and CFP-Hxt1p co-localized with Sec13-GFP at 37°C. Twenty minutes after the shift around 30% of both cargoes remained co-localized with ERES. This amount decreased to levels lower than 20% after one hour at 24°C. From these results, it seems that Sec31p recovered most of its function within the first 20 minutes at permissive temperature and that the ER exit kinetics of Cwp2p and Hxt1p appear to be similar. Next, we looked at the fate of Cwp2p and Hxt1p after ER exit. We incubated the *sec31-1* mutant at 37°C for 1 hour, shifted the cultures to 24°C and acquired movies at the rate of one image per 20 seconds during the first 8 minutes and examined the co-localization of Cwp2-Venus with CFP-Hxt1p and Cwp2-CFP with Ccw14-Venus (movies 1-2, Fig. 9A). We could observe that Cwp2-Venus and CFP-Hxt1p remained separated throughout the experiment and that the two GPI-anchored proteins Cwp2-CFP and Ccw14-Venus moved in the same dot-like structures. From the previous experiments, we know that sorting occurs prior to ER budding. This result suggests that the two cargoes remained sorted after ER budding. We obtained similar results when we acquired movies 10 or 20 minutes after the temperature shift to 24°C (data not shown).

Finally, we estimated the average speed of the different dots acquired in the movie 1 (Fig. 9B). In the first 8 minutes after the shift to 24°C, the CFP-Hxt1p dots were more mobile than the Cwp2-Venus dots. It is important to note that the speeds measured in these movies should not be considered as absolute values. In movies acquired with one image every 5 seconds (data not shown), the speeds calculated were two times superior to the ones displayed in Fig. 9B, but the ratio of the speed of Hxt1p dots to the speed of Cwp2p dots was conserved. Furthermore, some of the CFP-Hxt1p dots were occasionally so mobile that it became impossible to track them, leading to an underestimation of the average speeds.

These results demonstrate that Cwp2p and Hxt1p bud from distinct ERES and remain separate for some time afterwards.

DISCUSSION

Using microscopy to complement biochemical techniques, we identified three different types of ER exit sites (ERES), which differ by the type of cargo they concentrate and export out of the ER. One ERES population concentrates the soluble glycosylated pro-α-factor. Another ERES population carries Hxt1p. The third ERES population ensures the ER export of the GPI-anchored proteins Gas1p, Yps1p, Cwp2p, Ccw14p and Tos6p. The targeting of cargoes to different ERES required different machineries: one involving the COPII coat and the ER exit receptor Erv14p for transmembrane proteins, and one requiring GPI anchor remodeling for the GPI-anchored proteins.

ER-to-Golgi transport has been extensively studied in mammalian cells using light microscopy techniques, whereas in yeast biochemical approaches have been preferred. To obtain a more complete image of ER exit in yeast and to confirm our previous results about GPI-anchored protein sorting, we decided to develop light microscopy tools for yeast. Distinct advantages were obtained by visualization of the ER exit sites by a 15°C block in mammalian cells. In yeast, we did not observe such temperature dependence in wild-type cells (data not shown). So we decided to use the thermosensitive allele of the COPII component Sec31p. We reasoned that since it is part of the last COPII component to assemble onto the COPII coat, its non-functionality might not strongly disturb the assembly of the prebudding complex. In this way, the cargoes should be concentrated and bound to the prebudding complex at the ERES. It appeared that was the case at least for some cargo proteins.

Before going into this further, it is useful to discuss the microscopy techniques used. First, we had to choose between acquisition of live images or images of fixed cells. Acquisition from fixed cells has the advantage of fully controlling the timing and the temperature of the experiment, and provides more flexibility about acquisition exposure time, since the structures do not move. However, fixation has the tendancy to destroy the structures. After trying several fixation protocols, the 4% PFA fixation allowed us to visualize cargoes at ERES. However, this observation was true for only a small percentage of cells as the ERES was destroyed in most of the cells. For this reason, we decided to focus on live cell imaging. The limiting factors were the fluorescent signal, bleaching and the movement of the dots. We used two types of microscopes: a conventional fluorescence microscope or a confocal microscope. Confocal microscopy tends to display an image with a better signal to noise ratio compared to a conventional fluorescence microscopy. However the use of laser tends to increase the bleaching of the signal and in the case of the confocal microscopes available in our university the acquisition speed was too long for live co-localization studies of the ERES. For these reasons, we compromised by using conventional fluorescence microscopy, where acquisition can be done quickly with signals strong enough to allow the visualization of the ERES. To improve the signal to noise ratio, we used a 10 iterations blind deconvolution for the co-localization studies.

The best proof that the cargoes are indeed concentrated into ERES in *sec31-1* at 37°C is illustrated by their co-localization with the ERES marker Sec13-GFP. Moreover the dots do not colocalize with FM4-64 (fluorescent dye which labels endocytic membranes), excluding that these dots are derived from endocytosis (data not shown). We have tried different FM4-64 incubation protocols: adding the dye before the incubation at 37°C, during the incubation at 37°C, or with continous incubation with FM4-64 starting before the incubation at 37°C and washout just before the acquisition. In these experiments, there was no noticeable endocytosis defect, and no enrichment of cargoes into endocytic membranes. Considering the function of Sec31p in assembly of the COPII coat, it is surprising that in *sec31-1* there is no detectable defect in Sec13-GFP localization at 37°C. The restrictive temperature of *sec31-1* is 38°C. At 37°C, *sec31-1* cells grow more slowly than wild-type cells, but there is no striking increase in mortality. So in *sec31-1* at 37°C, there is still a sufficient amount of functional Sec31p for viability, but the Sec31p limitation seems to slow down the ER budding process rather than totally blocking the ER-derived vesicle formation. In this manner we were able to observe cargoes molecules accumulated in ERES. In our experiments, we have counted around 20 Sec13-GFP dots, which is substantially less than the 30 to 50 dots observed previously (22). We explain this difference by the difference in acquisition method. The 30 to 50 dots were quantified after 3D acquisition and Z-projection; in our experiment we counted 20 dots from a single 2D acquisition. One reason to visualize the accumulation of cargo in ERES *in vivo* was to confirm our previous results obtained using an *in vitro* budding assay (9). Previously, we observed that GPI-anchored proteins and non-GPI-anchored proteins are incorporated into different ER derived vesicle populations produced after addition of exogenous cytosol on pulse-labelled semi-intact cells. To provide confidence that the *in vitro* assay using crude cytosol reproduces faithfully the *in vivo* situation, we controlled that the ER resident protein Sec61p was not incorporated into ER-derived vesicles, ruling out ER fragmentation as a mechanism for vesicle generation in the assay. Moreover we observed that we could precipitate the Hxt1p containing vesicles using an anti-Venus antibody which recognizes Venus or CFP exposed at the cytoplasmic side of the vesicle. In the same assay, Cwp2-Venus, whose Venus tag is found on the luminal side of the vesicle, was not immunoprecipitated, reflecting the intactness of the produced ER-derived vesicles. One other argument against ER fragmentation is illustrated by the specific requirements of the different cargoes upon ER budding. Indeed Cwp2p budding requires Emp24p whereas Hxt1p requires Erv14p *in vivo* and *in vitro*. In this situation it is difficult to imagine that ER fragmentation leads to the specific formation of Hxt1p-containing vesicles in *emp24Δ* spheroplasts and to the generation of Cwp2p-containing vesicles in *erv14Δ* spheroplasts. Even though both approaches used here (biochemical and light microscopy) have their own weaknesses, both tend to demonstrate the same phenomena, which is that

GPI-anchored proteins and non-GPI-anchored proteins are incorporated into different ERES leading to the formation of different ER-derived vesicle populations in yeast.

We have further characterized the requirement of COPII, Erv14p, Emp24p and Bst1p for cargo concentration and sorting at the level of ERES (Fig. 10). GPI-anchored proteins and non-GPI-anchored proteins studied here required COPII to exit the ER, illustrated by their ER retention observed in *sec31-1*, *sec12-4* and *sec16-2*. However differences can be observed if we focus on the capability of cargoes to concentrate into specific ER domains. Indeed in *sec12-4* and *sec16-2*, Hxt1p was localized homogenously throughout the ER, whereas Cwp2p still displayed a punctate pattern. Since there is a disturbance of the Sec13-GFP pattern in such mutants, it is not clear whether the punctate pattern of Cwp2p reflects an accumulation into ERES or another ER domain. Nevertheless, this still implies that non-GPI-anchored proteins require COPII coat for proper concentration, whereas GPI-anchored protein concentration seems to depend upon another mechanism.

Erv14p has been postulated to be an ER exit receptor for Sma2p and Axl2p. Here we showed that it influences the ER exit of several other transmembrane proteins, such as Hxt1p, Hxt2p, Gap1p and Mid2p. In *sec31-1erv14Δ* cells, Hxt1p did not localize to ERES, suggesting that the concentration of Hxt1p to the ERES depends on Erv14p, presumably via binding to COPII. Interestingly, in the few *sec16-2* cells where Hxt1p was still concentrated into dots, we observed a sorting defect with Cwp2p. This suggests that COPII, or at least Sec16p, and presumably Erv14p are determinants for sorting by concentrating Hxt1p to sites from which Cwp2p is excluded or simply not concentrated. Gap1p is one of the proteins that require Erv14p. This is interesting for two reasons. First, we found Hxt1p and Gap1p incorporated into different ER-derived vesicles. This might suggest that Erv14p is not required for sorting between Hxt1p and Gap1p, but for sorting between GPI-anchored proteins and non-GPI-anchored proteins. Second, Gap1p contains a di-acidic motif in C-terminus, known to be an ER exit signal that allows direct binding of Gap1p to Sec24p. If Gap1p can be tightly associated to COPII via its diacidic motif, why is Erv14p required for efficient ER exit? As illustrated by the difference in budding efficiencies of Gap1p and Hxt1p (for which no ER exit signal has been identified so far), the presence of an ER exit signal confers a superior capacity for concentration by increasing the binding of Gap1p to COPII. Therefore we can imagine that Erv14p might promote the interaction of the ER exit signal with COPII.

We have seen that Cwp2p can concentrate into ER domains independantly of COPII. The concentration into dots required the inositol deacylase Bst1p. Deacylation is an important step prior the anchor remodeling. In *bst1Δ* and remodeling mutants, GPI-anchored proteins cannot associate with DRMs, which is presumably the illustration of the failure of GPI-anchored proteins to enter into ceramide-enriched membranes. Remodeling and ceramide synthesis are required for efficient ER exit of GPI-anchored proteins. From this information, we postulate that assembly of remodelled GPI-anchored protein with ceramide-rich domains might play a role in concentration of GPI-anchored proteins in the ER in a COPII-independent manner. Alternatively, their lack of remodelling may cause them to be recognized by the machinery recognizing unfolded proteins and thereby prevent their concentration.

Emp24p also clearly plays a role in ER exit of GPI-anchored proteins because its absence strongly decreases budding efficiency. Moreover Emp24p binds to GPI-anchored proteins (36). From these results, it was tempting to think that Emp24p function is similar to Erv14p but for GPI-anchored proteins. In that case we expected that in *sec31-1emp24Δ*, GPI-anchored proteins would not accumulate into ERES. The opposite phenotype was observed. Moreover the sorting was not affected between Cwp2-Venus and CFP-Hxt1p (data not shown). This suggests that Emp24p is not required for concentration and sorting, this step requiring anchor remodeling and perhaps association with ceramides. The most likely role of Emp24p in ER exit seems to be to somehow mediate the interaction of preconcentrated GPI-anchored proteins with COPII to ensure efficient ER budding.

The comparison of GPI-anchored protein remodeling between yeast and mammalian cells can provide some clues about the mechanism of sorting upon ER exit in yeast. In yeast remodeling of GPI-anchored proteins occurs in the ER, whereas in mammalian remodeling occurs in the Golgi compartment (4, 8, 44). Remodeling seems universally important for GPI-anchored protein trafficking and correlated with association with DRMs in the ER in yeast and in the Golgi compartment in mammalian cells (4, 45). Furthermore, ER exit of GPI-anchored proteins in yeast is dependent on the ceramide synthases Lag1p and Lac1p (46). This suggests that ceramides are essential in the ER membrane for membrane association and ER exit of GPI-anchored proteins. This was not observed in mammalian cells (47). But association of GPI-anchored proteins with lipid rafts in the Golgi compartment is essential for apical sorting in several epithelial cell lines and to the axonal region of neuronal cells (48-52). Why should remodeling take place is different locations in yeast and mammalian cells? In contrast to mammalian cells, ER-to-Golgi transport of ceramides is largely ensured by vesicular rather than non-vesicular transport in yeast (53, 54). A defect in GPI synthesis has been shown to reduce the vesicular transport of ceramides to the Golgi. This suggests that ceramides and GPI-anchored proteins cooperate in order to be both efficiently transported to the Golgi compartment. In mammalian cells, transport of ceramide from ER-to-Golgi is mainly carried out by a non-vesicular mechanism using CERT (ceramide transport protein) (55) and is likely to be independent of GPI-anchored protein transport. One reason for this difference in organization may be the chain length of ceramides. In yeast, ceramide have almost

exclusively C26 acyl chains, whereas in mammalian cells, most ceramides have shorter acyl chains. CERT is only capable of transporting ceramides with shorter chain length(56).

To summarize our hypothesis about GPI-anchored protein exit; in mammalian cells GPI-anchored proteins are not remodeled in the ER and not associated to DRMs, and ceramides use non vesicular transport to exit ER. In yeast, ceramides and GPI-anchored proteins are cotransported out of the ER in a tightly coupled manner in vesicles that are distinct from other secreted proteins. A possible reason for this may be that ER-derived vesicles enriched in ceramides might not allow efficient incorporation of transmembrane cargo proteins. It remains to be seen if special mechanisms for ER exit will exist in mammalian cells that synthesize long chain ceramides, and if endogenous GPI-anchored proteins are sorted or not from endogenous transmembrane cargo proteins in mammalian cells upon ER exit.

Materials and Methods

Yeast strains and plasmids

Yeast strains used in this study are listed in Table 1. For construction of the plasmid pRS416ADH-CWP2-VENUS, we amplified by PCR a fragment of 789 bp containing the signal sequence of *CWP2* and the sequence coding for the fluorescent protein VENUS (57) using a forward primer containing the *Xba*I site, the 63 bp of the signal sequence of *CWP2* and the 20 first nucleotides of VENUS and a reverse primer containing the 20 last nucleotides of VENUS and the *Xma*I site. In parallel, we amplified from genomic DNA the *CWP2* gene using a forward primer containing an *Xma*I site and 20 nucleotides starting from the 64th nucleotide of *CWP2* sequence and a reverse primer containing the 23 last nucleotides of *CWP2* including the stop codon and a *Xho*I site. We digested the pRS416ADH plasmid at the *Xba*I and *Xho*I sites, the signal sequence VENUS fragment at the *Xba*I and *Xma*I sites and the CWP2 fragment at the *Xma*I and *Xho*I sites. After a triple ligation we obtained the pRS416ADH-CWP2-VENUS plasmid. The same method has been used to produce pRS416ADH-CCW14-VENUS and pRS416ADH-TOS6-VENUS.

We amplified by PCR the *CWP2* gene from genomic DNA using a forward primer containing an *Xba*I site, the signal sequence of *CWP2*, a *Bam*HI site and the 20 nucleotides starting from the 64th nucleotide of *CWP2* sequence and a reverse primer containing the 23 last nucleotides of *CWP2* including the stop codon and a *Xho*I site. We inserted this fragment into pRS415ADH at the *Xba*I and *Xho*I sites and obtained pRS415ADH-CWP2. We then amplified by PCR the sequence coding for the fluorescent protein CERULEAN (58) with a forward primer containing a *Bam*HI site and a reverse primer excluding the stop codon of CERULEAN and a *Bam*HI site. The fragment containing CERULEAN was inserted into *Bam*HI digested pRS415ADH-CWP2 plasmid to obtain pRS415ADH-CWP2-CERULEAN.

We amplified the *HXT1* gene from genomic DNA to obtain a *HXT1* fragment flanked by the *Bam*HI and *Xho*I sites. Then we amplified the VENUS gene or the CERULEAN gene flanked by *Xba*I and *Bam*HI. We ligated the *Xba*I/*Xho*I digested pRS416ADH with the *Bam*HI/*Xho*I digested *HXT1* fragment and the *Xba*I/*Bam*HI digested VENUS fragment to obtain pRS416ADH-VENUS-HXT1. Similar procedures and restriction enzymes were used to clone pRS416ADH-VENUS-HXT2. We ligated the *Xba*I/*Xho*I digested pRS415ADH with *Bam*HI/*Xho*I digested *HXT1* fragment and the *Xba*I/*Bam*HI digested CERULEAN fragment to obtain pRS415ADH-CERULEAN-HXT1.

From the pRS415ADH-CERULEAN-HXT1 plasmid, we extracted the CERULEAN-HXT1 fragment using *Xba*I and *Xho*I, then blunted it and inserted at the *Bam*HI site of pRS414TEF to obtain pRS414TEF-CERULEAN-HXT1.

We amplified the *MID2* and *TAT2* genes from genomic DNA to obtain both ORF flanked by the *Xba*I and *Bam*HI sites. Then we amplified the VENUS gene flanked by *Bam*HI and *Xho*I. We ligated the *Xba*I/*Xho*I digested pRS415ADH with the *Xba*I/*Bam*HI digested *MID2* and the *Bam*HI/*Xho*I digested VENUS fragment to obtain pRS415ADH-MID2-VENUS, and ligated the digested *TAT2* fragment and the digested VENUS fragment with pRS416ADH to obtain pRS416ADH-TAT2-VENUS.

We constructed a VENUS-PMA1 that is inducible with doxycycline. A fragment of 3059pb containing the doxycyline inducible system was obtained after the *Eco*RI/*Sap*I digestion of PCM252(59). This fragment was blunted and inserted into Ycplac33 after digestion by *Eco*RI/*Hind*III and blunted. The obtained plasmid called Ycplac33-tet was digested with *Xho*I. We amplified the VENUS ORF using a forward primer containing the 40 nucleotides homologous to the upstream sequence of the *Xho*I site of Ycplac33-tet, a *Xho*I site, a *BamH*I site and the 20 first nucleotides of VENUS, and a reverse primer containing the 40 nucleotides homologous to the downstream sequence of the *Xho*I site of Ycplac33-tet, a XhoI site, a NotI site and the 20 last nucleotides of VENUS. We co-transformed the PCR product and the digested Ycplac33-tet into yeast, and could retrieve the Ycplac33-tet-VENUS plasmid from colonies growing on synthetic medium lacking uracil (SD-URA) and fluorescent after incubation with doxycycline. Then we amplified the PMA1 ORF with a forward primer containing the 20 last nucleotides of VENUS without the STOP codon and the 20 first nucleotides of PMA1, and a reverse primer containing the 40 nucleotides homologuous to the downstream sequence of VENUS on Ycplac33-tet-VENUS, and the 20 last nucleotides of PMA1. After digestion of Ycplac33-tet-VENUS by *Not*I, we co-transformed the digested plasmid with the PCR product into yeast, and retrieved the Ycplac33-tet-VENUS-PMA1 from a yeast colony growing on SD-URA and expressing Venus-Pma1p after incubation with doxycyline. To construct the plasmid yECgpαF, we amplified the sequence coding for yECitrine from plasmid pKT140 (60), adding restriction sites *Bgl*II and *EcoR*I; and the pro-α-factor encoding sequence from *S. cerevisiae* DNA with a forward primer containing an *Xma*I site and a reverse primer adding a *Bgl*II site after the first MFα-repeat. The introduced restriction sites were used to perform a triple ligation of both fragments into *Xma*I/*EcoR*I digested pRS416ADH(61) to obtain yECgpαF.

In vitro ER-budding assay and vesicle immunoisolation

The *in vitro* budding and sorting assay was performed as described (10). Vesicle fractions were isolated by floatation through Nycodenz layers and processed for immunoprecipitation with suitable antibodies. The samples were separated by SDS-PAGE and quantified using a cyclone phosphorimager (Packard). Vesicle immunoisolation was performed as described previously (10). Pellet (P) corresponds to immunoisolated vesicles and supernatant (S) corresponds to a vesicle fraction that was not precipitated. Individual fractions were processed for immunoprecipitation and analyzed as above. To quantify the percentage of proteins in Hxt1p- or Gap1p-containing vesicles, we divided the percentage of individual proteins found in the pellet fraction by the percentage of immunoisolated Hxt1p or Gap1p. This process enabled comparison of

several independent experiments in which the immunoisolation efficiency of vesicles can vary.

Microscopy

Transformed cells were incubated overnight in synthetic medium at 24°C. The next day, the cells were diluted into YPUAD. After 1 hour at 24°C, the cells were incubated at 37°C for 1 hour. For the micrographs of live cells, the cells were washed once and resuspended in a small amount of pre-warmed synthetic medium with 5mM HEPES, and directly observed under the microscope. For micrographs of fixed cells, the cells were incubated for 1 hour at 37°C in 4% paraformaldehyde plus 3.4%(w/v) sucrose then washed and resuspended in small amount of KPO_4/sorbitol (1,2 M sorbitol, 100mM potassium phosphate pH7,5). The micrographs were acquired under a 100X 1.4NA oil objective with the AXIOZ1 microscope (ZEISS) and the Zeiss AxioCam MRm CCD camera controled by the software AxioVision Rel. 4.6. If co-localization was required, then the acquisitions were deconvoluted by ten iterations with the 2D blind protocol using the Auto-Deblur software from AutoQuant. The data were quantified and processed with Image J.

Movies

Cells were prepared as described above. Movies were acquired under a 100X 1.4NA oil objective with the widefield fluorescence microscope Leica AF6000LX and the Coolsnap HQ camera (Roper Scientific). 2 or 3 Z stacks spaced by 220nm were acquired every 20 seconds, deconvoluted by 10 iterations and Z-projected. Tracking was performed by the manual tracking pluging of Image J, and speeds were adjusted by cell movement.

Acknowledgments

We thank the Yeast Resource Center, P.O. Ljungdahl, B.S. Glick, B. André and R. Schekman for providing antibodies, plasmids and strains, Gisèle Dewhurst, Isabelle Riezman, Brigitte Bernadets and the Bioimaging Platform of NCCR Frontiers in Genetics for technical help. We thank past and present members in Riezman laboratory for comments and discussion. This work was supported by the Human Frontiers Science Program Organization through a long-term fellowship (to RW), a research grant (to HR), the National Sciences and Engineering Research Council of Canada through a post-doctoral fellowship (to MT), the German Academic Exchange Service through a post-doctoral fellowship (to TMES), the Swiss National Science Foundation through a Marie Heim-Vögtlin fellowship (to RW) and a research grant (to HR).

References

1. Lee MC, Miller EA, Goldberg J, Orci L, Schekman R. Bi-directional protein transport between the ER and Golgi. Annu Rev Cell Dev Biol 2004;20:87-123.
2. Fujita M, Jigami Y. Lipid remodeling of GPI-anchored proteins and its function. Biochim Biophys Acta 2008;1780(3):410-420.
3. Pittet M, Conzelmann A. Biosynthesis and function of GPI proteins in the yeast Saccharomyces cerevisiae. Biochim Biophys Acta 2007;1771(3):405-420.
4. Fujita M, Umemura M, Yoko-o T, Jigami Y. PER1 is required for GPI-phospholipase A2 activity and involved in lipid remodeling of GPI-anchored proteins. Mol Biol Cell 2006;17(12):5253-5264.
5. Fujita M, Yoko OT, Jigami Y. Inositol deacylation by Bst1p is required for the quality control of glycosylphosphatidylinositol-anchored proteins. Mol Biol Cell 2006;17(2):834-850.
6. Watanabe R, Funato K, Venkataraman K, Futerman AH, Riezman H. Sphingolipids are required for the stable membrane association of glycosylphosphatidylinositol-anchored proteins in yeast. J Biol Chem 2002;277(51):49538-49544.
7. Kinoshita T, Fujita M, Maeda Y. Biosynthesis, remodeling and functions of mammalian GPI-anchored proteins: recent progress. J Biochem 2008.
8. Maeda Y, Tashima Y, Houjou T, Fujita M, Yoko-o T, Jigami Y, Taguchi R, Kinoshita T. Fatty acid remodeling of GPI-anchored proteins is required for their raft association. Mol Biol Cell 2007;18(4):1497-1506.
9. Muniz M, Morsomme P, Riezman H. Protein sorting upon exit from the endoplasmic reticulum. Cell 2001;104(2):313-320.
10. Watanabe R, Castillon GA, Meury A, Riezman H. The presence of an ER exit signal determines the protein sorting upon ER exit in yeast. Biochem J 2008.
11. Stephens DJ, Pepperkok R. Differential effects of a GTP-restricted mutant of Sar1p on segregation of cargo during export from the endoplasmic reticulum. J Cell Sci 2004;117(Pt 16):3635-3644.
12. Pao SS, Paulsen IT, Saier MH, Jr. Major facilitator superfamily. Microbiol Mol Biol Rev 1998;62(1):1-34.
13. Malkus P, Jiang F, Schekman R. Concentrative sorting of secretory cargo proteins into COPII-coated vesicles. J Cell Biol 2002;159(6):915-921.
14. Otte S, Barlowe C. Sorting signals can direct receptor-mediated export of soluble proteins into COPII vesicles. Nat Cell Biol 2004;6(12):1189-1194.
15. Sherwood PW, Carlson M. Efficient export of the glucose transporter Hxt1p from the endoplasmic reticulum requires Gsf2p. Proc Natl Acad Sci U S A 1999;96(13):7415-7420.
16. Ram AF, Van den Ende H, Klis FM. Green fluorescent protein-cell wall fusion proteins are covalently incorporated into the cell wall of Saccharomyces cerevisiae. FEMS Microbiol Lett 1998;162(2):249-255.
17. Lederkremer GZ, Cheng Y, Petre BM, Vogan E, Springer S, Schekman R, Walz T, Kirchhausen T. Structure of the Sec23p/24p and Sec13p/31p complexes of COPII. Proc Natl Acad Sci U S A 2001;98(19):10704-10709.
18. Kuehn MJ, Herrmann JM, Schekman R. COPII-cargo interactions direct protein sorting into ER-derived transport vesicles. Nature 1998;391(6663):187-190.
19. Miller EA, Beilharz TH, Malkus PN, Lee MC, Hamamoto S, Orci L, Schekman R. Multiple cargo binding sites on the COPII subunit Sec24p ensure capture of diverse membrane proteins into transport vesicles. Cell 2003;114(4):497-509.
20. Barlowe C, Orci L, Yeung T, Hosobuchi M, Hamamoto S, Salama N, Rexach MF, Ravazzola M, Amherdt M, Schekman R. COPII: a membrane coat formed by Sec proteins that drive vesicle budding from the endoplasmic reticulum. Cell 1994;77(6):895-907.
21. Bannykh SI, Rowe T, Balch WE. The organization of endoplasmic reticulum export complexes. J Cell Biol 1996;135(1):19-35.
22. Rossanese OW, Soderholm J, Bevis BJ, Sears IB, O'Connor J, Williamson EK, Glick BS. Golgi structure correlates with transitional endoplasmic reticulum organization in Pichia pastoris and Saccharomyces cerevisiae. J Cell Biol 1999;145(1):69-81.
23. Morsomme P, Prescianotto-Baschong C, Riezman H. The ER v-SNAREs are required for GPI-anchored protein sorting from other secretory proteins upon exit from the ER. J Cell Biol 2003;162(3):403-412.
24. De Groot PW, Hellingwerf KJ, Klis FM. Genome-wide identification of fungal GPI proteins. Yeast 2003;20(9):781-796.
25. Hamada K, Fukuchi S, Arisawa M, Baba M, Kitada K. Screening for glycosylphosphatidylinositol (GPI)-dependent cell wall proteins in Saccharomyces cerevisiae. Mol Gen Genet 1998;258(1-2):53-59.
26. Barlowe C, Schekman R. SEC12 encodes a guanine-nucleotide-exchange factor essential for transport vesicle budding from the ER. Nature 1993;365(6444):347-349.
27. Nakano A, Brada D, Schekman R. A membrane glycoprotein, Sec12p, required for protein transport from the endoplasmic reticulum to the Golgi apparatus in yeast. J Cell Biol 1988;107(3):851-863.
28. Gimeno RE, Espenshade P, Kaiser CA. COPII coat subunit interactions: Sec24p and Sec23p bind to adjacent regions of Sec16p. Mol Biol Cell 1996;7(11):1815-1823.
29. Supek F, Madden DT, Hamamoto S, Orci L, Schekman R. Sec16p potentiates the action of COPII proteins to bud transport vesicles. J Cell Biol 2002;158(6):1029-1038.
30. Connerly PL, Esaki M, Montegna EA, Strongin DE, Levi S, Soderholm J, Glick BS. Sec16 is a determinant of transitional ER organization. Curr Biol 2005;15(16):1439-1447.
31. Marzioch M, Henthorn DC, Herrmann JM, Wilson R, Thomas DY, Bergeron JJ, Solari RC, Rowley A. Erp1p and Erp2p, partners for Emp24p and Erv25p in a yeast p24 complex. Mol Biol Cell 1999;10(6):1923-1938.

32. Belden WJ, Barlowe C. Distinct roles for the cytoplasmic tail sequences of Emp24p and Erv25p in transport between the endoplasmic reticulum and Golgi complex. J Biol Chem 2001;276(46):43040-43048.
33. Fullekrug J, Suganuma T, Tang BL, Hong W, Storrie B, Nilsson T. Localization and recycling of gp27 (hp24gamma3): complex formation with other p24 family members. Mol Biol Cell 1999;10(6):1939-1955.
34. Rojo M, Pepperkok R, Emery G, Kellner R, Stang E, Parton RG, Gruenberg J. Involvement of the transmembrane protein p23 in biosynthetic protein transport. J Cell Biol 1997;139(5):1119-1135.
35. Sohn K, Orci L, Ravazzola M, Amherdt M, Bremser M, Lottspeich F, Fiedler K, Helms JB, Wieland FT. A major transmembrane protein of Golgi-derived COPI-coated vesicles involved in coatomer binding. J Cell Biol 1996;135(5):1239-1248.
36. Muniz M, Nuoffer C, Hauri HP, Riezman H. The Emp24 complex recruits a specific cargo molecule into endoplasmic reticulum-derived vesicles. J Cell Biol 2000;148(5):925-930.
37. Powers J, Barlowe C. Transport of axl2p depends on erv14p, an ER-vesicle protein related to the Drosophila cornichon gene product. J Cell Biol 1998;142(5):1209-1222.
38. Powers J, Barlowe C. Erv14p directs a transmembrane secretory protein into COPII-coated transport vesicles. Mol Biol Cell 2002;13(3):880-891.
39. Queenan AM, Barcelo G, Van Buskirk C, Schupbach T. The transmembrane region of Gurken is not required for biological activity, but is necessary for transport to the oocyte membrane in Drosophila. Mech Dev 1999;89(1-2):35-42.
40. Roth S, Neuman-Silberberg FS, Barcelo G, Schupbach T. cornichon and the EGF receptor signaling process are necessary for both anterior-posterior and dorsal-ventral pattern formation in Drosophila. Cell 1995;81(6):967-978.
41. Bokel C, Dass S, Wilsch-Brauninger M, Roth S. Drosophila Cornichon acts as cargo receptor for ER export of the TGFalpha-like growth factor Gurken. Development 2006;133(3):459-470.
42. Simpson JC, Cetin C, Erfle H, Joggerst B, Liebel U, Ellenberg J, Pepperkok R. An RNAi screening platform to identify secretion machinery in mammalian cells. J Biotechnol 2007;129(2):352-365.
43. Nakanishi H, Suda Y, Neiman AM. Erv14 family cargo receptors are necessary for ER exit during sporulation in Saccharomyces cerevisiae. J Cell Sci 2007;120(Pt 5):908-916.
44. Sipos G, Reggiori F, Vionnet C, Conzelmann A. Alternative lipid remodelling pathways for glycosylphosphatidylinositol membrane anchors in Saccharomyces cerevisiae. EMBO J 1997;16(12):3494-3505.
45. Bosson R, Jaquenoud M, Conzelmann A. GUP1 of Saccharomyces cerevisiae encodes an O-acyltransferase involved in remodeling of the GPI anchor. Mol Biol Cell 2006;17(6):2636-2645.
46. Barz WP, Walter P. Two endoplasmic reticulum (ER) membrane proteins that facilitate ER-to-Golgi transport of glycosylphosphatidylinositol-anchored proteins. Mol Biol Cell 1999;10(4):1043-1059.
47. Yasuda S, Kitagawa H, Ueno M, Ishitani H, Fukasawa M, Nishijima M, Kobayashi S, Hanada K. A novel inhibitor of ceramide trafficking from the endoplasmic reticulum to the site of sphingomyelin synthesis. J Biol Chem 2001;276(47):43994-44002.
48. Brown DA, Crise B, Rose JK. Mechanism of membrane anchoring affects polarized expression of two proteins in MDCK cells. Science 1989;245(4925):1499-1501.
49. Lisanti MP, Caras IW, Davitz MA, Rodriguez-Boulan E. A glycophospholipid membrane anchor acts as an apical targeting signal in polarized epithelial cells. J Cell Biol 1989;109(5):2145-2156.
50. Lisanti MP, Le Bivic A, Saltiel AR, Rodriguez-Boulan E. Preferred apical distribution of glycosyl-phosphatidylinositol (GPI) anchored proteins: a highly conserved feature of the polarized epithelial cell phenotype. J Membr Biol 1990;113(2):155-167.
51. Benting JH, Rietveld AG, Simons K. N-Glycans mediate the apical sorting of a GPI-anchored, raft-associated protein in Madin-Darby canine kidney cells. J Cell Biol 1999;146(2):313-320.
52. Paladino S, Sarnataro D, Pillich R, Tivodar S, Nitsch L, Zurzolo C. Protein oligomerization modulates raft partitioning and apical sorting of GPI-anchored proteins. J Cell Biol 2004;167(4):699-709.
53. Funato K, Riezman H. Vesicular and nonvesicular transport of ceramide from ER to the Golgi apparatus in yeast. J Cell Biol 2001;155(6):949-959.
54. Kajiwara K, Watanabe R, Pichler H, Ihara K, Murakami S, Riezman H, Funato K. Yeast ARV1 Is Required for Efficient Delivery of an Early GPI Intermediate to the First Mannosyltransferase during GPI Assembly and Controls Lipid Flow from the Endoplasmic Reticulum. Mol Biol Cell 2008;19(5):2069-2082.
55. Fukasawa M, Nishijima M, Hanada K. Genetic evidence for ATP-dependent endoplasmic reticulum-to-Golgi apparatus trafficking of ceramide for sphingomyelin synthesis in Chinese hamster ovary cells. J Cell Biol 1999;144(4):673-685.
56. Kumagai K, Yasuda S, Okemoto K, Nishijima M, Kobayashi S, Hanada K. CERT mediates intermembrane transfer of various molecular species of ceramides. J Biol Chem 2005;280(8):6488-6495.
57. Nagai T, Ibata K, Park ES, Kubota M, Mikoshiba K, Miyawaki A. A variant of yellow fluorescent protein with fast and efficient maturation for cell-biological applications. Nat Biotechnol 2002;20(1):87-90.
58. Rizzo MA, Springer GH, Granada B, Piston DW. An improved cyan fluorescent protein variant useful for FRET. Nat Biotechnol 2004;22(4):445-449.
59. Belli G, Gari E, Piedrafita L, Aldea M, Herrero E. An activator/repressor dual system allows tight tetracycline-regulated gene expression in budding yeast. Nucleic Acids Res 1998;26(4):942-947.
60. Sheff MA, Thorn KS. Optimized cassettes

for fluorescent protein tagging in Saccharomyces cerevisiae. Yeast 2004;21(8):661-670.
61. Mumberg D, Muller R, Funk M. Yeast vectors for the controlled expression of heterologous proteins in different genetic backgrounds. Gene 1995;156(1):119-122.

Figure legends

Figure 1

Hxt1p and Cwp2p localize in ERES in *sec31-1* at 37°C.

(A) Localization of CFP-Hxt1p (cyan), Cwp2-Venus (yellow) and Sec13-GFP in live wild-type cells at 37°C. (B) Localization of Sec13-GFP in live wild-type cells and *sec31-1* cells at 37°C. (C) Live images of *sec31-1* yeast expressing Cwp2-CFP (cyan) and Sec13-GFP (yellow) at 37°C. (D) Quantification of the several images described in (C). In the left panel, means of the number of dots of Cwp2-CFP and Sec13-GFP per cell. In the right panel, quantification of the co-localization of the Cwp2-CFP dots and Sec13-GFP dots. (n=number of cells quantified=62) (E) Live images of *sec31-1* yeast expressing CFP-Hxt1p (cyan) and Sec13-GFP (yellow) at 37°C. (F) Quantification of several micrographs described in (E). In the left panel, means of number of dots of CFP-Hxt1p and Sec13-GFP per cell. In the right panel, quantification of the co-localization of the CFP-Hxt1p dots and Sec13-GFP dots. (n=54). (G) Live images of *sec31-1* cells expressing Sec13-GFP (yellow) and Cwp2-CFP (blue) or CFP-Hxt1p (blue) after shift from 37°C to 24°C. (H) Quantification of several micrographs described in (G). Means of the percentage of co-localization per cell of Cwp2-CFP with Sec13-GFP (black bars, 45≤n≤54, n= number of cells plotted per time point) and of CFP-Hxt1p with Sec13-GFP (white bars, 42≤n≤51) in *sec31-1*. The quantifications were done at 37°C and 20, 40, 60 minutes in *sec31-1* after the shift from 37°C to 24°C. (C, E, G) CFP-Hxt1p and Cwp2-CFP have been acquired through the CFP channel. Sec13-GFP has been acquired through the YFP channel. Images deconvoluted by 10 iterations using blind deconvolution protocol. Star: vacuole. Fine dashed line: cell shape. White arrow heads: co-localizing dots. Scale bar: 3 μm.

Figure 2

Hxt1p and Cwp2p localize in different ERES in *sec31-1* at 37°C.

(A) Live images of *sec31-1* yeast expressing CFP-Hxt1p and Cwp2-Venus at 37°C. (B) Quantification of several micrographs described in (A). In the left panel, the number of dots of CFP-Hxt1p and Cwp2-Venus per cell was averaged. In the right panel, quantification of the co-localization of the Venus and CFP dots. (n=75). (C) Fluorescent micrographs of live *sec31-1* yeast expressing Cwp2-CFP and Cwp2-Venus at 37°C. (D) Quantification of several micrographs acquired as described in (C) and done as in (B). n=37. (E) Fluorescent micrographs of live *sec31-1* yeast expressing CFP-Hxt1p and Venus-Hxt1p at 37°C. (F) Quantification of several micrographs acquired as described in (E) and done as in (B). n=40. Scale bar: 3 μm. Star: vacuole. Fine dashed line: cell shape. White arrow heads: co-localizing dots. Open arrow heads: non-co-localizing dots. Images deconvoluted by 10 iterations using a blind deconvolution protocol.

Figure 3

Hxt1p sorts into a third ER derived vesicle population.

(A) *In vitro* budding was performed using wild-type semi-intact cells expressing Gap1pHA, Venus-Hxt1p and Cwp2-Venus for 1 hour at 24°C in absence or presence of wild-type cytosol. The numbers correspond to budding efficiency. Budding efficiencies were calculated as the percentage of the total input that was recovered in the purified vesicles for each individual protein. (B) Graphic representation of the average budding efficiencies observed in 4 independent experiments performed as in (A). (C) Budding of the ER resident protein Sec61p as performed in (A) and revealed by Western-blot. (D) Vesicles generated as in (A) from cells expressing Gap1p, Cwp2-Venus and CFP-Hxt1p were immunoisolated with or without purified polyclonal anti-Venus antibody. (E) Vesicles generated as in (A) from cells expressing Gap1pHA and Cwp2-Venus were immunoisolated with or without monoclonal anti-HA antibody. (F) Vesicles generated as in (A) from cells expressing Gap1pHA and Venus-Hxt1p were immunoisolated with or without monoclonal anti-HA antibody or purified polyclonal anti-Venus antibody. (D-F) The numbers correspond to the percentage of cargo found in the pellets. (G) Percentage of cargo proteins found in Hxt1p containing vesicles after *in vitro* sorting assay as performed in (D). (H) Percentage of cargo proteins found in Gap1p-containing vesicles after *in vitro* sorting assay as performed in (E). (I) Percentage of cargo proteins found in Gap1p and Hxt1p containing vesicles after *in vitro* sorting assay as performed in (F). (G-I) The bars represent the mean of 3 independent experiments.

Figure 4

GPI-anchored proteins colocalize in the same ERES, whereas glycosylated proαfactor does not co-localize with Hxt1p or Cwp2p in *sec31-1* at 37°C.

(A) Fluorescent micrographs of live *sec31-1* yeast expressing Cwp2-CFP and Ccw14-Venus at 37°C. (B) Quantification of several micrographs acquired as described in (A) and done as in Fig. 2B. n=45. (C) Fluorescent micrographs of live *sec31-1* yeast expressing Cwp2-CFP and Tos6-Venus at 37°C. (D) Quantification of several micrographs described in (C) and done as in (B). n=43. (E) Fluorescent micrographs of live *sec31-1* yeast expressing Cwp2-CFP and glycosylated ye-citrine-tagged αfactor yECgpαF) at 37°C. (F) Quantification of several micrographs described in (E) and done as in (B). n=49. (G) Fluorescent micrographs of live *sec31-1* yeast expressing CFP-Hxt1p and yECgpαF at 37°C. (H) Quantification of several micrographs described in (G) and done as in (B). n=55. Scale, acquisition and processing of the live images are the same as in Fig. 2.

Figure 5

Hxt1p but not Cwp2p concentration depends on COPII.

(A) Fluorescent micrographs of live *sec12-4* and *sec16-2* cells expressing CFP-Hxt1p or Cwp2-Venus at 37°C. (B) Fluorescent micrographs of live *sec12-4* and *sec16-2* cells expressing Sec13-GFP at 37°C. (C) Quantification of several micrographs described in (A) and Fig. S1B-C. The graph plots the average percentage of the *sec12-4*, *sec16-2* and *sec31-1* cells, for which Cwp2-Venus and CFP-Hxt1p are found in dots or in the ER. 67≤n≤83. (D) Quantification of several micrographs described in (A) and (S1B-C). The graph plots the average

number of dots of Cwp2-Venus and CFP-Hxt1p observed in the *sec12-4*, *sec16-2* and *sec31-1* cells. 14≤n≤68. Only cells in which dots were present are taken into account. (E) Deconvoluted fluorescent micrographs of live *sec16-2* cells expressing CFP-Hxt1p and Cwp2-Venus at 37°C. (F) Quantification of several micrographs acquired as described in (E) and Fig. 2A. The graph plots the average percentage of co-localization between Cwp2-Venus and CFP-Hxt1p in *sec16-2* and *sec31-1* cells at 37°C. 31≤n≤68. Only cells in which dots were present are taken into account. (A,B) Raw images. (E) Images deconvoluted by 10 iterations using blind deconvolution protocol. White arrow heads: co-localizing dots. Scale bar: 5 μm.

Figure 6

Cwp2p requires Bst1p to be concentrated into ERES.

(A) Fluorescent micrographs of live *bst1Δ* and *sec31-1bst1Δ* cells expressing CFP-Hxt1p and Cwp2-Venus at 37°C. (B) Quantification of several micrographs described in (A). The graph plots the average percentage of the *bst1Δ* cells, for which Cwp2-Venus and CFP-Hxt1p are found in the ER. n=72. (C) Quantification of several micrographs described in (A). The graph plots the average percentage of the *sec31-1bst1Δ* cells, for which Cwp2-Venus and CFP-Hxt1p are found in dots or in the ER. n=89. (D) Quantification of several micrographs described in (A).The graph plots the average number of dots of Cwp2-Venus and CFP-Hxt1p observed in the *sec31-1bst1Δ* cells. n=17. Only cells in which dots were present are taken into account. (A,B) Raw images. Scale bar: 5 μm.

Figure 7

Hxt1p ER export is defective in *erv14Δ* and Cwp2p ER export is defective in *emp24Δ.*

(A) Fluorescent micrographs of live wild-type cells, *erv14Δ* mutant cells and *emp24Δ* mutant cells expressing Venus-Hxt1p, Cwp2-Venus, Gap1-GFP or Gap1-GFP mutated at ubiquitination sites (Gap1ubGFP) at 30°C. (B) Fluorescent micrographs of live wild-type, *erv14Δ* and *emp24Δ* cells expressing Ccw14-Venus, Venus-Hxt2p, Mid2-Venus or Venus-Pma1p at 30°C. (A, B) Raw images are displayed here. The white arrow points out the perinuclear ER. Scale bar: 5 μm. (C) Quantification of several micrographs described in (A) and (B). The graph plots the average percentage of the wild-type, *erv14Δ* and *emp24Δ* cells, for which the different cargoes are found in the ER. 57≤n≤72. (D) *In vitro* budding assay of Gap1p, Venus-Hxt1p and Cwp2-Venus using WT, *erv14Δ* and *emp24Δ* semi-intact cells and WT cytosol and performed at 24°C. Tot: total, (-): -cytosol, (+): +cytosol. The numbers correspond to budding efficiency. Budding efficiencies were calculated as in Fig. 3A. (E) Graphic representation of the average budding efficiencies observed in 3 independent experiments performed as in (D).

Figure 8

Erv14p is required for concentration of Hxt1p and Emp24p is not required for Cwp2p concentration.

(A) Fluorescent micrographs of live *erv14Δ* mutant cells and *emp24Δ* mutant cells expressing Sec13-GFP at 37°C. (B) Fluorescent micrographs of live *erv14Δsec31-1* mutant cells and *emp24Δsec31-1* mutant cells expressing Cwp2-Venus or CFP-Hxt1p at 37°C. (A, B) Raw images are displayed here. Scale bar: 5 μm. (C) Quantification of several micrographs described in (B). The graph plots the average percentage of the *erv14Δsec31-1* and *emp24Δsec31-1* cells, for which Cwp2-Venus and CFP-Hxt1p are found in dots or in the ER. 83≤n≤92. (D) Quantification of several micrographs described in (B).The graph plots the average number of dots of Cwp2-Venus and CFP-Hxt1p observed in the *erv14Δsec31-1* and *emp24Δsec31-1* cells. n=60 for *emp24Δsec31-1* and n=15 for *erv14Δ sec31-1*. Only cells in which dots were present are taken into account.

Figure 9

Hxt1p and Cwp2p traffic at different speeds early in the secretory pathway.

(A) Quantification of several movies acquired as in movie 1 and 2. The graph plots the average percentage of co-localization of Cwp2-CFP with Ccw14-Venus (movie 2) and Cwp2-Venus with CFP-Hxt1p (movie 1) in *sec31-1* along the time after the temperature shift from 37°C to 24°C. For co-localization between Cwp2-CFP and Ccw14-Venus, n1=6 with n1= number of cells plotted and 6≤n2≤12 with n2= number of dots plotted per cell. For co-localization between Cwp2-Venus and CFP-Hxt1p, n1=6 and 8≤n2≤20. (B) Quantification of the dots average speeds. The black bars represent the mean of the average speed of the Cwp2-Venus dots tracked in several movies acquired as in movie 1. The white bars represent the mean of the average speed of the CFP-Hxt1p dots. n1=6 and 8≤n2≤20.

Figure 10

Model of cargo concentration and sorting upon ER exit

The GPI-anchored protein Cwp2p is concentrated into DRM via remodeling initiated by the inositol deacylase Bst1p. Patches of concentrated GPI-anchored proteins are associated to ERES, and stably bound to COPII coated vesicles because of Emp24p. The transmembrane protein Hxt1p is concentrated and loaded to the ERES and forming COPII coated vesicles throught its potential interaction to COPII via Erv14p. The co-existence of the two concentrative mechanisms, and probably the exclusion of Hxt1p from DRM might contribute to sorting. After full assembly of the COPII coat, there is generation of two ER-derived vesicles different by the cargoes they carry.

Figure S1

Control of deconvolution and specificity of signal.

(A) Localization of Sec13-GFP in live *sec31-1* cells at 37°C. (B) Localization of CFP-Hxt1p in live *sec31-1* cells at 37°C. (C) Localization of Cwp2-Venus in live *sec31-1* cells at 37°C. Raw images are indicated by "*raw"*. The term "*10 it"* indicates that the images have been deconvoluted by 10 iterations using a blind deconvolution protocol. Scale bar: 3 μm.

Figure S2

Hxt1p and Cwp2p do not co-localize in fixed *sec31-1* cells at 37°C, but co-localized in *bos1-1* cells at 37°C.

(A) Fluorescent micrographs of 4% paraformaldehyde fixed *sec31-1* yeast cells

expressing CFP-Hxt1p and Cwp2-Venus at 37°C. (B) Quantification of several micrographs described in (A), and done as in Fig.2B. n=71. (C) Fluorescent micrographs of live *bos1-1* yeast expressing CFP-Hxt1p and Cwp2-Venus at 37°C. (D) Quantification of several micrographs described in (C) and done as in Fig.2B. n=56.

Movies

Movie 1 shows *sec31-1* cells expressing CFP-Hxt1p (blue), Cwp2-Venus (green) with 1 acquisition per 20 seconds. Each image is the result of 3 Z-stacks spaced by 220 nm, deconvoluted by 10 iterations and projected in Z. In the bottom part, tracking of individual dots have been added. Movie 1 covers the time between 0 minutes to 8 minutes after the shift from 37°C to 24°C.

Movie 2 shows *sec31-1* cells expressing Cwp2-CFP (cyan) and Ccw14-Venus (yellow) with 1 acquisition per 20 secondes. Each image is the result of 2 Z-stacks spaced by 220 nm, deconvoluted by 10 iterations and projected in Z. In the bottom part, tracking of individual dots have been added. Movie 2 covers the time between 0 minutes to 10 minutes after the shift from 37°C to 24°C.

Table 1. Strains used in this study

Strains	Genotype	Source
RH732	*Mata pep4Δ::URA3 his4 leu2 lys2 ura3 bar1*	Lab strain
RH1491	*Mata sec12-4 leu2 ura3 lys2 his4*	Lab strain
RH1498	*Matα sec16-2 leu2 ura3 lys2 his4*	Lab strain
RH2874	*Matα leu2 lys2 trp1 ura3 bar1*	Lab strain
RH5877	*Mata sec31-1 leu2 ura3 lys2 trp1 his3*	Lab strain
RH5942	*Mata bst1Δ::*KanMX *leu2 ura3 lys2 met15 his3*	Lab strain
RH6850	*Matα bos1-1 leu2 ura3*	Lab strain
RH6878	*Mata erv14Δ::*KanMX *leu2 ura3 lys2 trp1*	Lab strain
RH6881	*Mata sec31-1 erv14Δ::KANMX leu2 ura3 lys2 trp1*	Lab strain
RH6910	*Mata emp24Δ::*KanMX *leu2 ura3 lys2 trp1 his3*	Lab strain
RH6912	*Mata sec31-1 emp24Δ::*KanMX *leu2 ura3 lys2 trp1*	Lab strain
RH6965	*Matα sec31-1 bst1Δ::*KanMX *leu2 ura3 lys2 trp1 his3*	Lab strain

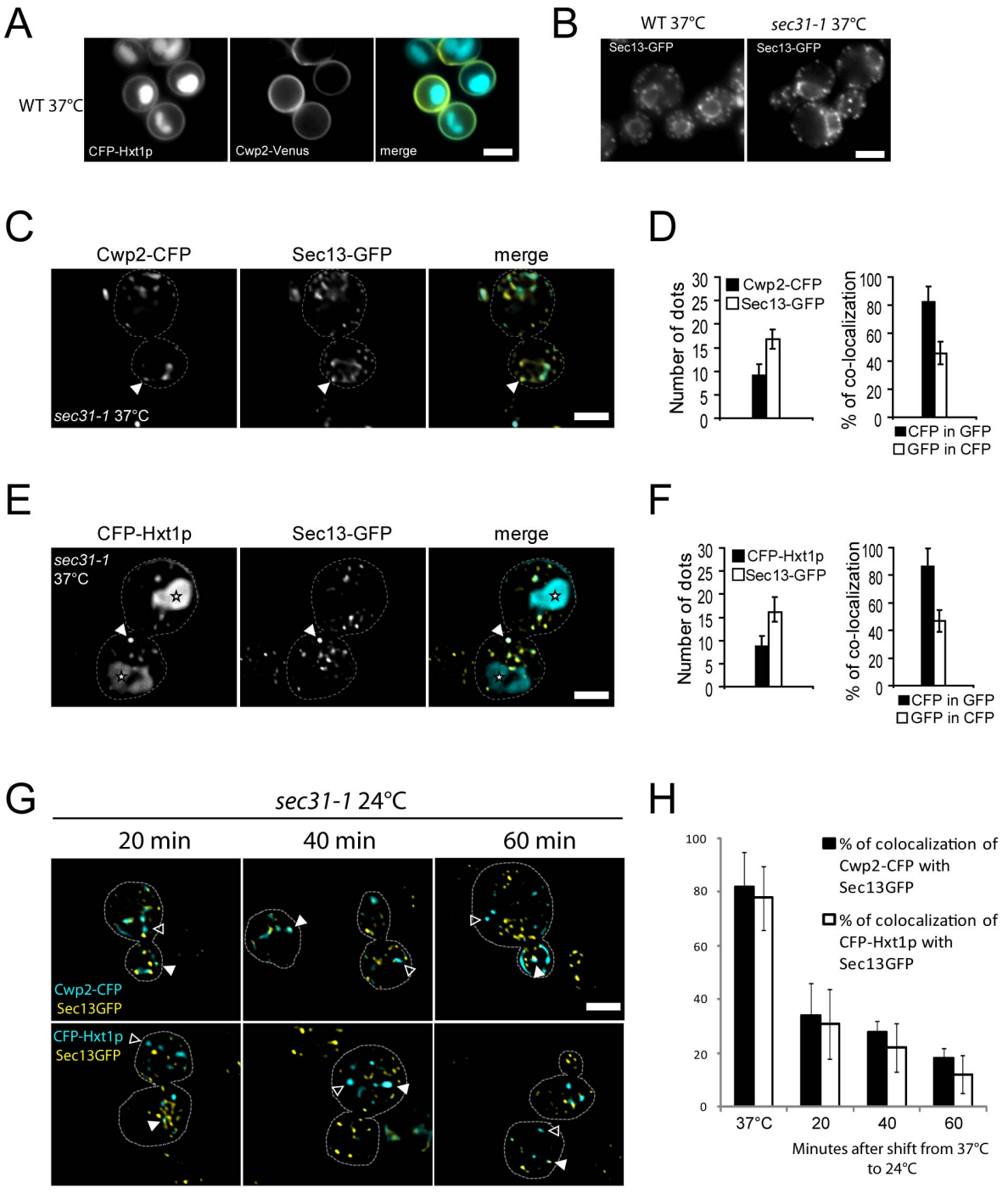
A
WT 37°C
CFP-Hxt1p
Cwp2-Venus
merge
B
WT 37°C
sec31-1 37°C
Sec13-GFP
Sec13-GFP
C
Cwp2-CFP
Sec13-GFP
merge
sec31-1 37°C
D
Number of dots
Cwp2-CFP
Sec13-GFP
% of co-localization
CFP in GFP
GFP in CFP
E
CFP-Hxt1p
Sec13-GFP
merge
sec31-1
37°C
F
Number of dots
CFP-Hxt1p
Sec13-GFP
% of co-localization
CFP in GFP
GFP in CFP
G
sec31-1 24°C
20 min
40 min
60 min
Cwp2-CFP
Sec13GFP
CFP-Hxt1p
Sec13GFP
H
% of colocalization of Cwp2-CFP with Sec13GFP
% of colocalization of CFP-Hxt1p with Sec13GFP
37°C
20
40
60
Minutes after shift from 37°C to 24°C

Fig. 1

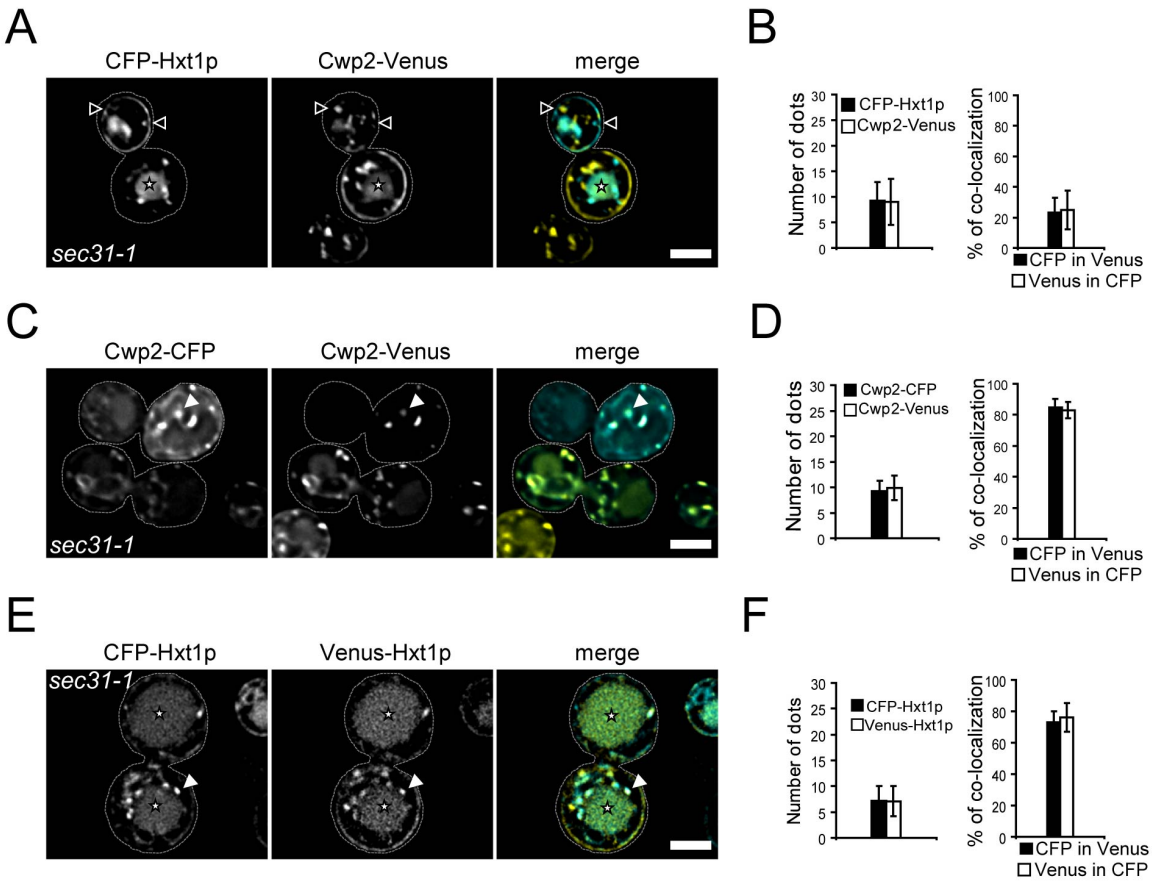
A
CFP-Hxt1p
Cwp2-Venus
merge
sec31-1
B
Number of dots
CFP-Hxt1p
Cwp2-Venus
% of co-localization
CFP in Venus
Venus in CFP
C
Cwp2-CFP
Cwp2-Venus
merge
sec31-1
D
Number of dots
Cwp2-CFP
Cwp2-Venus
% of co-localization
CFP in Venus
Venus in CFP
E
CFP-Hxt1p
Venus-Hxt1p
merge
sec31-1
F
Number of dots
CFP-Hxt1p
Venus-Hxt1p
% of co-localization
CFP in Venus
Venus in CFP

Fig. 2

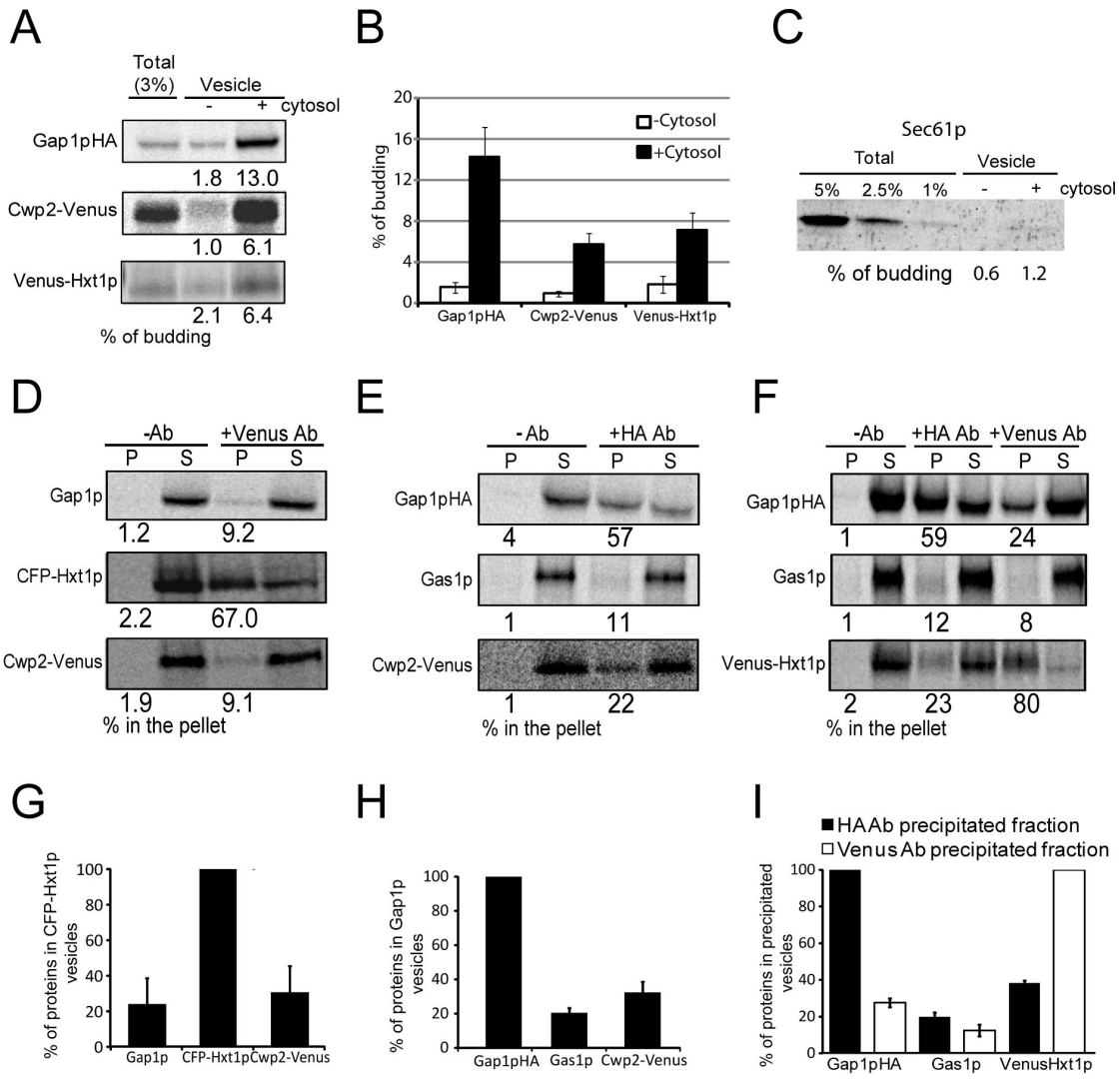
A
Total (3%)
Vesicle
- + cytosol
Gap1pHA
1.8 13.0
Cwp2-Venus
1.0 6.1
Venus-Hxt1p
2.1 6.4
% of budding
B
% of budding
-Cytosol
+Cytosol
Gap1pHA
Cwp2-Venus
Venus-Hxt1p
C
Sec61p
Total
Vesicle
5% 2.5% 1% - + cytosol
% of budding 0.6 1.2
D
-Ab
+Venus Ab
P S P S
Gap1p
1.2 9.2
CFP-Hxt1p
2.2 67.0
Cwp2-Venus
1.9 9.1
% in the pellet
E
-Ab
+HA Ab
P S P S
Gap1pHA
4 57
Gas1p
1 11
Cwp2-Venus
1 22
% in the pellet
F
-Ab
+HA Ab
+Venus Ab
P S P S P S
Gap1pHA
1 59 24
Gas1p
1 12 8
Venus-Hxt1p
2 23 80
% in the pellet
G
% of proteins in CFP-Hxt1p vesicles
Gap1p
CFP-Hxt1p
Cwp2-Venus
H
% of proteins in Gap1p vesicles
Gap1pHA
Gas1p
Cwp2-Venus
I
HA Ab precipitated fraction
Venus Ab precipitated fraction
% of proteins in precipitated vesicles
Gap1pHA
Gas1p
VenusHxt1p

Fig. 3

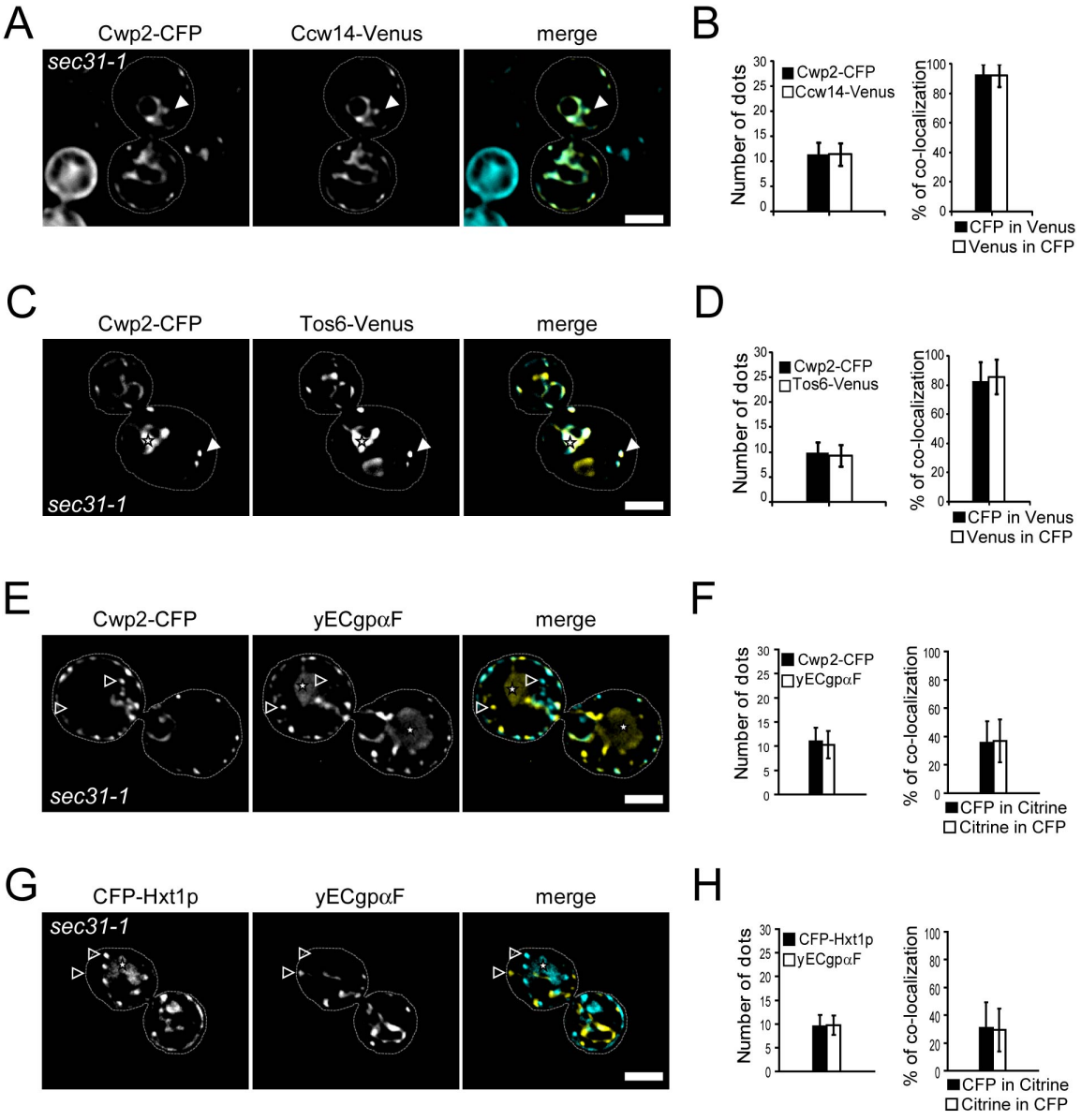
A
Cwp2-CFP
Ccw14-Venus
merge
sec31-1
B
Number of dots
Cwp2-CFP
Ccw14-Venus
% of co-localization
CFP in Venus
Venus in CFP
C
Cwp2-CFP
Tos6-Venus
merge
sec31-1
D
Number of dots
Cwp2-CFP
Tos6-Venus
% of co-localization
CFP in Venus
Venus in CFP
E
Cwp2-CFP
yECgpαF
merge
sec31-1
F
Number of dots
Cwp2-CFP
yECgpαF
% of co-localization
CFP in Citrine
Citrine in CFP
G
CFP-Hxt1p
yECgpαF
merge
sec31-1
H
Number of dots
CFP-Hxt1p
yECgpαF
% of co-localization
CFP in Citrine
Citrine in CFP

Fig. 4

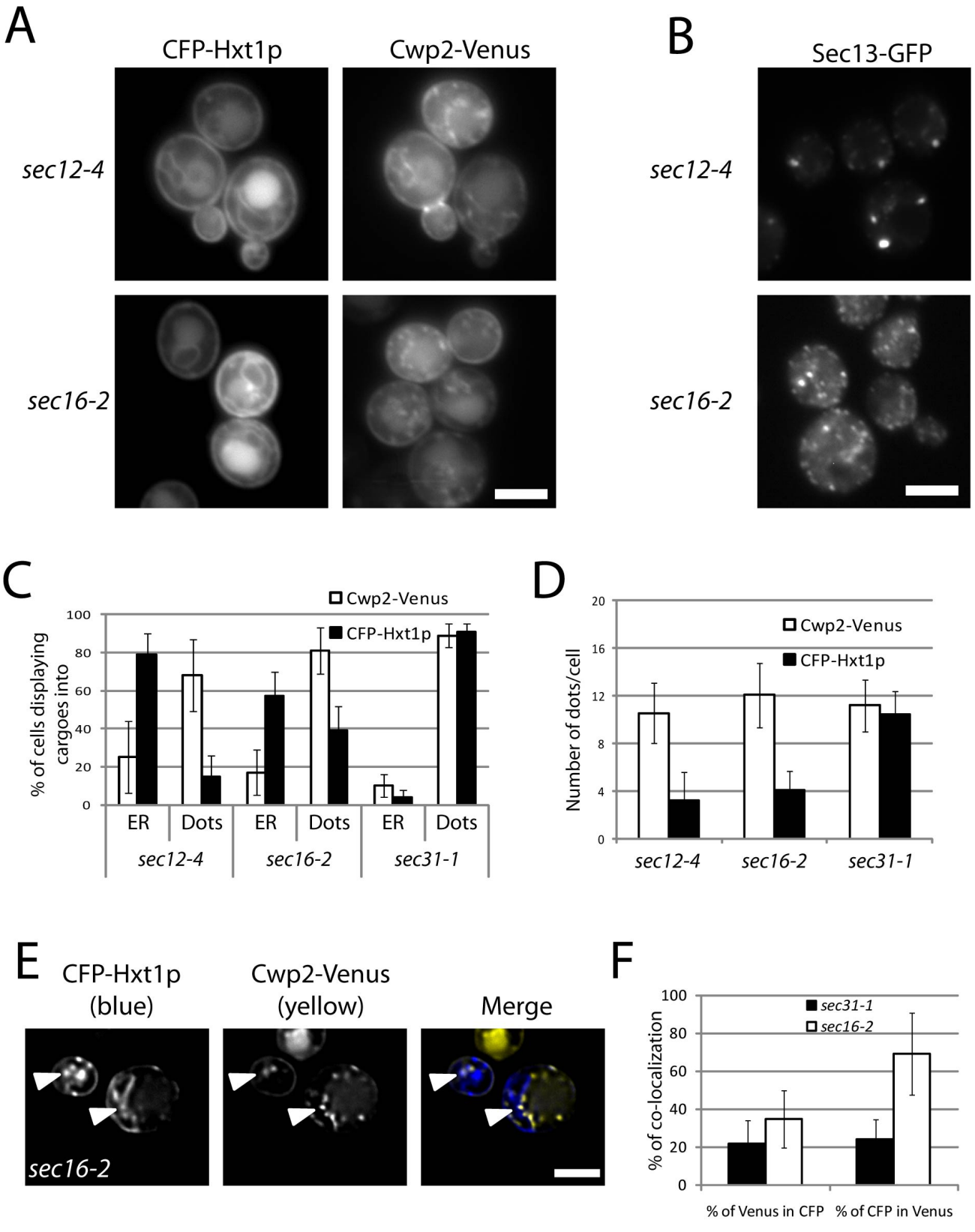
A
CFP-Hxt1p
Cwp2-Venus
sec12-4
sec16-2
B
Sec13-GFP
sec12-4
sec16-2
C
Cwp2-Venus
CFP-Hxt1p
% of cells displaying cargoes into
100
80
60
40
20
0
ER
Dots
ER
Dots
ER
Dots
sec12-4
sec16-2
sec31-1
D
Cwp2-Venus
CFP-Hxt1p
Number of dots/cell
20
16
12
8
4
0
sec12-4
sec16-2
sec31-1
E
CFP-Hxt1p (blue)
Cwp2-Venus (yellow)
Merge
sec16-2
F
sec31-1
sec16-2
% of co-localization
100
80
60
40
20
0
% of Venus in CFP
% of CFP in Venus

Fig. 5

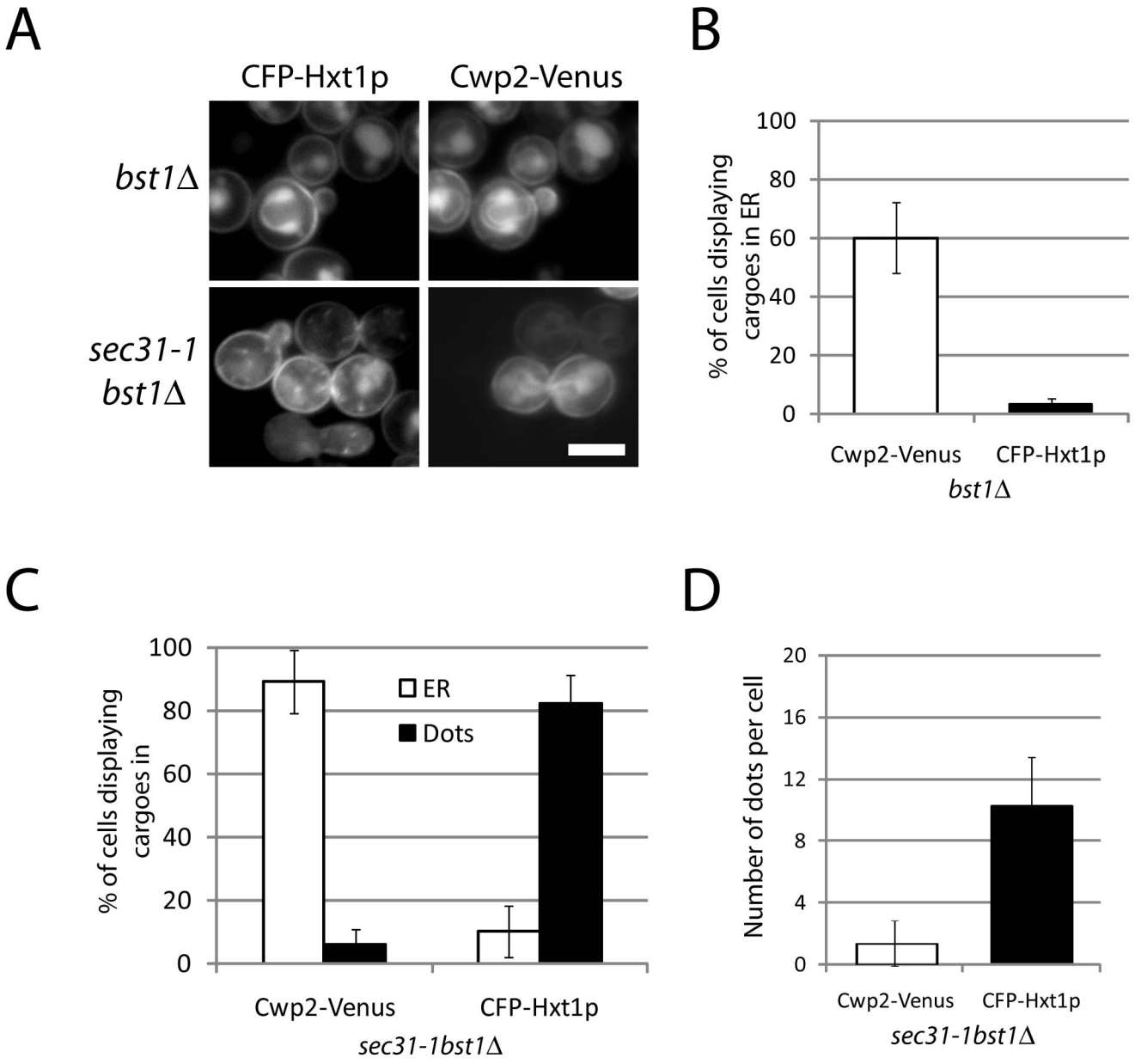
A
CFP-Hxt1p
Cwp2-Venus
bst1Δ
sec31-1
bst1Δ
B
% of cells displaying cargoes in ER
100
80
60
40
20
0
Cwp2-Venus
CFP-Hxt1p
bst1Δ
C
% of cells displaying cargoes in
ER
Dots
100
80
60
40
20
0
Cwp2-Venus
CFP-Hxt1p
sec31-1bst1Δ
D
Number of dots per cell
20
16
12
8
4
0
Cwp2-Venus
CFP-Hxt1p
sec31-1bst1Δ

Fig. 6

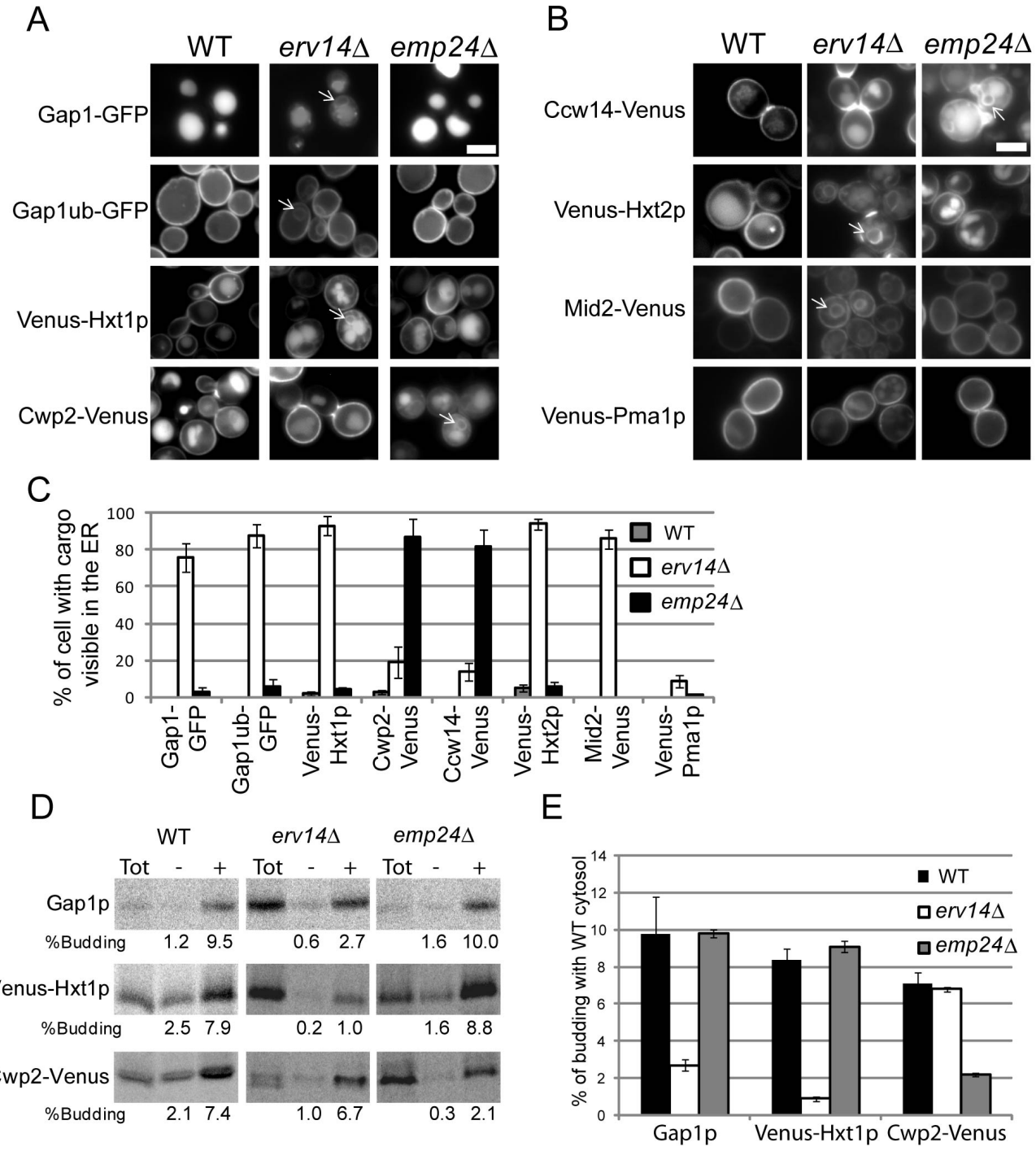
A
WT
erv14Δ
emp24Δ
Gap1-GFP
Gap1ub-GFP
Venus-Hxt1p
Cwp2-Venus
B
WT
erv14Δ
emp24Δ
Ccw14-Venus
Venus-Hxt2p
Mid2-Venus
Venus-Pma1p
C
% of cell with cargo visible in the ER
100
80
60
40
20
0
WT
erv14Δ
emp24Δ
Gap1-GFP
Gap1ub-GFP
Venus-Hxt1p
Cwp2-Venus
Ccw14-Venus
Venus-Hxt2p
Mid2-Venus
Venus-Pma1p
D
WT
erv14Δ
emp24Δ
Tot - + Tot - + Tot - +
Gap1p
%Budding 1.2 9.5 0.6 2.7 1.6 10.0
Venus-Hxt1p
%Budding 2.5 7.9 0.2 1.0 1.6 8.8
Cwp2-Venus
%Budding 2.1 7.4 1.0 6.7 0.3 2.1
E
% of budding with WT cytosol
14
12
10
8
6
4
2
0
WT
erv14Δ
emp24Δ
Gap1p
Venus-Hxt1p
Cwp2-Venus

Fig. 7

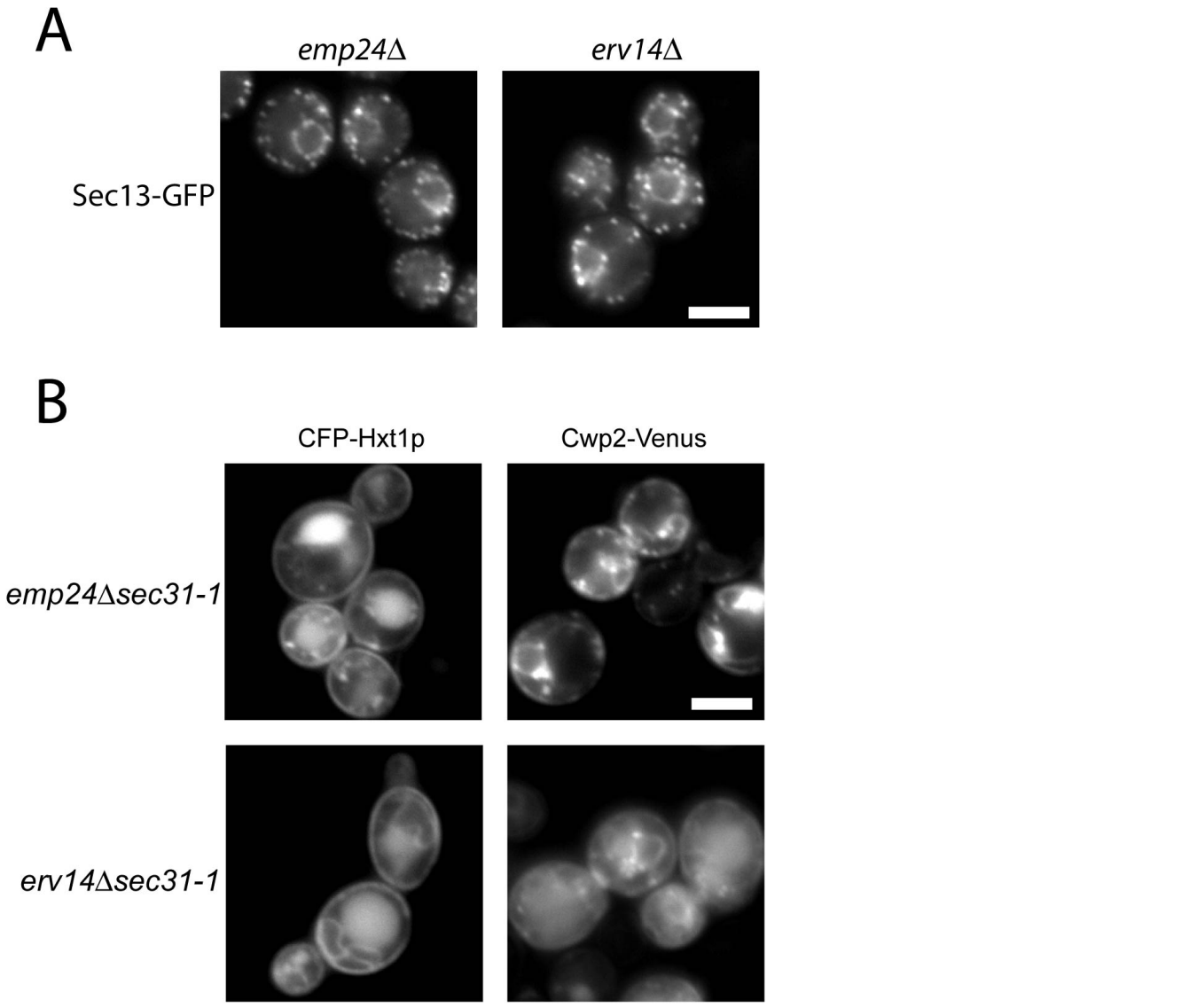
A
emp24Δ
erv14Δ
Sec13-GFP
B
CFP-Hxt1p
Cwp2-Venus
emp24Δsec31-1
erv14Δsec31-1
C
% of cells displaying cargoes in
100
80
60
40
20
0
Cwp2-Venus
CFP-Hxt1p
ER
Dots
ER
Dots
emp24Δsec31-1
erv14Δsec31-1
D
Number of dots per cell
20
16
12
8
4
0
Cwp2-Venus
CFP-Hxt1p
emp24Δ sec31-1
erv14Δ sec31-1

Fig. 8

A

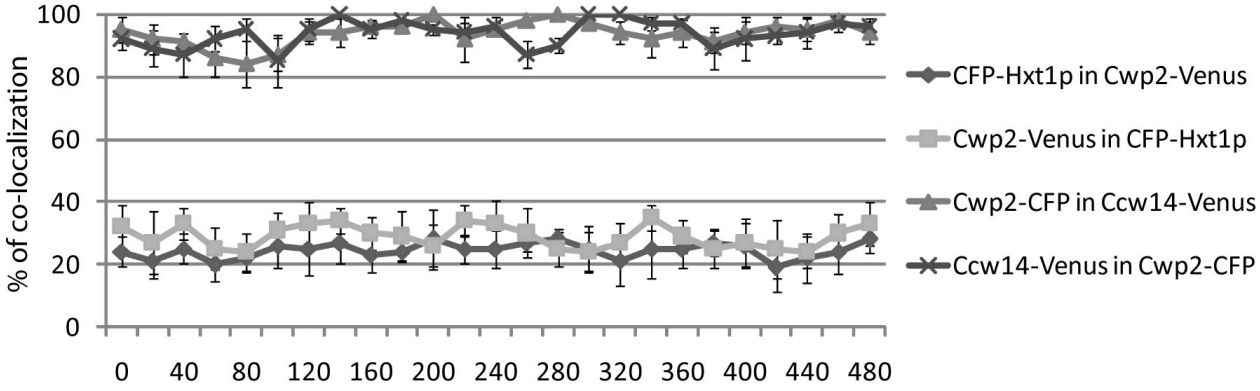
100
80
60
40
20
0
% of co-localization
0
40
80
120
160
200
240
280
320
360
400
440
480
CFP-Hxt1p in Cwp2-Venus
Cwp2-Venus in CFP-Hxt1p
Cwp2-CFP in Ccw14-Venus
Ccw14-Venus in Cwp2-CFP

B

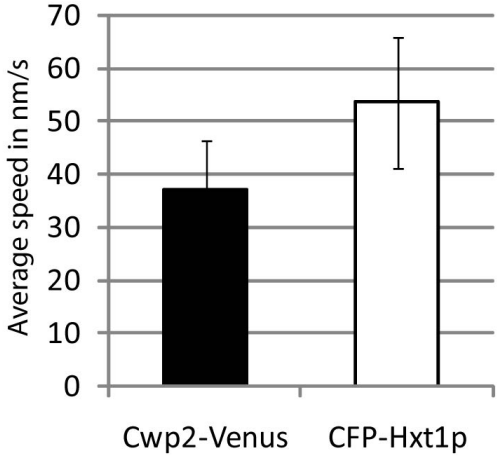
70
60
50
40
30
20
10
0
Average speed in nm/s
Cwp2-Venus
CFP-Hxt1p

Fig. 9

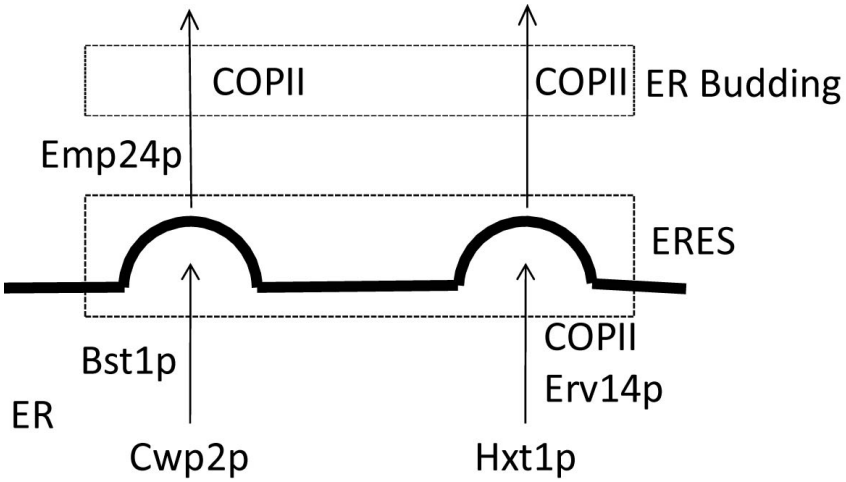
COPII
COPII
ER Budding
Emp24p
ERES
Bst1p
COPII
Erv14p
ER
Cwp2p
Hxt1p

Fig. 10

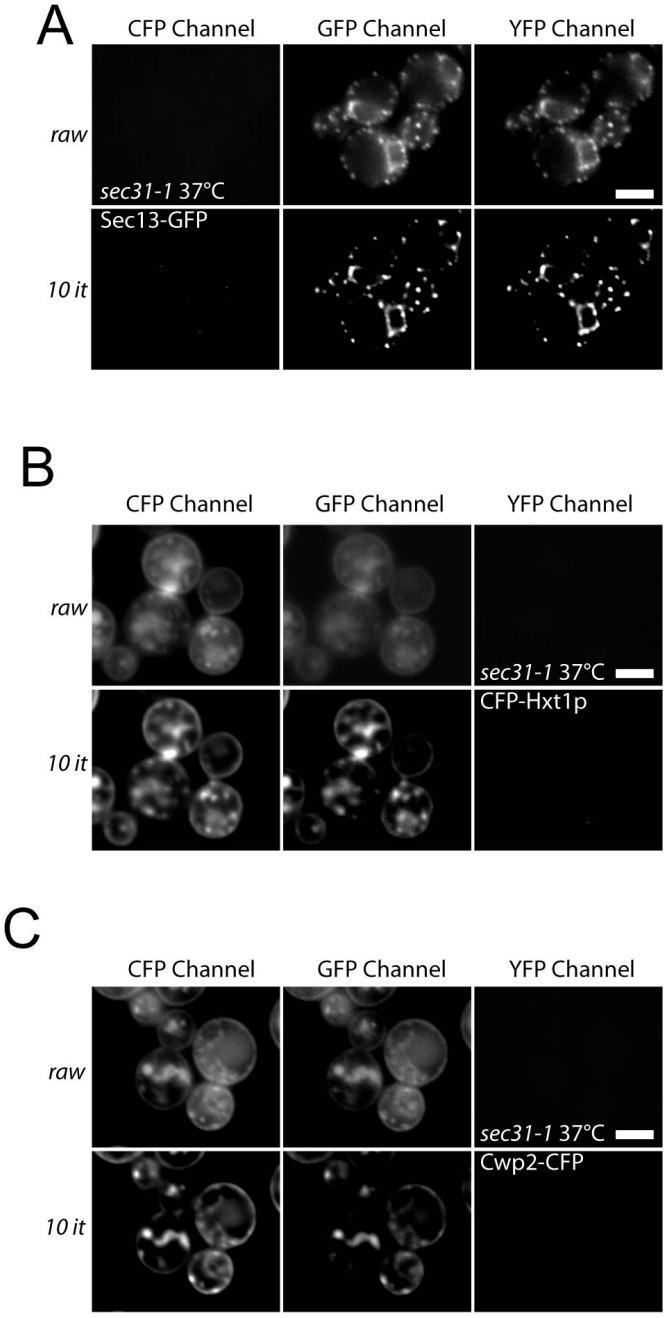
A
CFP Channel
GFP Channel
YFP Channel
raw
sec31-1 37°C
Sec13-GFP
10 it
B
CFP Channel
GFP Channel
YFP Channel
raw
sec31-1 37°C
CFP-Hxt1p
10 it
C
CFP Channel
GFP Channel
YFP Channel
raw
sec31-1 37°C
Cwp2-CFP
10 it

Fig. S1

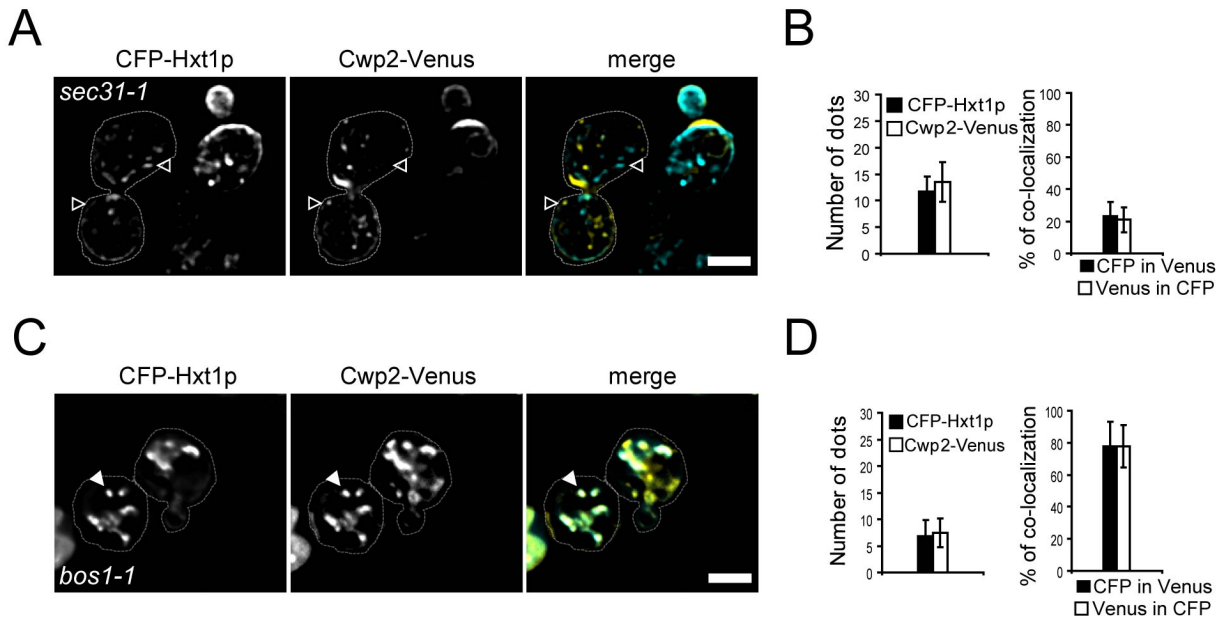
A
CFP-Hxt1p
Cwp2-Venus
merge
sec31-1
B
Number of dots
CFP-Hxt1p
Cwp2-Venus
% of co-localization
CFP in Venus
Venus in CFP
C
CFP-Hxt1p
Cwp2-Venus
merge
bos1-1
D
Number of dots
CFP-Hxt1p
Cwp2-Venus
% of co-localization
CFP in Venus
Venus in CFP

Fig. S2

III.C- Additional results

III.C1- Emp24p and GPI-anchored protein ER exit in yeast.

We previously hypothesized that Emp24p and Erv14p are ER exit receptors for two parallel ER-to-Golgi pathways. As described previously (Schuldiner et al., 2005), we wanted to confirm the synthetic interaction between Emp24p/Per1p (remodeling) and Erv14p. At 24°C (fig.1) and higher temperatures (data not shown), the growth of *emp24Δerv14Δ* and *per1Δerv14Δ* is slower that the single mutants. The double mutant *per1Δemp24Δ* grows almost as well as the corresponding single mutants. This implies that lipid remodeling of GPI-anchored proteins and Emp24p work in the same pathway, whereas Erv14p contributes to a second pathway. Disturbance of both pathways results in a severe growth phenotype and has a strong effect on morphogenesis (fig.2). If Emp24p and Erv14p are ER exit receptors, we suppose that they should co-localize with their respective cargo at the ERES. Therefore, we decide to fuse Emp24p and Erv14p with fluorescent proteins. After

Fig.1. Genetic interaction between *EMP24*, *ERV14* and *PER1*. The cells were grown on YPD plates at 24°C.

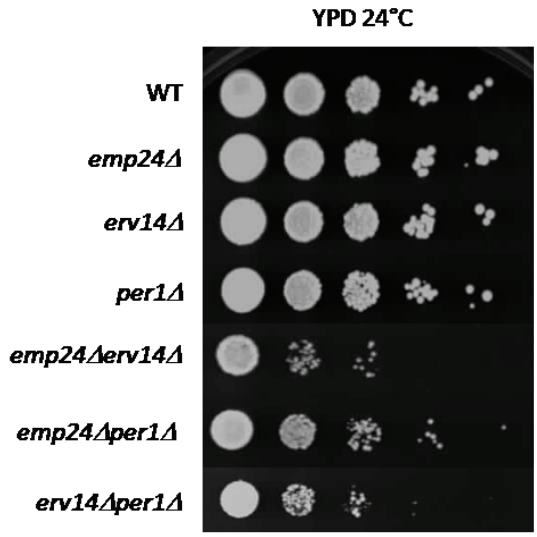

Fig.2. Morphogenesis of WT, *emp24Δ*, *erv14Δ* and *emp24Δerv14Δ* cells at 30°C. Phase contrast of live cells at 30°C.

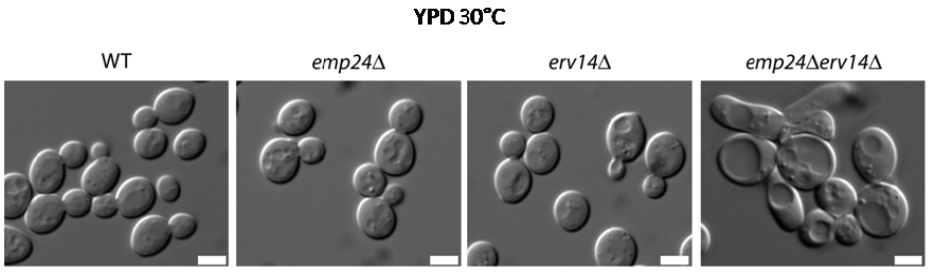

several trials, we inserted the gene coding for cerulean (CFP) inside the sequence of EMP24 in order to obtain a functional protein (fig. 3, 4A).

Fig. 3. Emp24p sequence and insertion of CFP. EMP24 and its promoter have been inserted into the centromeric plasmid ycplac111.

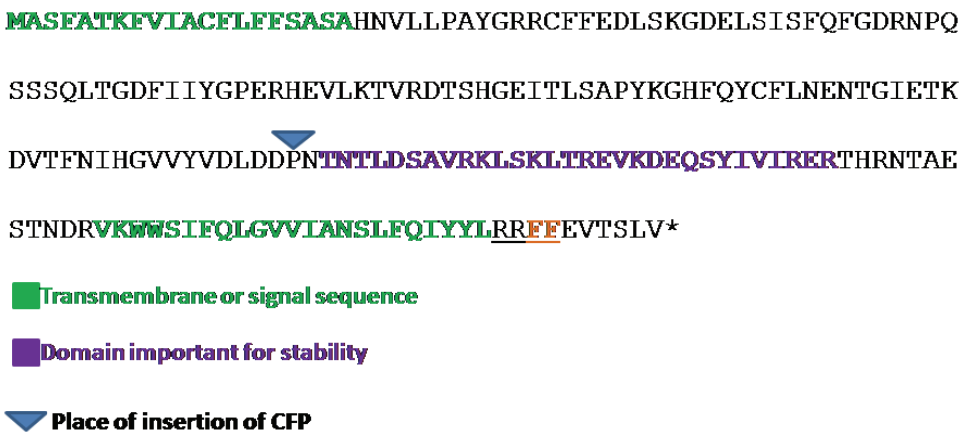

We integrated at the genomic locus the coding sequence for mCitrine downstream of *ERV14.* As seen in fig.4B, Erv14-mCi is functional since Hxt1p is normally sent to the plasma membrane. In wild-type cells, Emp24p and Erv14p co-localize with the cis-Golgi marker Sed5p (fig. 4C-E). In *sec31-1* Emp24p and Erv14p still co-localize with Sed5p (fig. 4F-H), which itself co-localizes with Sec13-GFP (fig.5). These results imply that Emp24p and Erv14p are incorporated into ERES in *sec31-1* at 37°C. However, considering the sorting of Cwp2p and Hxt1p we would have expected that Emp24p and Erv14p do not co-localize. Therefore we examined the co-localization of Emp24p and Erv14p with their respective cargo in *sec31-1*. Erv14p and Hxt1p do co-localize, reinforcing the idea that Erv14p is an ER exit receptor (fig. 6C-D). On the other hand, only 40% of Cwp2p dots co-localized with Emp24p (fig. 6A-B). This surprising result forced us to revisit the function of Emp24p. If Emp24p is an ER exit receptor, then we have to assume that there are two pools of Emp24p: one that functions for GPI-anchored protein ER exit and another that does not.

Fig. 4. Localization of Emp24p and Erv14p. (A) Expression of Cwp2-Venus in wild-type cells (WT), in *emp24Δ* cells expressing the empty plasmid ycplac111 and in *emp24Δ* cells expressing ycplac111 containing EMP24-CFP. (B) Expression of CFP-Hxt1p in wild-type cells (WT), in *erv14Δ* cells and in *erv14::mCi* cells. (C) Expression of ycplac111 containing EMP24CFP in wild-type cells expressing Erv14-mCi and mRFP-Sed5p. (D,E) Quantification of several images acquired as in (C). (F) Expression of ycplac111 containing EMP24CFP in *sec31-1* cells expressing Erv14-mCi and mRFP-Sed5p. (G,H) Quantification of several images acquired as in (F). Raw images. Arrow : ER. Plain white arrow : co-localizing dots. Scale bar : 5μm.

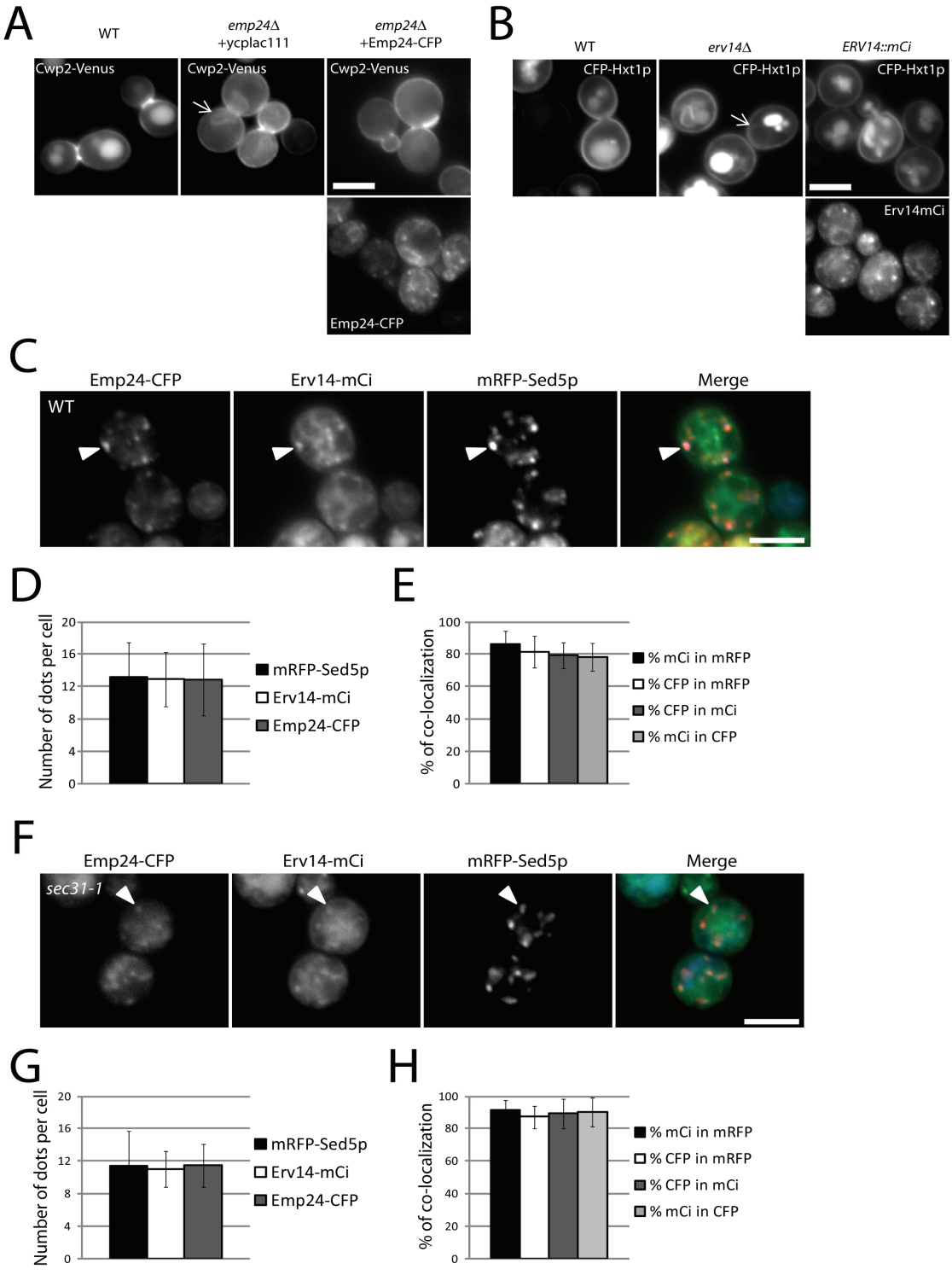

Fig. 5. Localization of Sec13-GFP and mRFP-Sed5p in WT and *sec31-1* at 37°C. (A) Live images of WT and *sec31-1* at 37°C expressing Sec13-GFP and mRFP-Sed5p. (B) Quantification of several images acquired as in (A). Images deconvoluted by 10 iterations. Open arrow head : no-colocalizing dots. White plain arrow head : colocalizing dots. Scale bar : 3µm.

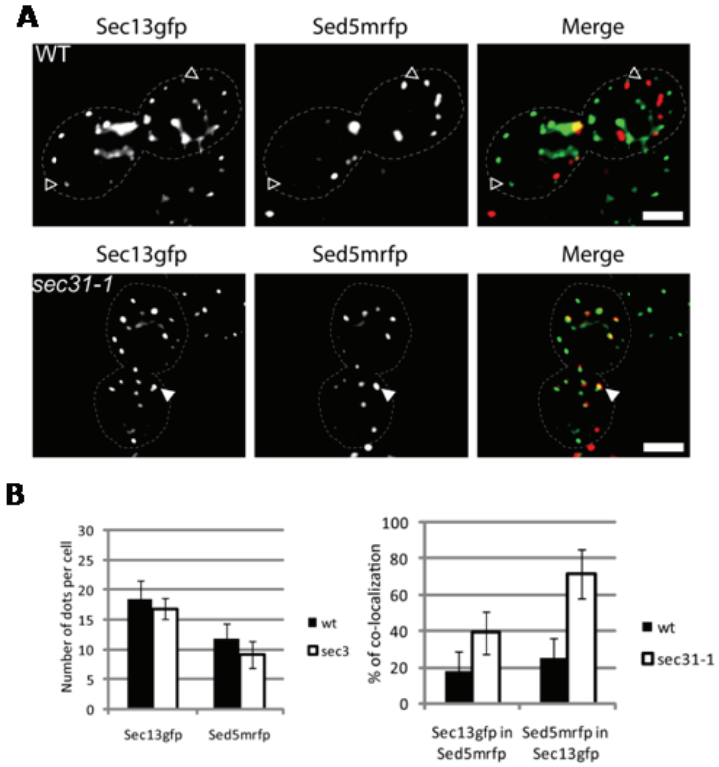

Fig. 6. Co-localization of Erv14p and Emp24p with Hxt1p and Cwp2p respectively. (A) live images of *sec31-1* at 37°C expressing Emp24-CFP and Cwp2-Venus. (B) Quantification of several images acquired as in (A). (C) live images of *sec31-1* at 37°C expressing Erv14-mCi and CFP-Hxt1p. (C) Quantification of several images acquired as in (D). Images deconvoluted by 10 iterations. Open arrow head : no-colocalizing dots. White plain arrow head : colocalizing dots. Scale bar : 5µm.

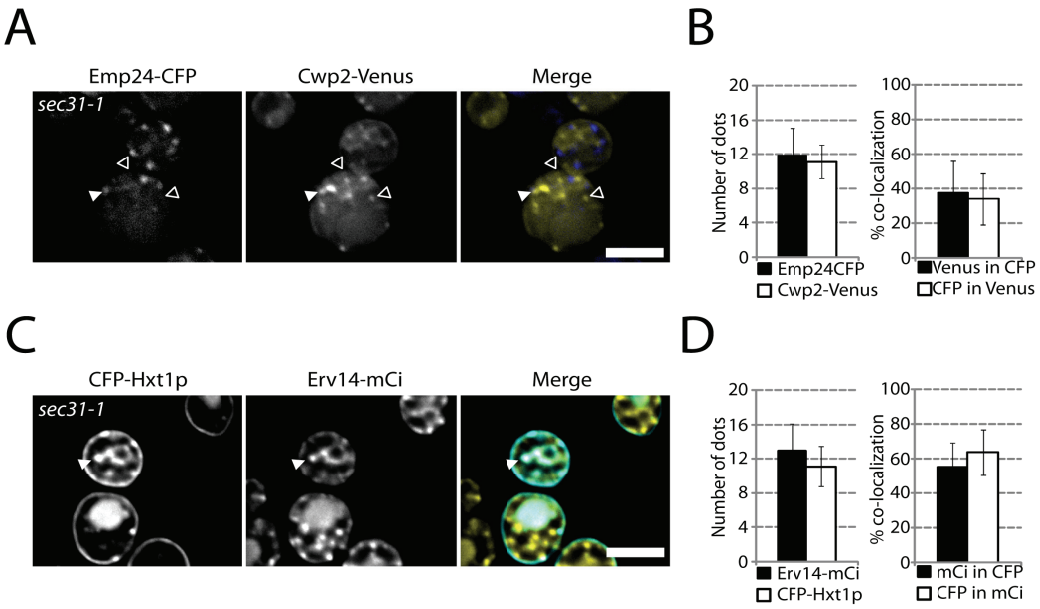

Furthermore, not all of the Cwp2p dots colocalize with Emp24p. To explain this one might envisage that there are two pools of concentrated Cwp2p, one that colocalizes with Emp24p and is ready for ER exit and another that has not yet interacted with Emp24p and is not ready for ER exit. The other alternative is that Emp24p plays some other function in ER exit and is not an ER exit receptor. Among alternative explanations for Emp24p function it could be that Emp24p is involved in retrieval from the Golgi of the real exit receptor or it is a regulator of the ER exit receptor.

To explore Emp24p function further, we wanted to know the relationship between Emp24p and remodeling. As previously mentioned, Cwp2p cannot accumulate in ER structures prior budding in *bst1Δ* cells. We looked at the localization of Cwp2p in the other mutants for remodeling: *per1Δ, gup1Δ* and *cwh43Δ*. With the exception of *cwh43Δ*, Cwp2p failed to exit ER efficiently in *per1Δ* and *gup1Δ* cells (fig.7A-B). In *cwh43Δ* cells, Cwp2p did not accumulate in the ER but displayed a diffuse localization throughout the cell and in the vacuole. In *cwh43Δ* cells, we observed a more pronounced defect in Gas1p maturation than in *emp24Δ* by western-blotting and by pulse-chase (data not shown). Either the effect of *cwh43Δ* knockout is specific for Gas1p or *cwh43Δ* cells display a glycosylation defect.

After combining the *sec31-1* mutation with the knockout of the different genes coding for remodeling enzymes, we looked if Cwp2p was able to be concentrated into specific ER domains (fig. 7B-E). As seen previously for *bst1Δsec31-1*, Cwp2p failed to localized into dots if any step of remodeling was compromised, including the one accomplished by Cwh43p. This suggests that either Cwh43p is involved in Cwp2p remodelling or in microdomain formation. However, this does not explain the localization of Cwp2p in *cwh43Δ* cells. This intriguing localization might be related to what was observed in *lcb1-100* cell. Lcb1p is

directly involved in ceramide synthesis. In *lcb1-100*, Gas1p maturation is strongly impaired, due to a weak membrane association of Gas1p (Watanabe et al., 2002). But similar to *cwh43Δ* cells, in *lcb1-100* we could not observe an accumulation of Cwp2p in the ER, but a diffused localization in the cytosol and in the vacuole (data not shown). Considering that Cwh43p has been described to catalyze the transfer of phytoceramides to the GPI anchor, then the direct targeting to the vacuole through a non-concentrative pathway out of the ER, can be related to the presence of diacylglycerol on the GPI anchor ; the phenotype being stronger in *lcb1-100* because of the absence of ceramides in the ER membrane.

Despite the fact that Emp24p did not colocalize with Cwp2p in *sec31-1*, we examined the localization of Emp24p in the remodeling mutants in order to provide evidence that Emp24p acts downstream of remodeling (fig. 8). Whereas the localization of Erv14p is not significantly modified in the remodeling mutants, Emp24p is relocalized into the ER in *bst1Δ, per1Δ* and g*up1Δ*. In *cwh43Δ* cells, the defect is not obvious, however there is a higher heterogeneity of phenotypes with a mix of cells where Emp24p is found in the ER and cells with no significant defect.

These results suggest that Emp24p functions downstream of remodeling, however the conversion of diacylglerol to phytoceramide is not a absolute prerequisite for proper localization of Emp24p. Even though this is a good indication that Emp24p may interact with remodeled GPI-anchored proteins and that this interaction might influence the localization of Emp24p, the co-localization of Emp24p with Cwp2p in *sec31-1* supposes a complex regulation of GPI-anchored protein ER exit (see discussion).

Fig.7. Cwp2p localization in remodeling mutants. (A) live images of wild-type and remodeling mutant cells expressing Cwp2-Venus and CFP-Hxt1p at 37°C. (B) Quantification of several images acquired as in (A). The graphic displays the percentage of cells showing Cwp2p or Hxt1p in the ER. (C) live images of *sec31-1* and remodeling mutant cells combined with the *sec31-1* mutation expressing Cwp2p and Hxt1p at 37°C. (D,E) Quantification of several images acquired as in (C). (D)The graphic displays the percentage of cells showing Cwp2p or Hxt1p in the ER or in dots. (E) The graphic displays the number of dots of Cwp2p and Hxt1p visualized in cells exhibiting dots. Scale bar : 5µm.

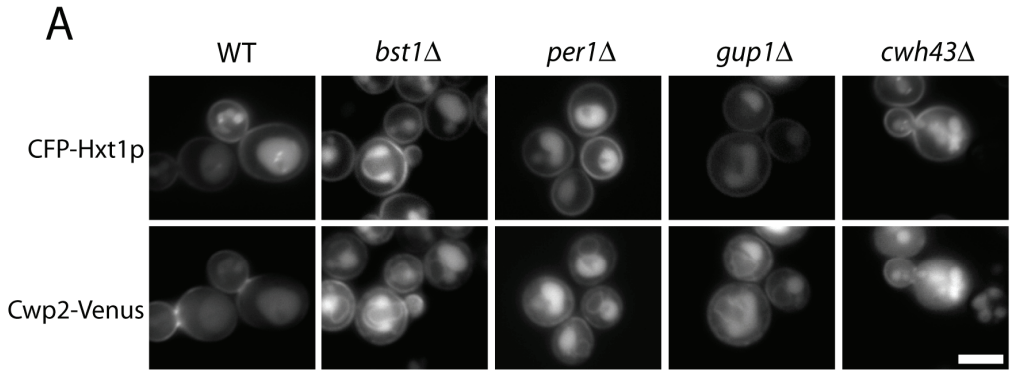

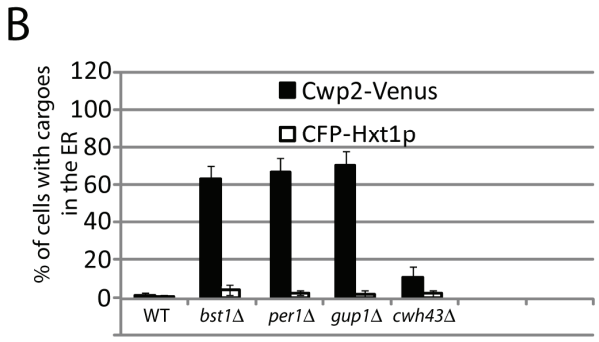

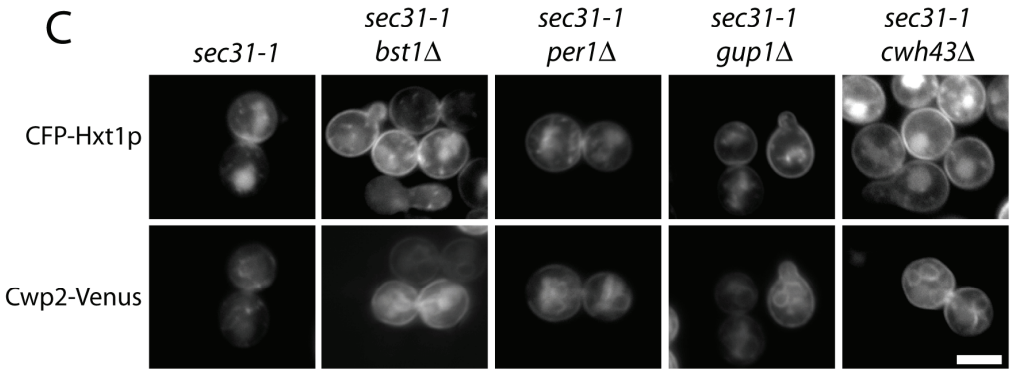

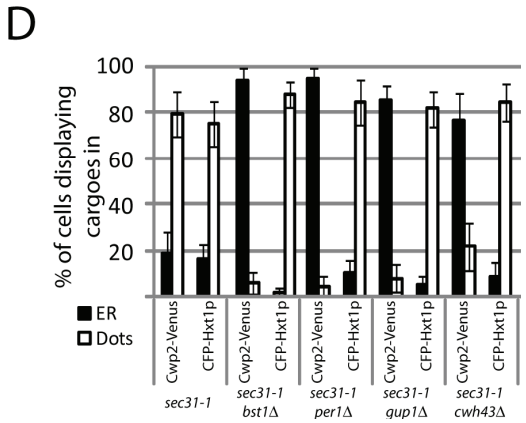

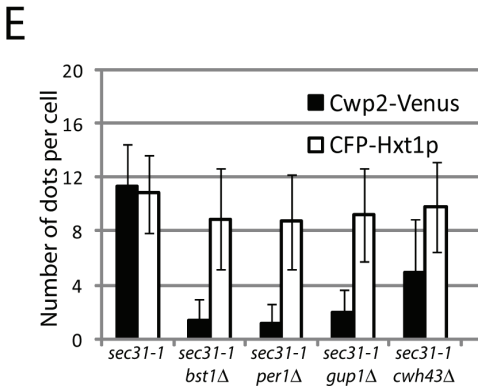

Fig. 8. Localization of Emp24p and Erv14p in remodeling mutants. (A) live images of wild-type and remodeling mutant cells expressing Emp24-CFP and Erv14-mCi at 37°C. (B) Quantification of several images acquired as in (A). The graphic displays the number of dots of Emp24p and Erv14p visualized in cells exhibiting dots. Scale bar : 5μm.

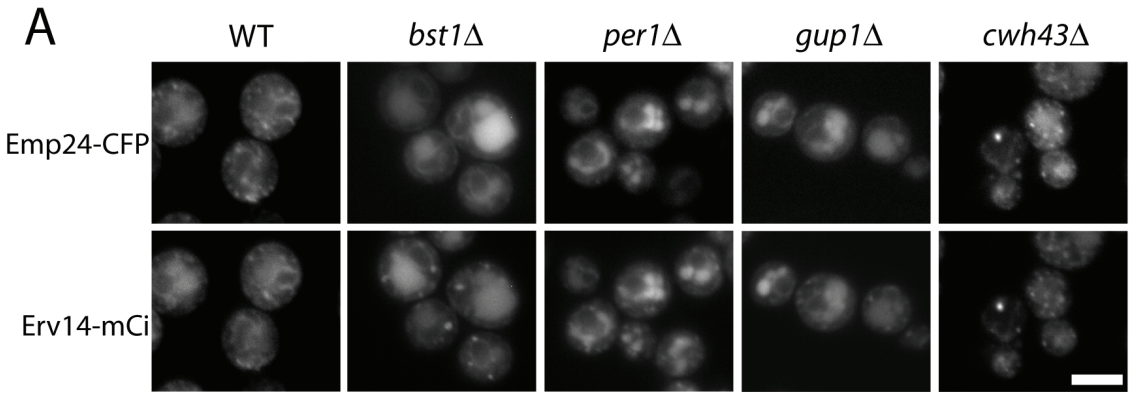

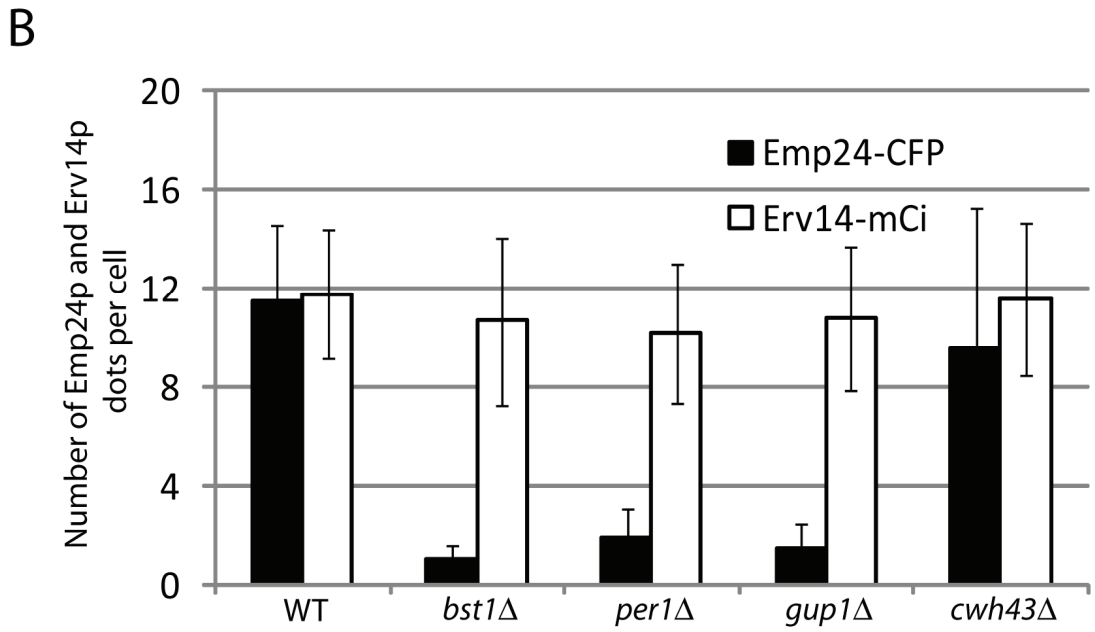

III.C2-Sar1p and sorting.

As mentioned in the introduction, Sar1p is the small Ras GTPase, which upon activation by the guanine nucleotide exchange factor (GEF) Sec12p, triggers cargo loading and COPII coat assembly. The GTP hydrolysis by Sar1p is mediated by the activity of GTPase activating protein (GAP), which accelerates GTP hydrolysis and reverses the Sec23p/Sec24p-Sar1p interaction. Interestingly Sec23p is the GAP for Sar1p and the GAP activity is further stimulated by recruitment of Sec13p/Sec31p (Antonny et al., 2001; Yoshihisa et al., 1993). This phenomena should theoretically prevent the formation of a stable prebudding complex. But actually it has been shown *in vitro* that the Sec23p/Sec24p complex is maintained on the membrane by the presence of the GEF Sec12p, which counteracts the GTPase-stimulating activity of the coat by continually recharging Sar1p with GTP (Futai et al., 2004). Furthermore Sec23p/Sec24p can associate with assembled cargo even after Sar1p GTP hydrolysis, but this interaction is disrupted upon GTP hydrolysis if cargo molecules are not properly assembled/ oligomerized (Sato and Nakano, 2005). By this relationship, Sar1p selectively promotes exclusion of unassembled cargo molecules from forming COPII vesicles by virtue of its GTP hydrolysis (Sato and Nakano, 2004).

Sar1p being the central actor of the COPII coat formation, we assayed its requirement for GPI-anchored protein ER exit. Therefore we performed budding assay in presence of the GTP-locked form of Sar1p (Dn H77L) or using the thermosensitive allele of Sar1p (fig.1). We observed that the GTP hydrolysis of Sar1p is not strictly required for ER budding of the GPI-anchored proteins Gas1p and Cwp2p and the transmembrane protein Hxt1p in contrast to Gap1p (fig.1A, B). Furthermore the Sar1p activity is partially dispensable for ER exit of GPI-

anchored proteins, whereas Gap1p and to a lower extent, Hxt1p, required Sar1p for ER budding (fig.1C,D).

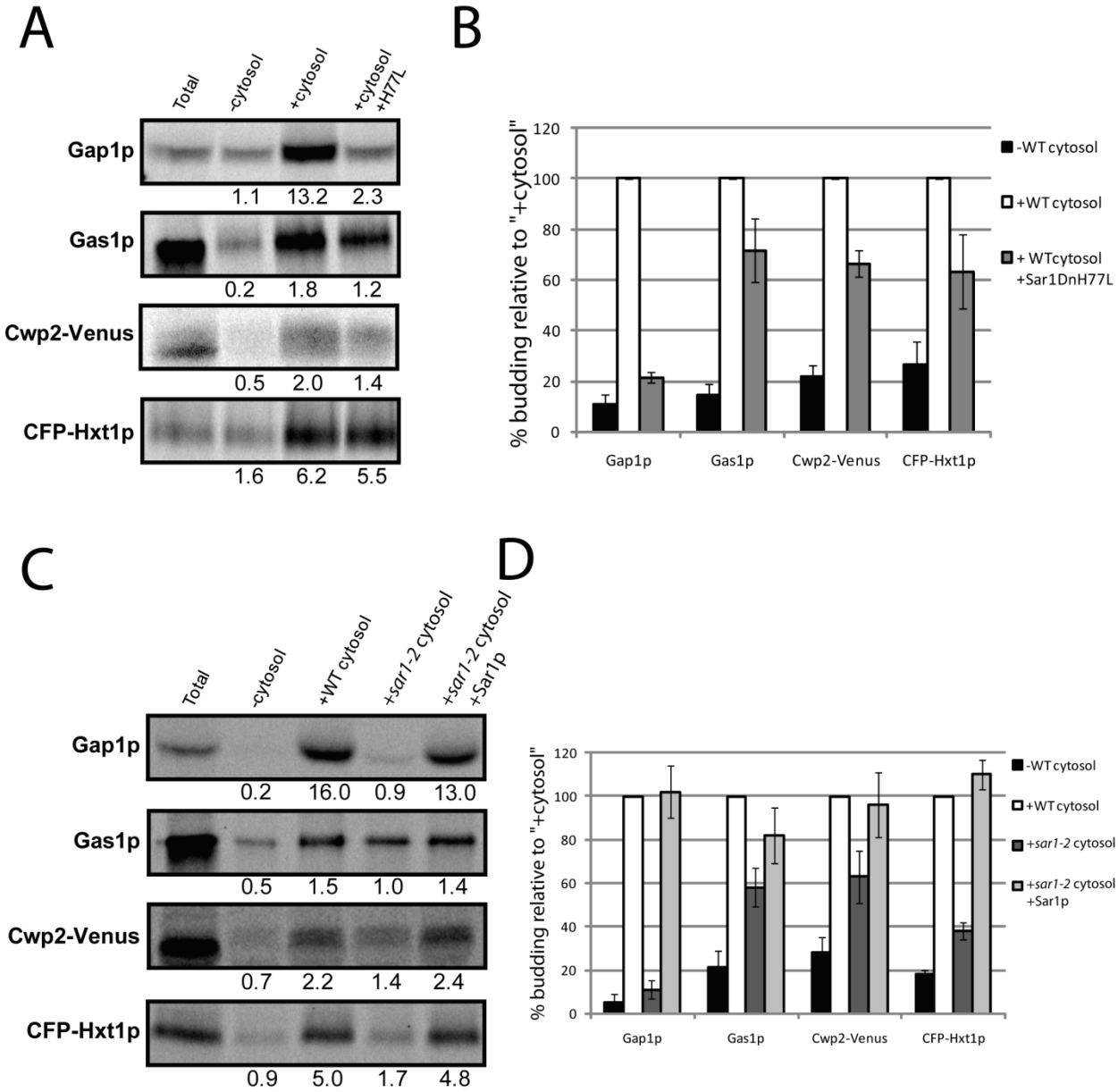

Fig.1. GPI-anchored protein ER budding is Sar1p independent.
A. Budding assay in presence of Sar1 DNnH77L. B Quantification of several assays as performed in A. The Y axis represents the % of budding relative to the % of budding calculated in presence of WT cytosol. C. Budding assay in presence of *sar1-2* cytosol. D Quantification of several assays as performed in C. The Y axis represents the % of budding relative to the % of budding calculated in presence of WT cytosol.

From these surprising results, we decided to look at Emp24p and another GPI-anchored protein Ccw14p budding in order to extract some model concerning the requirement of Sar1p. In the Fig.2, we observed that the GPI-anchored protein Ccw14p ER budding is Sar1p

independent in contrast to the soluble cargo incorporated into the Gap1p containing vesicle, alpha factor. Emp24p budding in presence of the GTP-locked form of Sar1p displayed an intermediate phenotype. This probably illustrates the fact that Emp24p is required for the ER exit of GPI-anchored proteins and that a majority of Emp24p could be found in Erv14p positive ER-derived vesicles.

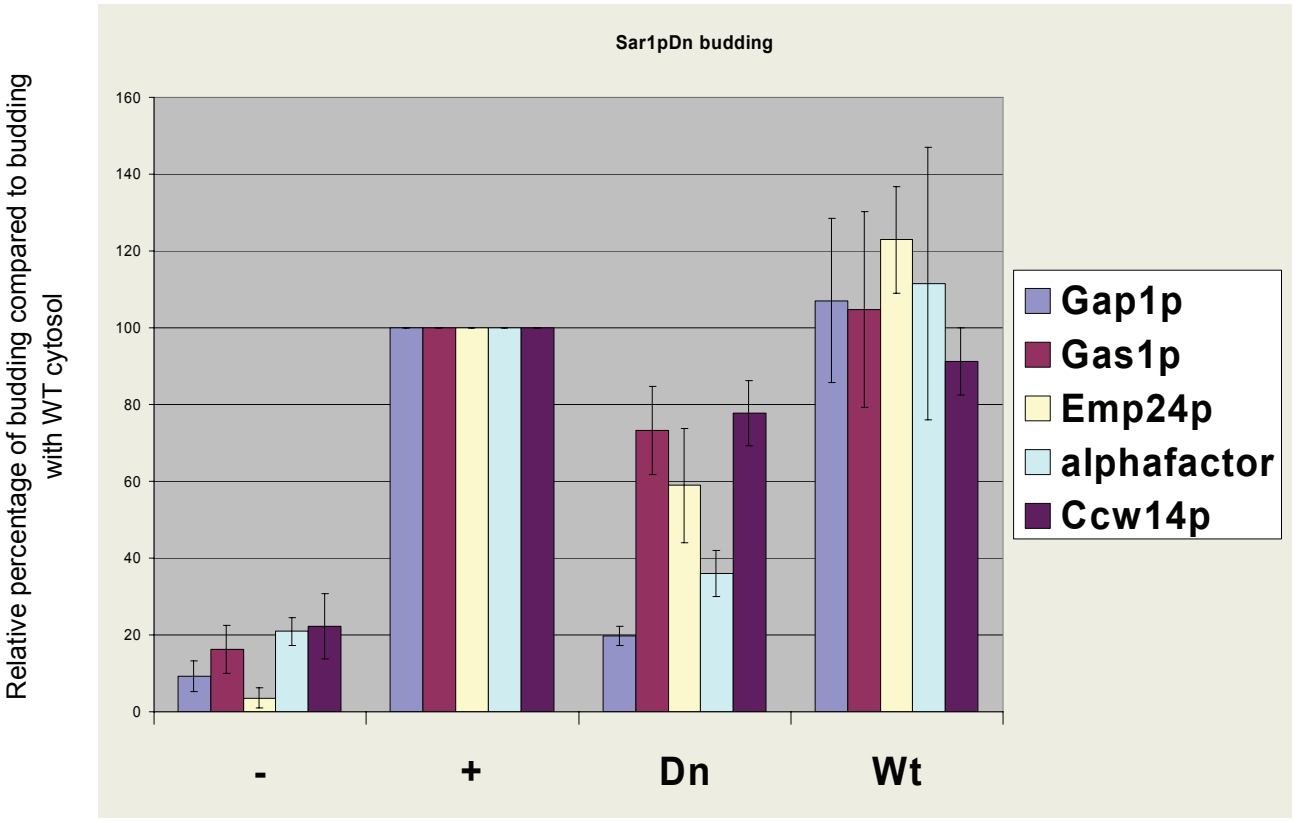

Fig.2. ER budding in presence of GTP-locked form of Sar1p.
Budding assay in presence of Sar1 DNnH77L. Quantification of 3 assays as performed in fig.1A. The Y axis represents the % of budding relative to the % of budding calculated in presence of WT cytosol. (-): budding without cytosol; (+): budding with WT cytosol; (Dn): budding with WT cytosol and the GTP-locked form of Sar1p; (Wt): budding with WT cytosol and wild-type Sar1p.

The study of the transmembrane protein Sfk1p may help us to better understand the requirement of Sar1p upon ER budding. Sfk1p contains 6 potential transmembrane domains and is localized at the plasma membrane (Audhya and Emr, 2002). Sfk1p recruits the type III phosphatidylinositol 4-kinase Stt4p at the plasma membrane, involved in the activation of the MAP kinase cascade in response to heat shock (Audhya and Emr, 2002). We decided to fuse Sfk1p with Venus at the C-terminus (Sfk1-V) and the N-terminus (V-Sfk1p) since we

could not identify any known ER exit signal (fig.3). Both constructs localized to the plasma membrane, suggesting that the fusion with Venus did not

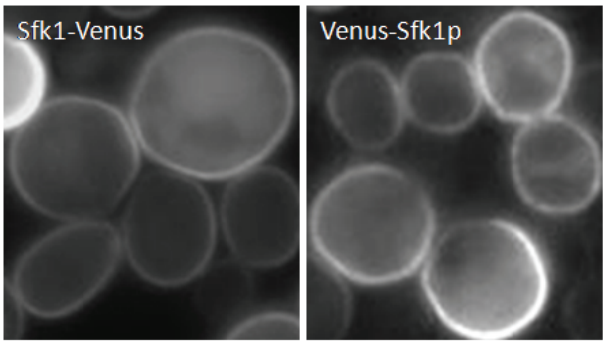

Fig.3. Localization of Sfk1p fused with Venus in Ct and Nt in wild-type cells

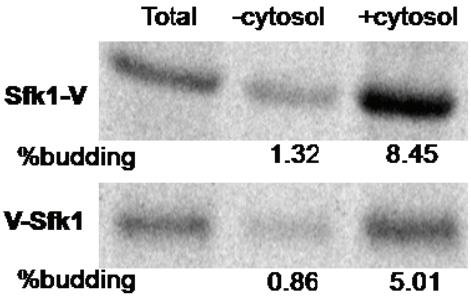

Fig.4. *In vitro* budding assay of Sfk1p fused with Venus in Ct and Nt using wild-type spheroplasts and cytosol.

disturb the ER exit of Sfk1p. Both fusions bud from ER with efficiencies of the same order (fig.4).

Surprisingly the two fusions exit ER in different ER-derived vesicle populations (fig.5). Indeed when fused in N-terminus with Venus, a significant fraction of Sfk1p is found in Gap1p containing vesicles, whereas when fused in C-terminus with Venus, Sfk1p is excluded from the Gap1p containing vesicles. From these results we can imagine that Sfk1p contains a specific signal for sorting in N-terminus or C-terminus, which is disturbed by the fusion with Venus. From our previous results, where we have shown that ER exit signal

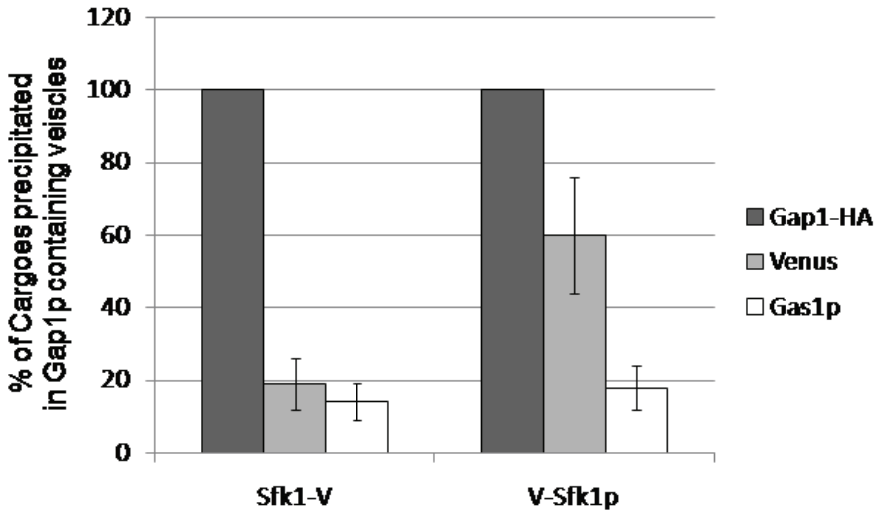

Fig.5. Sorting assay of Sfk1p.
Quantification of 3 sorting assays. Gap1p containing vesicles have been precipitated with HA antibody. The Y axis displays the percentage of cargo co-immuno-precipitated with Gap1-HA containing vesicles. Sfk1-V and V-Sfk1p are latter precipitated with the anti-Venus antibody.

drives cargoes into the Gap1p containing vesicles, we suppose that Sfk1p contains a sorting signal in its C-terminus. However as seen for Gap1p (Malkus et al., 2002), removal of ER exit signal leads to a strong decrease in budding efficiency, which is not the case for Sfk1p. Coming back to this later, we then looked at the Sar1p dependency for Sfk1p ER exit (fig.6). Sfk1-V ER budding does not require the GTP hydrolysis of Sar1p, similarly to the GPI-anchored protein Gas1p. Even though not that striking V-Sfk1 ER budding is more dependent of Sar1p GTP hydrolysis.

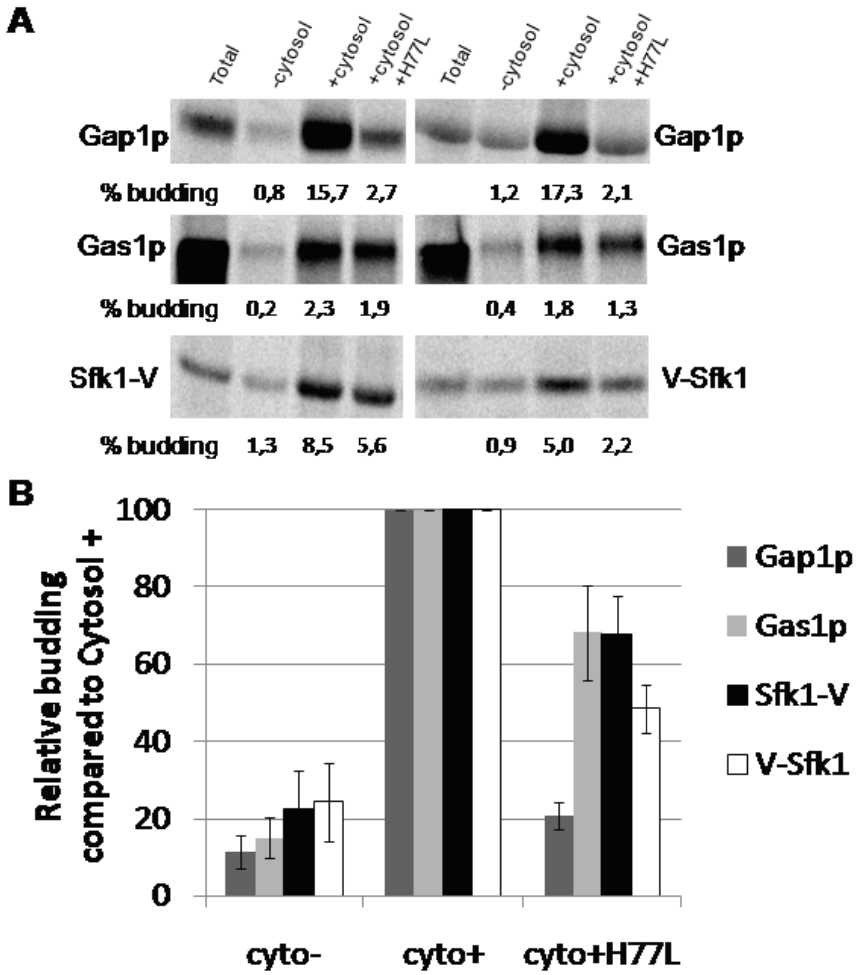

Fig.6. Sar1p dependency of Sfk1p. A. In vitro budding assay in presence of GTP-locked form of Sar1p (H77L). B Quantification of several assays as performed in A. The Y axis represents the % of budding relative to the % of budding calculated in presence of WT cytosol.

These results suggest a relationship between sorting and Sar1p dependency. To further understand this relationship, we looked at the localization of both constructs in *erv14Δ* cells (fig.7). At 30°C, V-Sfk1p localized in the perinuclear ER in *erv14Δ* cells, whereas Sfk1-V is normally found at the plasma membrane. However, Sfk1-V ER exit does not depend on Emp24p (data not shown). We could not test the functionality of both constructs, but if we suppose that both constructs are functional and not misfolded, then, likely Erv14p recognizes the C-terminus of Sfk1p and in combination with the GTP hydrolysis of Sar1p, Sfk1p is concentrated into ER-derived vesicles as seen for V-Sfk1p. Concerning Sfk1-V, the situation is unclear. If the interaction with Erv14p is disturbed because of the Venus fusion, we should expect a decrease in ER exit kinetics, which was not the case. Instead Sfk1p was sorted into another ER-derived vesicle population for which the requirement of Sar1p GTP hydrolysis is not strict. This could suggest the presence of an additionnal ER exit signal(s) in the Sfk1p sequence which are recessive to the potential C-terminus ER exit signal and are sufficient for entry into alternative ER-derived vesicles. Even though it may be too early to conclude on sorting mechanisms of Sfk1p, these results suggest there is a relationship between sorting, the GTP hydrolysis of Sar1p and Erv14p.

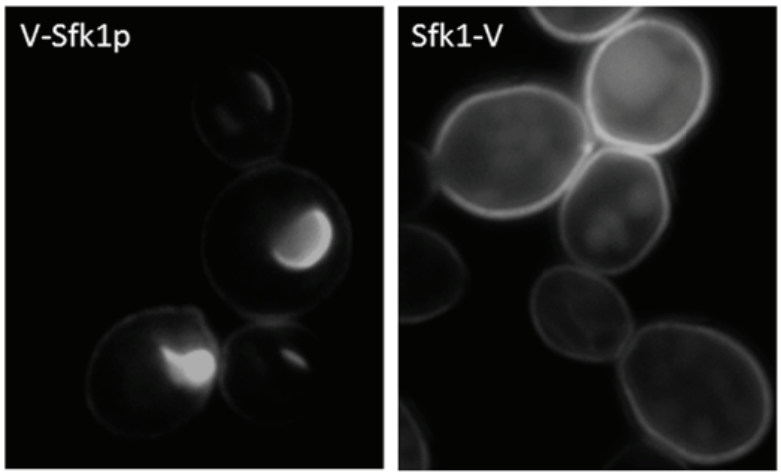

Fig.7. Localization of Sfk1p in *erv14Δ* cells

III.C3- Bos1p requirement and sorting.

We previously observed that SNAREs, tethering factors and the Rab GTPase Ypt1p are involved in sorting upon ER exit (Morsomme et al., 2003; Morsomme and Riezman, 2002). Considering that the fate of ER-derived vesicles is to fuse to the Golgi apparatus, we wondered if there was a specific set of molecules enriched on GPI-anchored protein containing vesicles. We tried to address this question by producing ER-derived vesicles and observed if we were able to precipitate specifically the GPI-anchored protein containing vesicles with antibodies against the v-SNARE Bos1p (Fig.8) and the potential ER exit receptor Emp24p (fig.9).

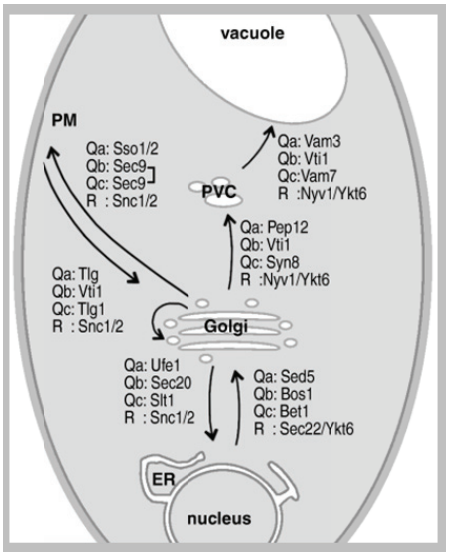

Fig.8. SNAREs and vesicular traffic in Yeast

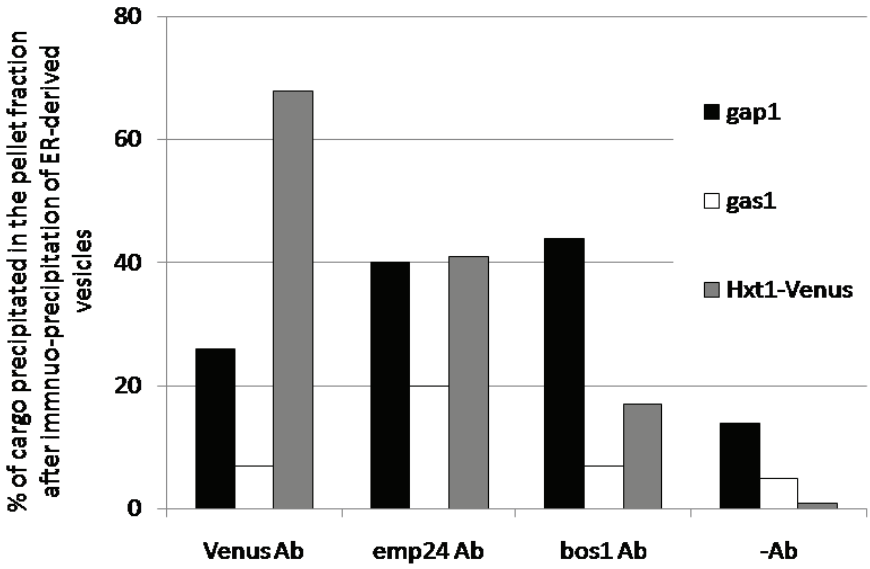

Fig. 9. Precipitation of specific ER-derived vesicles.
After being produced from wild-type spheroplasts and cytosol, ER-derived vesicles are immuno-precipitated with specific antibodies against Venus, Emp24p and Bos1p.

The antibody against Emp24p preferentially precipitated the Gap1p and Hxt1p containing vesicles, confirming what was seen *in vivo*. We could confirm that the v-SNARE Bos1p is

incorporated into the Gap1p containing vesicles, but Bos1p could not be found on the Gas1p and Hxt1p containing vesicles. This suggests that Hxt1p and Gas1p containing vesicles either do not expose any SNAREs or contain a different set of SNAREs molecules. In this perspective, we attempted to precipitate ER-derived vesicles with the antibodies against the SNARES Gos1p and Ykt6p, but this was unsuccessful in the sense that we could not precipitate any ER-derived vesicles even the Gap1p containing ones (data not shown). These results leave the open question: How GPI-anchored protein containing vesicles are able to fuse with the Golgi apparatus?

We previously observed that in *bos1-1* cells at 37°C, Cwp2-Venus and CFP-Hxt1p strongly co-localized in structures (Part III.B and fig.10A-B) which partially co-localize with the ERES markers Sec13-GFP (fig. 10C-F). This result suggests that both cargoes accumulate in a compartment post ER unable to fuse with the Golgi apparatus. In order to determinate if the sorting defect observed in *bos1-1* cells at 37°C occurs before or after budding, we observed the co-localization of Cwp2-Venus and CFP-Hxt1p in the mutant *bos1-1sec31-1* (fig. 10). Cwp2-Venus and CFP-Hxt1p no longer localized in the large structures seen in *bos1-1* cells, but in discrete punctate structures similar to what was observed in the *sec31-1* mutant. Additionally the co-localization percentage between Cwp2-Venus and CFP-Hxt1p is now equal to 40%. This result indicates that most of the sorting defect observed in *bos1-1* cells is the result of an event occurring after budding of ER-derived vesicles, suggesting that the SNARE Bos1p prevents heterotypic fusion of ER-derived vesicles.

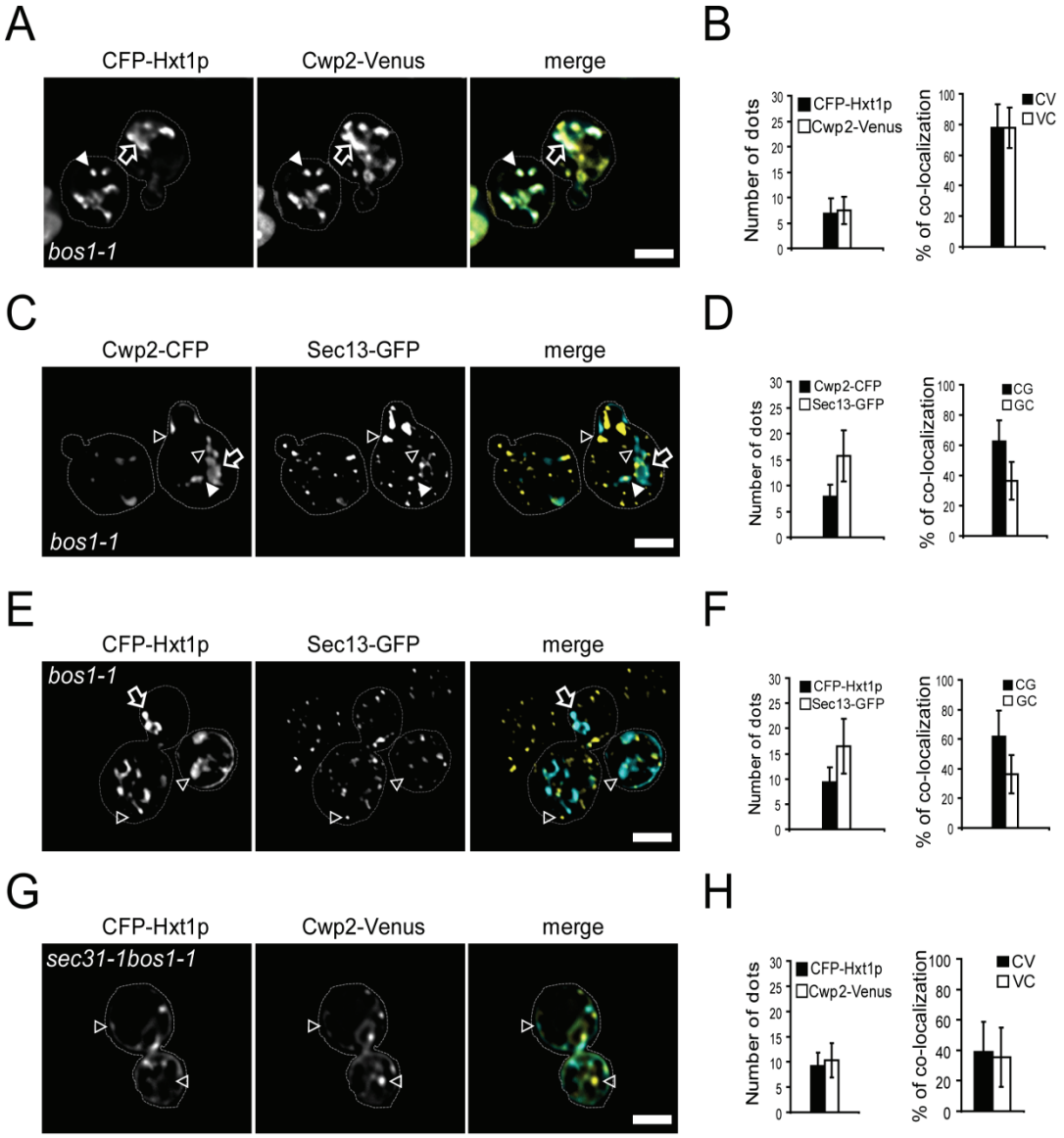

Fig. 10.The sorting defect observed in *bos1-1* at restrictive temperature occurs after the ER derived vesicles formation.

(A) CFP-Hxt1p and Cwp2-Venus in *bos1-1* yeast at 37°C. (B) Quantification of the micrographs described in (A). In the left panel, the number of dots of CFP-Hxt1p and Cwp2-Venus per cell were averaged. In the right panel, the black bar (CV) represents the mean of the percentage per cell of the CFP-Hxt1p dots co-localizing with the Cwp2-Venus dots. The white bar (VC) represents the mean of the percentage per cell of the Cwp2-Venus dots co-localizing with the CFP-Hxt1p dots. (n=56). (C) Cwp2-CFP and Sec13GFP in *bos1-1* yeast at 37°C. (D) Quantification of the several micrographs described in (C). In the left panel, the number of dots of Cwp2-CFP and Sec13GFP per cell were averaged. In the right panel, the black bar (CG) represents the mean of the percentage per cell of the Cwp2-CFP dots co-localizing with the Sec13GFP dots. The white bar (GC) represents the mean of the percentage per cell of the Sec13GFP dots co-localizing with the Cwp2-CFP dots. (n=53). (E) CFP-Hxt1p and Sec13GFP in *bos1-1* yeast at 37°C. (F) Quantification of the micrographs described in (E) and done as in (D). n=56.(G) Fluorescent micrographs of live *bos1-1sec31-1* yeast cells expressing CFP-Hxt1p and Cwp2-Venus at 37°C. (H) Quantification of the micrographs described in (G) and done as in (B). n=45. Scale bar: 3 μm. Star: vacuole. Fine dashed line: cell shape. White arrow heads: co-localizing dots. Open arrow heads: non-co-localizing dots. Large open arrow: large structure.

III.C4- Sorting along the secretory pathway.

To address the fate of Cwp2p and Hxt1p after ER exit, we synchronized transport through the secretory pathway using the *sec31-1* mutant. We incubated the *sec31-1* mutant at 37°C for 1 hour, shifted the cultures to 24°C and observed cargo localization at different time points.

Fig. 11. Synchronized ER exit of Cwp2-CFP and CFP-Hxt1p in *sec31-1* after shift from 37°C to 24°C.
(A) Live images of *sec31-1* cells expressing Sec13-GFP (yellow) and Cwp2-CFP (blue) or CFP-Hxt1p (blue) after shift from 37°C to 24°C. (B) Quantification of several micrographs described in (A). Means of the percentage of co-localization per cell of Cwp2-CFP with Sec13-GFP (black bars, 45≤n≤54, n= number of cells plotted per time point) and of CFP-Hxt1p with Sec13-GFP (white bars, 42≤n≤51) in *sec31-1*. The quantifications were done at 0, 20, 40, 60 minutes in *sec31-1* after the shift from 37°C to 24°C. Scale bar: 3 μm. Star: vacuole. Fine dashed line: cell shape. White arrow heads: co-localizing dots. Open arrow heads: non-co-localizing dots. Images deconvoluted by 10 iterations using a blind deconvolution protocol.

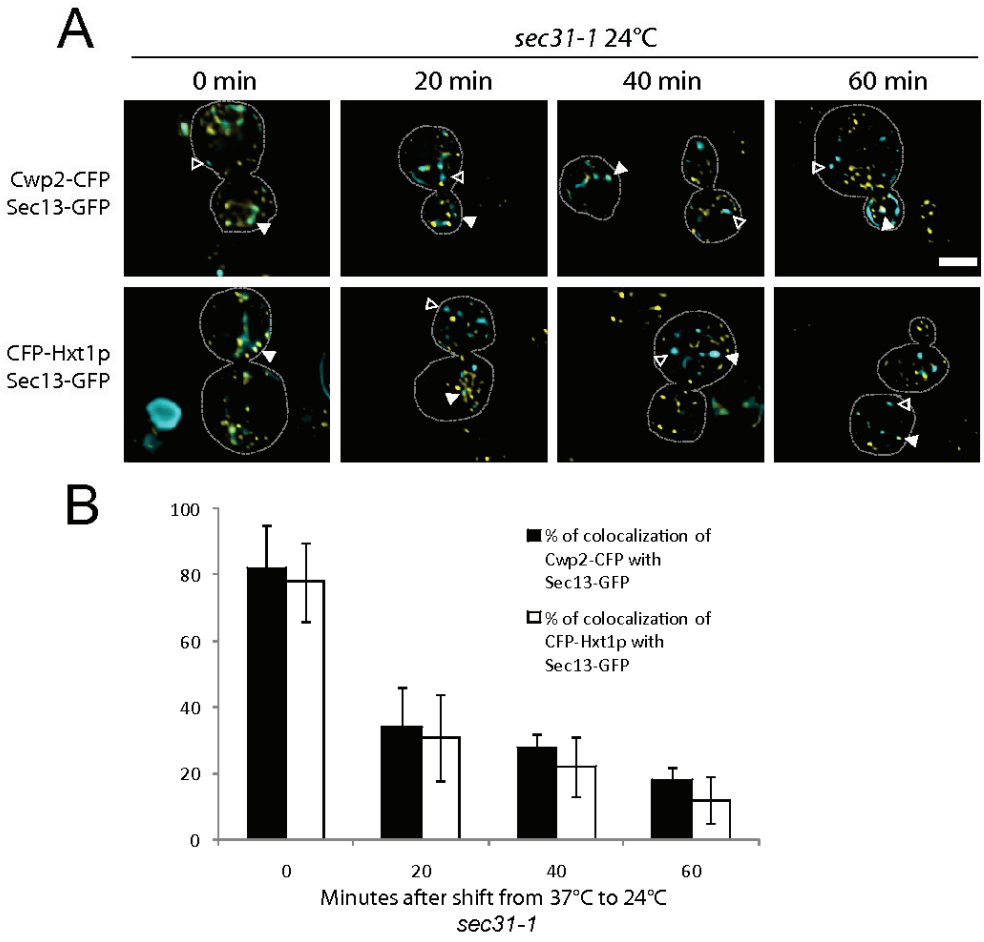

At first, we examined the kinetics of ER exit of Cwp2-Venus and Hxt1p, by following their co-localization with the ERES marker Sec13-GFP after the shift to 24°C (Part III.B and Fig. 11A-B). At 37°C, around 80% of Cwp2-Venus and CFP-Hxt1p co-localized with Sec13-GFP. Twenty minutes after the shift around 30% of both cargoes remained co-localized with ERES. This amount decreased to levels lower than 20% after one hour at 24°C. From these results, it seems that Sec31p recovered most of its function within the first 20 minutes at permissive temperature and that the ER exit kinetics of Cwp2p and Hxt1p appear to be similar. Then we looked at the progression of the cargo proteins through the secretory pathway, and quantified their localization every twenty minutes after the shift to 24°C (Fig. 12A-B). At time 0, Hxt1p and Cwp2p are found in majority in the ER and dots, which correspond to ERES. After 20 minutes, more than 50% of cargoes have left the ER and are found in dots. Forty minutes after the shift to 24°C a significant amount of cargo is found at the cell surface, and this proportion became the majority one hour after the shift. During this experiment, Cwp2-Venus and CFP-Hxt1p progressed through the secretory pathway with similar kinetics.

With the same protocol, we measured the co-localizaton of Cwp2-Venus and CFP-Hxt1p in *sec31-1* cells every 5 minutes after the shift to 24°C (Fig. 12A,C). Both dot structures co-localized to only approximately 20% during the whole experiment with a peak at only 35%, 15 minutes after the shift to 24°C (Fig. 12C). Interestingly, after one hour the majority of cells displayed a nascent bud and Cwp2-Venus was concentrated at the bud neck, while CFP-Hxt1p was found at the cell surface of the mother cell (Fig. 12D-E). This strongly suggests that the two cargoes follow parallel secretory pathways to reach different locations at the cell surface. We previously observed that a significant amount of Cwp2p and Hxt1p was found in the vacuole in wild-type and *sec31-1* cells.

Fig. 12. Hxt1p and Cwp2p remain sorted along the secretory pathway and display different localization at the cell surface.
(A) Fluorescent micrographs of live *sec31-1* yeast expressing CFP-Hxt1p (blue) and Cwp2-Venus (yellow) and incubated continuously with FM4-64 (red) after shift from 37°C to 24°C. Scale bar: 5 µm. Time points: every 5 minutes after the shift to 24°C. Only time points 0, 20, 40, 60 minutes are displayed. (B) Quantification of several micrographs described in (A). For CFP-Hxt1p and Cwp2-Venus at each time point, the percentage of cells displaying cargoes at the indicated localization compared to the total population has been calculated. The cargo protein seen in the vacuole has been disregarded. 21≤n≤68 per time point. (C) Mean of the percentage per cell of co-localization between Cwp2-Venus dots and CFP-Hxt1p dots. 21≤n≤68 per time point. (D) Fluorescent micrographs of live *sec31-1* yeast expressing CFP-Hxt1p and Cwp2-Venus 1 hour after the shift from 37°C to 24°C. (E) Quantification of the Cwp2-Venus and CFP-Hxt1p localization as in described in (D). Each bar shows the percentage of cells having CFP-Hxt1p or Cwp2-Venus in the mother cell, in the bud neck and in the daugther cell. n=40.

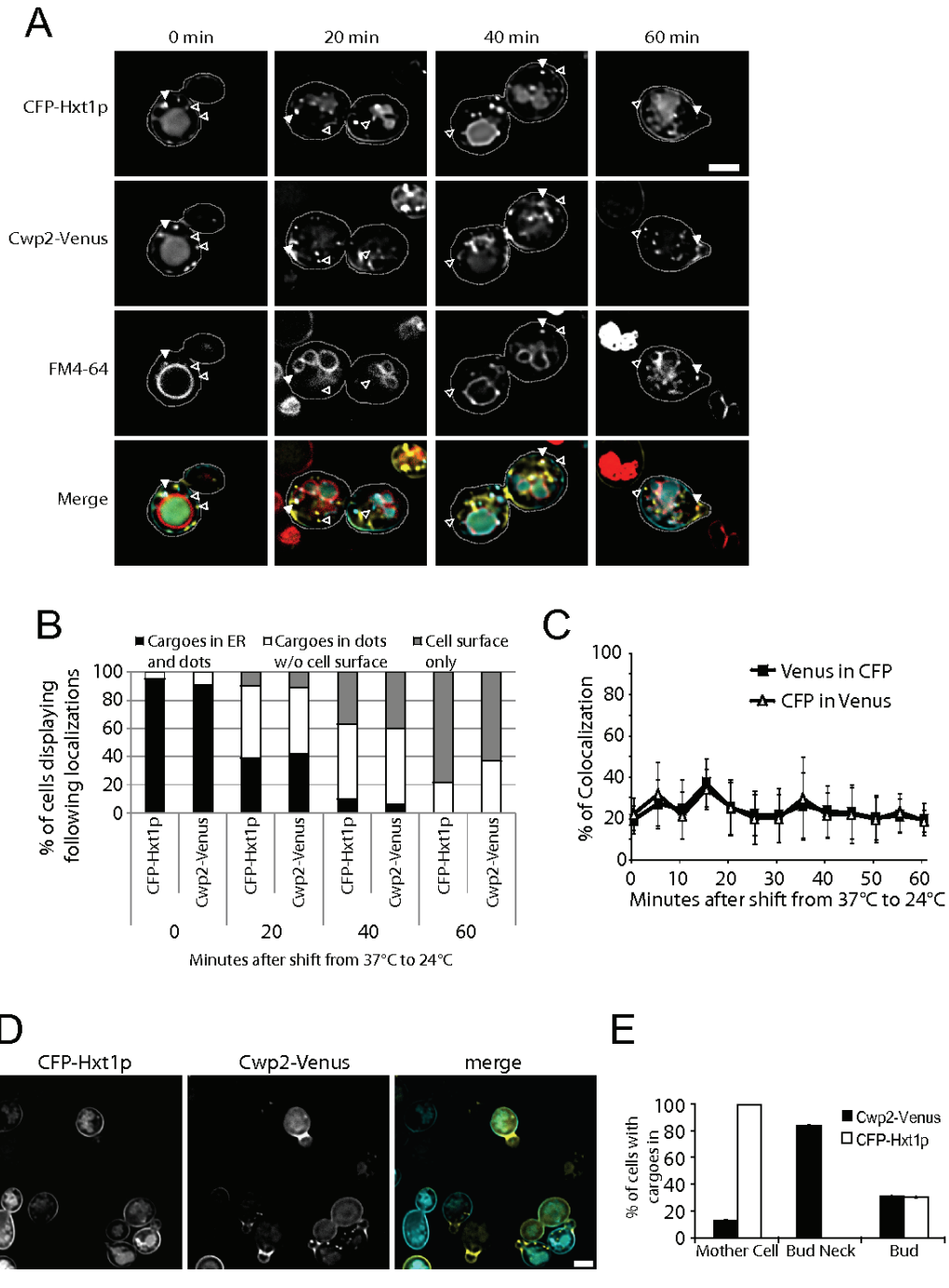

Therefore, it is possible that some of the cargo dots observed at 24°C were part of the endocytic pathway, suggesting the possibility that we monitored both the secretory and endocytic pathways. To examine this, *sec31-1* cells co-expressing Cwp2-Venus and CFP-Hxt1p were incubated at 37 °C for one hour in presence of FM4-64, which labels endocytic membranes, and the cultures were shifted to 24°C in presence of FM4-64 (Fig. 12A). Figure 13A shows the co-localization of Cwp2-Venus and CFP-Hxt1p with FM4-64. Cwp2-Venus, which is secreted to the cell wall, showed only few dots that co-localized with FM4-64 throughout the whole experiment. In contrast, we observed an increasing number of CFP-Hxt1p dots in FM4-64 containing compartments. After one hour, most of the CFP-Hxt1p dots observed were in the endocytic pathway. In summary, shortly after the shift to 24°C, Cwp2p and Hxt1p were secreted to the cell surface, where Hxt1p was endocytosed and Cwp2p was stably linked to the cell wall. Therefore, we quantified the co-localization of Cwp2-Venus with CFP-Hxt1p in the endocytic pathway, i.e among the cargo dots found in FM4-64 compartments (excluding the vacuole). We observed that the rare Cwp2-Venus dots found with FM4-64 co-localized with CFP-Hxt1p after the shift to 24°C (Fig. 13B). Then we focused on the co-localization of the cargo dots excluded from FM4-64, i.e the secretory pathway. Cwp2-Venus and CFP-Hxt1p dots co-localized only 10-30% (Fig. 13C). To reinforce these results, we acquired movies of *sec31-1* cells expressing Cwp2-Venus and CFP-Hxt1p treated as in Fig. 12A over 10 minutes with one acquisition every 20 seconds at 0, 20 and 50 minutes after the temperature shift to 24°C (Data not shown). In these three movies, we observed that Cwp2-Venus and CFP-Hxt1p dots moved independently from each other, except when Cwp2-Venus dots co-localized with FM4-64. In contrast, if we co-expressed the two GPI-anchored proteins Cwp2p and Ccw14p fused with CFP and Venus respectively in *sec31-1* cells, both cargo proteins move in the same dots (data not shown). These results clearly

demonstrate that Cwp2p and Hxt1p, which are incorporated into distinct ERES and therefore distinct ER-derived vesicles, traffic separately throughout the secretory pathway before reaching their final and distinct destinations. However it is still unclear whether or not both cargoes go through different subcompartments of the Golgi apparatus.

Fig. 13. Hxt1p and Cwp2p remain sorted along the secretory pathway but colocalize in the endocytic pathway.
Quantification of several micrographs described in Fig. 12A at 0, 20, 40 and 60 minutes after the shift at 24°C. 21≤n≤68 per time point. (A) Quantification of the co-localization of CFP-Hxt1p and Cwp2-Venus dots with FM4-64. (B) Quantification of the co-localization between CFP-Hxt1p and Cwp2-Venus dots within the FM4-64 stained compartment. (C) Quantification of the co-localization between CFP-Hxt1p and Cwp2-Venus dots for dots which do not co-localize with FM4-64. Co-localizations with the vacuole were excluded for the quantifications in A, B and C.

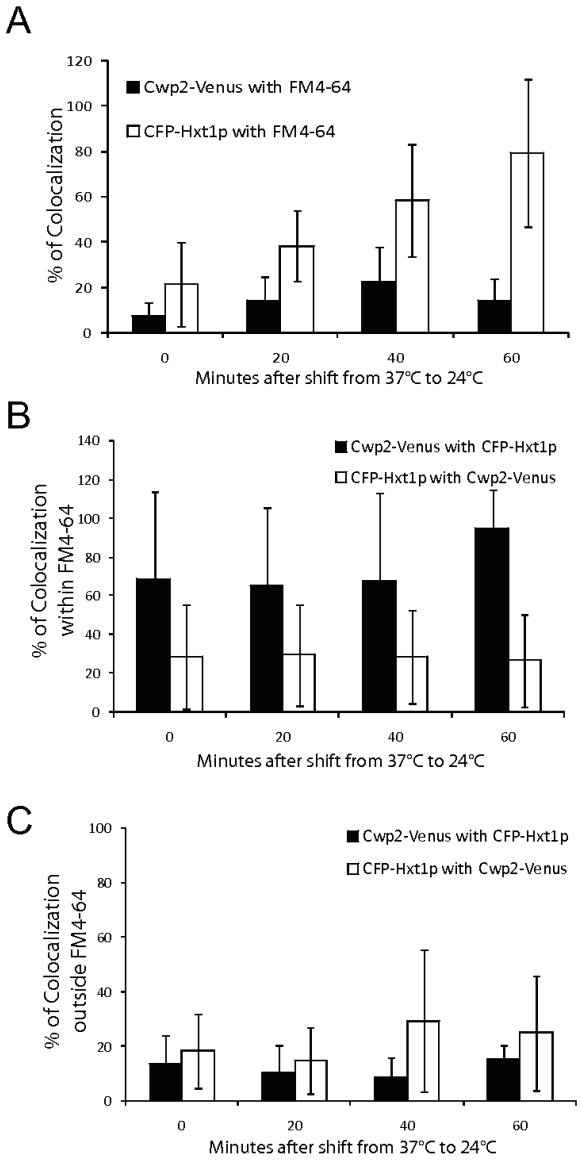

IV-Discussion, outlook and Conclusion

During this thesis work, I believe we made substantial progress in the understanding of GPI-anchored protein ER exit and protein sorting. We have seen that the GPI anchor is an important signal for GPI-anchored protein exit from the ER, but if it is required for sorting, then it is a recessive signal compared to the ER exit signal contained in the soluble cargo α–factor. The GPI anchor might be required for ER budding because lipid remodeling ensures concentration of GPI-anchored proteins into ER microdomains prior to ER budding (Fig.14). We propose that the adaptor proteins Emp24p and Erv25p allow the association of pre-concentrated GPI-anchored proteins to the forming COPII coated vesicles in a Sar1p independent manner.

Fig14. ER exit of GPI-anchored proteins in Yeast

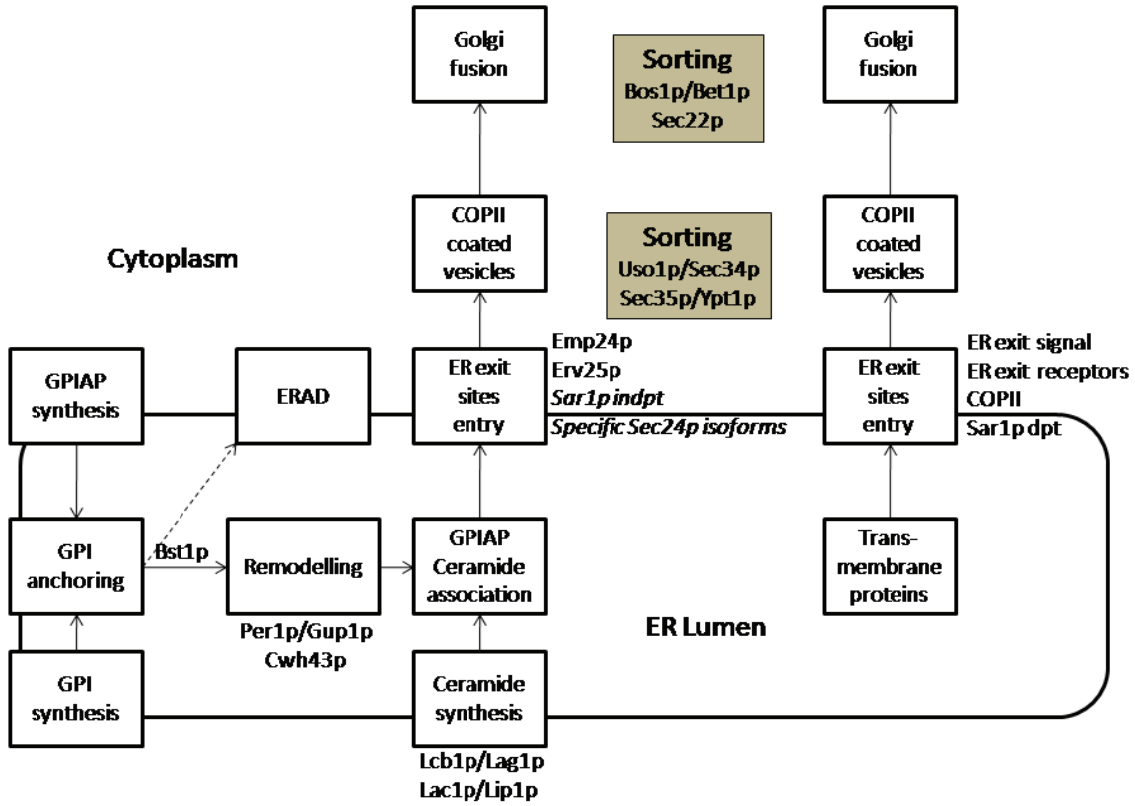

We have also shown that the transmembrane protein Hxt1p is concentrated into COPII vesicles because of its interaction with the ER exit receptor Erv14p, itself bound to the prebudding complex. After budding, the two ER-derived vesicle populations progress to the Golgi apparatus and the SNARE Bos1p somehow prevents the heterotypic fusion of the different populations of ER-derived vesicles. Then the two cargoes go through the entire secretory pathway following parallel routes until their delivery to the cell surface.

Function of Emp24p

Even though we have made some progress towards the understanding of GPI-anchored protein ER exit, the molecular function of the potential ER exit receptor of GPI-anchored proteins Emp24p remains unclear. First, Emp24p is essential for proper ER exit of GPI-anchored proteins, as seen by pulse-chase analysis, live imaging, and the *in vitro* budding assay. Second, Emp24p functions downstream of remodeling, because Cwp2p was still concentrated in *emp24Δsec31-1* cells, in contrast to what has been observed in the remodeling mutants. Gas1p and Cwp2p were still enriched in the DRMs in *emp24Δsec31-1* (data not shown), that was not true in *bst1Δsec31-1, per1Δsec31-1 and gup1Δsec31-1.* Moreover Emp24p was relocalized into the ER in the remodeling mutants. Third, Emp24p is not required for sorting because Cwp2p was still sorted in *emp24Δsec31-1* cells. Finally Emp24p is not involved in the general mechanism of COPII vesicle formation, because there is no defect in Sec13-GFP pattern in *emp24Δ* cells, in contrast what is seen in *sec12-4* for example. From these results, we can describe the following sequence: GPI-anchored proteins are concentrated and maybe sorted into specialized ER domains after remodeling and therefore Emp24p ensures proper packaging of GPI-anchored proteins into COPII coated

vesicles. According to this model Emp24p must be enriched into the GPI-anchored protein containing ER domains and ER-derived vesicles. However this postulate was not confirmed. This suggests a more complex mechanism regarding Emp24p function. Although Emp24p may be required for GPI-anchored protein ER exit in an unexpected manner, we will present in the following part some possible hypotheses regarding the Emp24p function.

If Emp24p is indeed an ER exit receptor of GPI-anchored proteins, we can suppose the existence of two pools of Emp24p: one competent as an ER exit receptor, and one inactive (the majority) which is transported like other transmembrane proteins exposing an ER exit signal. In this hypothesis, we can imagine that Emp24p activity is regulated by the interaction with Erv25p. To explore this hypothesis, the simplest experiment would be to look at the co-localization of Erv25p with Emp24p and GPI-anchored proteins in *sec31-1* cells. If Erv25p is strongly co-localized with Emp24p and but not with GPI-anchored proteins, this could suggest that Erv25p prevents the interaction of Emp24p with GPI-anchored proteins. However this is unlikely because in *erv25Δ* cells the maturation of Gas1p is strongly delayed. If Erv25p only co-localizes with Emp24p when Emp24p is co-localized with GPI-anchored proteins, then Erv25p could positively activate Emp24p as an ER exit receptor. Another possible observation would be that Erv25p strongly co-localizes with GPI-anchored proteins. In that case Erv25p is the ER exit receptor of GPI-anchored proteins and according to the co-localization with Emp24p, Emp24p would be the positive regulator. However the fact that Emp24p and not a fraction of it, is completely relocalized in the ER in *erv25Δ* cells (data not shown) goes against the function of Erv25p in generating two pools of Emp24p. Others candidates for a potential regulation of the Emp24p activity would be Erp1p, Erp2p and Ted1p (*YIL039W*). Erp1p and Erp2p are members of the p24 family and have been found

in complex with Erv25p and Emp24p (Marzioch et al., 1999). Moreover, *erp1Δ* and *erp2Δ* cells display a delay in Gas1p maturation (Marzioch et al., 1999). We can apply the same localization experiments done for Emp24p to Erp1p and Erp2p. First we can look at the co-localization of Emp24p with GPI-anchored proteins in *erp1Δ sec31-1* and *erp2Δ sec31-1* cells, and at the co-localization of Erp1p and Erp2p with Emp24p and GPI-anchored proteins in *sec31-1* cells. Ted1p has been recently isolated as an regulator of GPI-anchored protein ER exit (Haass et al., 2007). In *ted1Δ* cells, Gas1p maturation is impaired (Haass et al., 2007). Genetic interaction indicates that Ted1p functions together with Emp24p and Erv25p. Furthermore it has been hypothesized that Bst1p and Ted1p function in parallel pathways to regulate Emp24p/Erv25p function (Haass et al., 2007). Ted1p contains a predicted phosphoric ester hydrolase activity, which could mean that Ted1p is involved in remodeling. But it is too early to predict the mechanism by which Ted1p regulates Emp24p/Erv25p, but study of the localization of Emp24p in *ted1Δ* cells and the co-localization of Ted1p with Emp24p and GPI-anchored proteins might enlighten us on the mechanism by which GPI-anchored proteins exit ER.

Another hypothesis regarding the Emp24p function is that Emp24p is required for proper folding of GPI-anchored proteins. This would be consistent with the Unfolded Protein Response (UPR) activation in *emp24Δ* cells and the induction of *EMP24* upon UPR (Travers et al., 2000). In this context we can imagine two ways, supposing that unfolded proteins cannot exit ER efficiently: Emp24p functions as a chaperone protein or Emp24p is involved in ER exit of unfolded GPI-anchored proteins and after retrieval from the Golgi targets them to the ER associated degradation (ERAD) machinery. If Emp24p is required for proper folding of GPI-anchored protein in the ER, it may actually be required as well to maintain a proper folding

along ER-to-Golgi transport, otherwise we would expect an ER retention signal rather than an ER exit signal in the C-terminus of Emp24p. But then again the localization of Emp24p with GPI-anchored proteins in *sec31-1* is not consistent with this hypothesis. Furthermore it is intellectually difficult to connect the hypothetical chaperone function of Emp24p and its requirement for COPI coated vesicles formation (Aguilera-Romero et al., 2008). If Emp24p is required for traffic of unfolded GPI-anchored proteins, then again we should suppose two pools of Emp24p to be consistent with our results. One way to clear this point would be to run a Blue-Native PAGE in order to see whether GPI-anchored proteins are aggregated and misfolded in *emp24Δ* cells.

A last hypothesis would be that Emp24p and p24 family members are essential for the retrieval from the Golgi apparatus of a cycling GPI-anchored protein ER exit receptor. This hypothesis could be supported by the Gas1p maturation delay observed in the mutant for the α-subunit of the COPI coatmer(Sutterlin et al., 1997a). We can then wonder about the significance of the physical interaction observed between Emp24p and GPI-anchored proteins (Muniz et al., 2000). To identify this mysterious ER exit receptor several approaches can be imagined. The first one which is actually being attempted in our laboratory, is to purify the GPI-anchored protein containing vesicles, and after mass spectrometry identify specific proteins contained in this vesicle population. Among them there is a high probability to pinpoint the real ER exit receptor. This approach is challenging because besides GPI-anchored proteins, we do not know any others specific proteins contained in GPI-anchored proteins ER-derived vesicles, and GPI-anchored proteins being exclusively luminal, no cytoplasmically exposed bait can be used to pull-down the vesicles. To overcome this difficulty we can flip GPI-anchored proteins outside the vesicles after controlled sonication (Marcia Taylor, unpublished results). Another approach would be to determine or revisit the

genes presenting a genetic interaction with *ERV14*. Indeed *EMP24*, *ERV25*, *TED1*, *BST1* and *PER1* exhibit a strong synthetic defect with *ERV14* (Haass et al., 2007; Schuldiner et al., 2005). We can then narrow down the number of candidates by observation of Gas1p maturation defect in the mutants for these candidates. And finally we can assay physical interaction between GPI-anchored proteins and the candidates ER exit receptor in ER-derived vesicles.

In parallel to these experiments, supposing a real physical interaction between Emp24p or the p24 family members and GPI-anchored proteins, and in order to understand the molecular function of Emp24p, it would be necessary to identify the domains of interaction between Emp24p and GPI-anchored proteins. Cross-linking truncated versions of Emp24p with GPI-anchored proteins would allow the identification of the domain of interaction of Emp24p. We can perform the same kind of experiments using truncated versions of the GPI-anchored protein Cwp2p (52 amino acids after cleavage of the signal peptide and the GPI attachment site) rather than Gas1p (519 amino acids after post-translational cleavages). However, it is highly probable that Emp24p interacts with the glycans of GPI-anchored proteins and/or the GPI and/or the microdomains in which GPI-anchored proteins are enriched. In this regard it would be then more suitable to assay the interaction in mutants: in *pmt4Δ* and *pmt6Δ* cells to assay the glycan requirement for interaction, in *gaa1-1*, *bst1Δ*, *per1Δ*, *gup1Δ* and *cwh43Δ* cells to assay the GPI and remodeling requirement and in *lcb1-100* or in wild-type in presence of myriocin to test the influence of ceramides. Pmt4p and Pmt6p are O-mannosyltransferases, which catalayse the transfer of O-mannose to serine/threonine residues in the ER. O-mannosylation is essential for a variety of biological processes (Orlean, 1990). Gaa1p is involved in the attachment of the GPI to the newly synthesized protein, and as enounced before Bst1p, Per1p, Gup1p and Cwh43p are required

for lipid remodeling of the GPI. Lcb1p is a serine C-palmitoyltransferase, which catalyzes the first step in the biosynthesis of long-chain base component of sphingolipids, myriocin blocks the same step (Nagiec et al., 1994).

COPII coated vesicle formation

From our results we concluded that GPI-anchored protein concentration prior to ER budding does not require COPII in contrast to transmembrane proteins. More surprisingly, GPI-anchored protein budding from the ER does not seem to require the small Ras GTPase Sar1p. This result could suggest that Sar1p is not required for concentration or incorporation of GPI-anchored proteins into COPII coated vesicles, but it as well implies that Sar1p is not essential for COPII assembly for GPI-anchored protein-containing vesicles. It therefore becomes tempting to speculate that GPI-anchored proteins exit the ER via unconventional COPII coated vesicles. *In vivo* microscopy and pulse-chase experiment showed that GPI-anchored proteins require COPII coat for ER-to-Golgi transport. However, considering the severity of the COPII mutant phenotype, it is possible that the ER exit defect observed for GPI-anchored proteins is an indirect consequence of the disturbance of traffic in general. So we looked at budding using *sec23-1* spheroplasts and cytosol in presence or not of wild-type Sec23p/Sec24p complex (data not shown). Unfortunately, the results were not reproducible enough to demonstrate a strict requirement or not of Sec23p in the formation of COPII coat for the GPI-anchored protein ER-derived vesicles. Another but similar approach would be to promote ER budding using purified COPII components and observe the effect of the absence of one of the component at a time. But in this context, sorting of GPI-anchored proteins cannot be observed. To overcome this issue a mass spectrometry approach would be again

necessary. This supposes that we can specifically precipitate the GPI-anchored protein containing vesicles, either by using a yet unknown specific protein as a bait or by flipping the GPI-anchored proteins to the cytoplasmic side of the vesicles. But a second problem might occur: during our budding assay, we collect the ER-derived vesicles after ultracentrifugation in a Nycodenz gradient. The Nycodenz promotes the disassembly and removal of the COPII coat from the vesicle. The Nycodenz gradient is therefore not suitable for our purpose. We can propose then to produce ER-derived vesicles using *sec18* membranes and cytosol in presence of GTPγS or in presence of Sar1p GTP locked form. The use of *sec18* should prevent the fusion of ER-derived vesicles. GTPγS should prevent the disassembly of the COPII coat, and Sar1p GTP locked form will allow the specific formation of ER-derived vesicles containing GPI-anchored proteins and Hxt1p. The Hxt1p containing vesicles can be separated using an antibody against a tag fused at the N-terminus of Hxt1p, however the presence of the COPII coat may prevent the interaction of the antibody with the tag. By centrifugation without any gradient we probably can remove most of the heavy membranes, and using an antibody against GFP, for instance, we can pull-down COPII coated vesicles if Sec13p is tagged with GFP. This tag must be cleavable (a thrombin cleavage site), then we can perform a second precipitation using an antiboby against a specific protein of the GPI-anchored protein containing vesicles, if known, or against GPI-anchored proteins after sonication. If pure the vesicles fraction can be sent to mass spectrometry, if not we can use the same method to precipitate the Gap1p containing vesicles and look at eventual differences after mass spectrometry. The same approach can be used in order to know if any SNAREs or tethering factors are specific for the GPI-anchored protein containing vesicles. Alternatively, immuno-cryoelectron microscopy might be able to tell us if there is a difference regarding the COPII coat composition of the different ER-derived vesicle populations.

Directly related to COPII coat, there are two non-essential isoforms of Sec24p, which can be connected to ER exit of specific cargoes. Considering protein sorting it is legitimate to believe that the different isoforms are associated to different ER-derived vesicle populations. Probably the fastest way to confirm or not this hypothesis would be to observe the co-localization of the different isoforms. If they do not or partially co-localize, this would strongly reinforce the protein sorting upon ER exit hypothesis.

Sorting machinery.

Most of the proteins involved in sorting identified so far are SNAREs, tethering factors or Rab GTPase. This suggests that the sorting defect that we could observe was the result of an event occurring after ER budding. In only two mutants we could observe a sorting defect prior to budding. *sec16-2* was one of them. The second mutant was *gpi1Δ* (data not shown). Sec16p is involved in COPII coat formation and Hxt1p concentration, because in *sec16-2* cells the concentration of Hxt1p is mildly affected and we could still observe Hxt1p dots which were missorted. Gpi1p is involved in the first step of GPI synthesis. In this mutant most of Cwp2p is not GPI-anchored and cannot be concentrated. Since the concentration phenotype was mild as well, we could observe a small amount of Cwp2p dots in *gpi1Δsec31-1* which partially co-localized (40%±25%) with Hxt1p dots (data not shown). Until now we have not observed any mutants where sorting prior to budding is affected, without affecting cargo concentration. This suggests that the two processes are tightly coupled, implying that sorting occurs because of different concentration mechanisms for different cargos.

Golgi: One or several identities?

One remarkable discovery was that cargoes sorted upon ER exit follow parallel secretory pathways. This would imply that sorted cargoes go through distinct Golgi apparati or distinct subcompartments of the Golgi apparatus. The experiment set-up presented in this thesis is not sufficient to believe without a doubt the existence of several Golgi apparati. We could have missed the precise moment when the two cargoes are mixed in the Golgi. However this is unlikely because cargoes go through the Golgi in around five minutes (Losev et al., 2006; Matsuura-Tokita et al., 2006) and we performed movies with 1 frame per 20 seconds over 10 minutes in 6 movies from 0 to 10 minutes, 10 to 20 minutes, 20 to 30 minutes, etc… until most of the cargoes reached the cell surface. Another reason to remain skeptical is that even though the secretion of the two cargoes seems synchronized, the entry in the Golgi apparatus is spread along the time (fig. 15).

After quantification of the co-localization of the cargoes with the ERES marker Sec13p and the marker of the Trans-Golgi network Sec7p, we could observe that the wave of secretion of a particular cargo is rather flat. The maximum of co-localization of the cargoes with the Golgi occurs between 25 and 40 minutes after shifting the *sec31-1* cells from 37°C to 24°C, and this peak of co-localization is never higher than 35%. Therefore, if the cargoes mix in the Golgi apparatus the maximum of co-localization expected should not be higher than 35%. Furthermore, we know that some of the Hxt1p dots correspond to the compartments of the endocytic pathway, and after extraction of the signal from endocytosis, we observed that Cwp2p and Hxt1p co-localized only to around 20%. The calculations are too close to conclude that the different cargoes do not traverse the same Golgi.

Fig.15. Localization of the cargo proteins Cwp2p and Hxt1p in *sec31-1* after shift from 37°C to 24°C. The localization of the dots was determined by co-localization with the ERES marker Sec13p and the trans-Golgi marker Sec7p. ER and Cell surface was directly observed. « t » represents the time in minutes after the shift to 24°C.

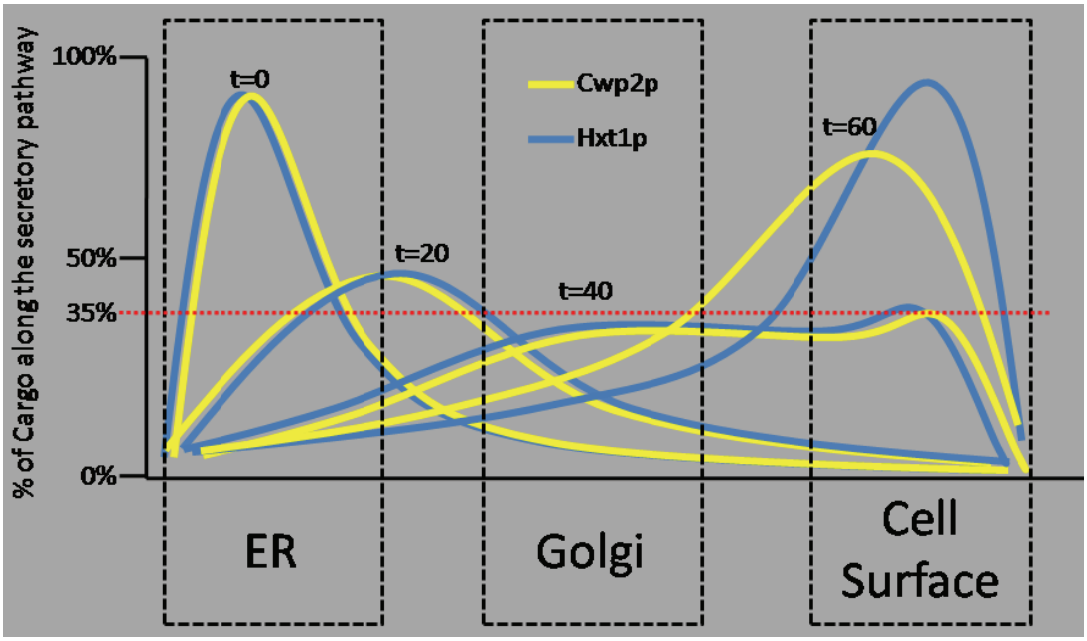

Similar to what was done with *sec31-1*, we thought to accumulate cargo proteins using mutants for exit from the Golgi compartment. Unfortunately in such mutants (*sec7-1, sec6-4*), there is no longer a clear distinction between the Golgi and endocytic compartments using FM4-64 (data not shown). Obviously fluorescence microscopy is not an appropriate approach to investigate this issue, even though it was sufficient concerning ER sorting. To assay this hypothesis, two approaches can be used. Probably the simplest would be to perform immunocryo EM in wild-type cells and in *sec31-1* 20 to 30 minutes after the shift from 37°C to 24°C and observe the co-localization of Gas1p and Gap1p in the Golgi apparatus. A second approach which would require many controls would be to first to precipitate the Golgi apparatus from wild-type cells or from *sec31-1* cells 20 to 30 minutes after the shift from 37°C to 24°C, then precipitate the Gap1p-HA containing Golgi, and observe if Gas1p comes down with it. The hardest part would probably to isolate specifically the Golgi apparatus without retrieving plasma membrane. For this we would have to use a

bait containing a cleavable tag. This bait should be specific for the Golgi compartment and exposed at the cytoplasmic side. Preferentially this should be a soluble protein in order to prevent the precipitation of the early events of the secretory pathways. One possible candidate for such bait could be the Rab protein Ypt6p, for instance. About the choice of the bait, we have to consider that this bait could be specific from cis-Golgi or trans-Golgi compartment. Moreover, if indeed there are several types of Golgi compartments, the bait may be specific for one type of Golgi compartment.

ER-to-Golgi mobility machinery

In mammalian cells microtubules are required for transport from the ER Golgi intermediate compartment (ERGIC) to the Golgi apparatus. In yeast nobody has ever shown a cytoskeleton dependence for ER-to-Golgi transport however experiments using cytoskeleton depolymerizing drugs did not reveal a cytoskeleton function in ER-to-Golgi traffic. From our movies, we could observe a difference in mobility of the Cwp2p and Hxt1p dots suggesting that there are at least two different mechanisms to make these dots move. The actual model is that as soon as formed, the ER-derived vesicles travel by diffusion to the Golgi apparatus, which is not consistent with our observations, because in that case all the dots should move at the same speed. However we can not be certain that the dots that we observed are ER-derived vesicles as they could still be attached to the ER. The movement of the dots might not be the illustration of longitudinal transport of vesicles to the Golgi but a lateral movement of ERES at the surface of the ER. To clarify this point, simple experiments can be performed. First, we can acquire movies of wild-type cells expressing a fluorescent COPII component and fluorescent microtubules (or actin), and observe if there is colocalization

and movement of vesicles along the cytoskeletal elements. At the same time, using *sec31-1* cells we can simultaneously visualize the movement of different cargo proteins and cytoskeletal structures. If indeed we find a link between dots movement and cytoskeleton, we can confirm these results using nocodazole and benomyl (for microtubules) and latruculin (for actin) and observe an eventual decrease in speeds of the dots. If this is observed then we can try to look more in details at the different requirements using mutants for dyneins and kinesins or myosins (the use of double or triple mutants might be required to overcome the redundancy of the molecular motors). Later we can come back to biochemistry and assay by pulse-chase the effect of motors on secretory protein maturation.

ER-to-Golgi transport has been extensively studied and a complete and solid picture of the mechanism has emerged recently. However this model has been established through the study of a limited number of cargo proteins. The discovery of ER sorting raises the possibility of different mechanisms allowing transport from the ER to Golgi apparatus. Indeed in this work, I believe we brought new elements showing that the mechanisms of GPI-anchored protein concentration and COPII coated vesicle formation diverge from the current model. At the moment we can only speculate of the significance of the ER sorting event in yeast. We believe that it is related to ceramide transport, because of the capacity of GPI-anchored proteins to concentrate into microdomains after remodelling (Fujita et al., 2006a), because ER exit of GPI-anchored proteins requires ceramides (Sutterlin et al., 1997a), because ceramide transport to the Golgi compartment is largely vesicular, and because ceramide transport is GPI dependent in yeast (Funato and Riezman, 2001; Kajiwara et al., 2008). In mammalian cells, ceramide transport to the Golgi is dependent of a non-vesicular

mechanism (Yasuda et al., 2001) and therefore is not likely to depende upon GPI. Nevertheless, it is important to determine if ER to Golgi transport of GPI-anchored proteins in mammalian cells, which depends upon the Emp24p homologue, also involves protein sorting upon ER exit.

V-References

Aguilera-Romero, A., J. Kaminska, A. Spang, H. Riezman, and M. Muniz. 2008. The yeast p24 complex is required for the formation of COPI retrograde transport vesicles from the Golgi apparatus. *J Cell Biol*. 180:713-20.

Antonny, B., D. Madden, S. Hamamoto, L. Orci, and R. Schekman. 2001. Dynamics of the COPII coat with GTP and stable analogues. *Nat Cell Biol*. 3:531-7.

Audhya, A., and S.D. Emr. 2002. Stt4 PI 4-kinase localizes to the plasma membrane and functions in the Pkc1-mediated MAP kinase cascade. *Dev Cell*. 2:593-605.

Bagnat, M., S. Keranen, A. Shevchenko, and K. Simons. 2000. Lipid rafts function in biosynthetic delivery of proteins to the cell surface in yeast. *Proc Natl Acad Sci U S A*. 97:3254-9.

Bagnat, M., and K. Simons. 2002a. Cell surface polarization during yeast mating. *Proc Natl Acad Sci U S A*. 99:14183-8.

Bagnat, M., and K. Simons. 2002b. Lipid rafts in protein sorting and cell polarity in budding yeast Saccharomyces cerevisiae. *Biol Chem*. 383:1475-80.

Bannykh, S.I., T. Rowe, and W.E. Balch. 1996. The organization of endoplasmic reticulum export complexes. *J Cell Biol*. 135:19-35.

Barlowe, C., and R. Schekman. 1993. SEC12 encodes a guanine-nucleotide-exchange factor essential for transport vesicle budding from the ER. *Nature*. 365:347-9.

Barz, W.P., and P. Walter. 1999. Two endoplasmic reticulum (ER) membrane proteins that facilitate ER-to-Golgi transport of glycosylphosphatidylinositol-anchored proteins. *Mol Biol Cell*. 10:1043-59.

Belden, W.J., and C. Barlowe. 1996. Erv25p, a component of COPII-coated vesicles, forms a complex with Emp24p that is required for efficient endoplasmic reticulum to Golgi transport. *J Biol Chem*. 271:26939-46.

Belden, W.J., and C. Barlowe. 2001a. Distinct roles for the cytoplasmic tail sequences of Emp24p and Erv25p in transport between the endoplasmic reticulum and Golgi complex. *J Biol Chem*. 276:43040-8.

Belden, W.J., and C. Barlowe. 2001b. Role of Erv29p in collecting soluble secretory proteins into ER-derived transport vesicles. *Science*. 294:1528-31.

Benachour, A., G. Sipos, I. Flury, F. Reggiori, E. Canivenc-Gansel, C. Vionnet, A. Conzelmann, and M. Benghezal. 1999. Deletion of GPI7, a yeast gene required for addition of a side chain to the glycosylphosphatidylinositol (GPI) core structure, affects GPI protein transport, remodeling, and cell wall integrity. *J Biol Chem*. 274:15251-61.

Benghezal, M., A. Benachour, S. Rusconi, M. Aebi, and A. Conzelmann. 1996. Yeast Gpi8p is essential for GPI anchor attachment onto proteins. *EMBO J*. 15:6575-83.

Benting, J.H., A.G. Rietveld, and K. Simons. 1999. N-Glycans mediate the apical sorting of a GPI-anchored, raft-associated protein in Madin-Darby canine kidney cells. *J Cell Biol*. 146:313-20.

Bi, X., R.A. Corpina, and J. Goldberg. 2002. Structure of the Sec23/24-Sar1 pre-budding complex of the COPII vesicle coat. *Nature*. 419:271-7.

Bielli, A., C.J. Haney, G. Gabreski, S.C. Watkins, S.I. Bannykh, and M. Aridor. 2005. Regulation of Sar1 NH2 terminus by GTP binding and hydrolysis promotes membrane deformation to control COPII vesicle fission. *J Cell Biol*. 171:919-24.

Bokel, C., S. Dass, M. Wilsch-Brauninger, and S. Roth. 2006. Drosophila Cornichon acts as cargo receptor for ER export of the TGFalpha-like growth factor Gurken. *Development*. 133:459-70.

Bosson, R., M. Jaquenoud, and A. Conzelmann. 2006. GUP1 of Saccharomyces cerevisiae encodes an O-acyltransferase involved in remodeling of the GPI anchor. *Mol Biol Cell*. 17:2636-45.

Brown, D.A., B. Crise, and J.K. Rose. 1989. Mechanism of membrane anchoring affects polarized expression of two proteins in MDCK cells. *Science*. 245:1499-501.

Brown, D.A., and E. London. 1998. Structure and origin of ordered lipid domains in biological membranes. *J Membr Biol*. 164:103-14.

Brown, D.A., and J.K. Rose. 1992. Sorting of GPI-anchored proteins to glycolipid-enriched membrane subdomains during transport to the apical cell surface. *Cell*. 68:533-44.

Bue, C.A., C.M. Bentivoglio, and C. Barlowe. 2006. Erv26p directs pro-alkaline phosphatase into endoplasmic reticulum-derived coat protein complex II transport vesicles. *Mol Biol Cell*. 17:4780-9.

Campana, V., A. Caputo, D. Sarnataro, S. Paladino, S. Tivodar, and C. Zurzolo. 2007. Characterization of the properties and trafficking of an anchorless form of the prion protein. *J Biol Chem*. 282:22747-56.

Canivenc-Gansel, E., I. Imhof, F. Reggiori, P. Burda, A. Conzelmann, and A. Benachour. 1998. GPI anchor biosynthesis in yeast: phosphoethanolamine is attached to the alpha1,4-linked mannose of the complete precursor glycophospholipid. *Glycobiology*. 8:761-70.

Chen, R., E.I. Walter, G. Parker, J.P. Lapurga, J.L. Millan, Y. Ikehara, S. Udenfriend, and M.E. Medof. 1998. Mammalian glycophosphatidylinositol anchor transfer to proteins and posttransfer deacylation. *Proc Natl Acad Sci U S A*. 95:9512-7.

Dominguez, M., K. Dejgaard, J. Fullekrug, S. Dahan, A. Fazel, J.P. Paccaud, D.Y. Thomas, J.J. Bergeron, and T. Nilsson. 1998. gp25L/emp24/p24 protein family members of the cis-Golgi network bind both COP I and II coatomer. *J Cell Biol*. 140:751-65.

Elrod-Erickson, M.J., and C.A. Kaiser. 1996. Genes that control the fidelity of endoplasmic reticulum to Golgi transport identified as suppressors of vesicle budding mutations. *Mol Biol Cell*. 7:1043-58.

Espenshade, P., R.E. Gimeno, E. Holzmacher, P. Teung, and C.A. Kaiser. 1995. Yeast SEC16 gene encodes a multidomain vesicle coat protein that interacts with Sec23p. *J Cell Biol*. 131:311-24.

Ferguson, M.A., J.S. Brimacombe, J.R. Brown, A. Crossman, A. Dix, R.A. Field, M.L. Guther, K.G. Milne, D.K. Sharma, and T.K. Smith. 1999. The GPI biosynthetic pathway as a therapeutic target for African sleeping sickness. *Biochim Biophys Acta*. 1455:327-40.

Fraering, P., I. Imhof, U. Meyer, J.M. Strub, A. van Dorsselaer, C. Vionnet, and A. Conzelmann. 2001. The GPI transamidase complex of Saccharomyces cerevisiae contains Gaa1p, Gpi8p, and Gpi16p. *Mol Biol Cell*. 12:3295-306.

Fujita, M., and Y. Jigami. 2008. Lipid remodeling of GPI-anchored proteins and its function. *Biochim Biophys Acta*. 1780:410-20.

Fujita, M., M. Umemura, T. Yoko-o, and Y. Jigami. 2006a. PER1 is required for GPI-phospholipase A2 activity and involved in lipid remodeling of GPI-anchored proteins. *Mol Biol Cell*. 17:5253-64.

Fujita, M., O.T. Yoko, and Y. Jigami. 2006b. Inositol deacylation by Bst1p is required for the quality control of glycosylphosphatidylinositol-anchored proteins. *Mol Biol Cell*. 17:834-50.

Funato, K., and H. Riezman. 2001. Vesicular and nonvesicular transport of ceramide from ER to the Golgi apparatus in yeast. *J Cell Biol*. 155:949-59.

Futai, E., S. Hamamoto, L. Orci, and R. Schekman. 2004. GTP/GDP exchange by Sec12p enables COPII vesicle bud formation on synthetic liposomes. *EMBO J*. 23:4146-55.

Ghugtyal, V., C. Vionnet, C. Roubaty, and A. Conzelmann. 2007. CWH43 is required for the introduction of ceramides into GPI anchors in Saccharomyces cerevisiae. *Mol Microbiol*. 65:1493-502.

Gimeno, R.E., P. Espenshade, and C.A. Kaiser. 1995. SED4 encodes a yeast endoplasmic reticulum protein that binds Sec16p and participates in vesicle formation. *J Cell Biol*. 131:325-38.

Gimeno, R.E., P. Espenshade, and C.A. Kaiser. 1996. COPII coat subunit interactions: Sec24p and Sec23p bind to adjacent regions of Sec16p. *Mol Biol Cell*. 7:1815-23.

Grimme, S.J., B.A. Westfall, J.M. Wiedman, C.H. Taron, and P. Orlean. 2001. The essential Smp3 protein is required for addition of the side-branching fourth mannose during assembly of yeast glycosylphosphatidylinositols. *J Biol Chem*. 276:27731-9.

Haass, F.A., M. Jonikas, P. Walter, J.S. Weissman, Y.N. Jan, L.Y. Jan, and M. Schuldiner. 2007. Identification of yeast proteins necessary for cell-surface function of a potassium channel. *Proc Natl Acad Sci U S A*. 104:18079-84.

Hamburger, D., M. Egerton, and H. Riezman. 1995. Yeast Gaa1p is required for attachment of a completed GPI anchor onto proteins. *J Cell Biol*. 129:629-39.

Heese-Peck, A., H. Pichler, B. Zanolari, R. Watanabe, G. Daum, and H. Riezman. 2002. Multiple functions of sterols in yeast endocytosis. *Mol Biol Cell*. 13:2664-80.

Hong, Y., K. Ohishi, J.Y. Kang, S. Tanaka, N. Inoue, J. Nishimura, Y. Maeda, and T. Kinoshita. 2003. Human PIG-U and yeast Cdc91p are the fifth subunit of GPI transamidase that attaches GPI-anchors to proteins. *Mol Biol Cell*. 14:1780-9.

Huang, M., J.T. Weissman, S. Beraud-Dufour, P. Luan, C. Wang, W. Chen, M. Aridor, I.A. Wilson, and W.E. Balch. 2001. Crystal structure of Sar1-GDP at 1.7 A resolution and the role of the NH2 terminus in ER export. *J Cell Biol*. 155:937-48.

Ikezawa, H. 2002. Glycosylphosphatidylinositol (GPI)-anchored proteins. *Biol Pharm Bull*. 25:409-17.

Kajiwara, K., R. Watanabe, H. Pichler, K. Ihara, S. Murakami, H. Riezman, and K. Funato. 2008. Yeast ARV1 Is Required for Efficient Delivery of an Early GPI Intermediate to the First Mannosyltransferase during GPI Assembly and Controls Lipid Flow from the Endoplasmic Reticulum. *Mol Biol Cell*. 19:2069-82.

Kappeler, F., D.R. Klopfenstein, M. Foguet, J.P. Paccaud, and H.P. Hauri. 1997. The recycling of ERGIC-53 in the early secretory pathway. ERGIC-53 carries a cytosolic endoplasmic reticulum-exit determinant interacting with COPII. *J Biol Chem*. 272:31801-8.

Kapteyn, J.C., H. Van Den Ende, and F.M. Klis. 1999. The contribution of cell wall proteins to the organization of the yeast cell wall. *Biochim Biophys Acta*. 1426:373-83.

Kinoshita, T., N. Inoue, and J. Takeda. 1995. Defective glycosyl phosphatidylinositol anchor synthesis and paroxysmal nocturnal hemoglobinuria. *Adv Immunol*. 60:57-103.

Kuehn, M.J., J.M. Herrmann, and R. Schekman. 1998. COPII-cargo interactions direct protein sorting into ER-derived transport vesicles. *Nature*. 391:187-90.

Ladasky, J.J., S. Boyle, M. Seth, H. Li, T. Pentcheva, F. Abe, S.J. Steinberg, and M. Edidin. 2006. Bap31 enhances the endoplasmic reticulum export and quality control of human class I MHC molecules. *J Immunol*. 177:6172-81.

Lederkremer, G.Z., Y. Cheng, B.M. Petre, E. Vogan, S. Springer, R. Schekman, T. Walz, and T. Kirchhausen. 2001. Structure of the Sec23p/24p and Sec13p/31p complexes of COPII. *Proc Natl Acad Sci U S A*. 98:10704-9.

Leidich, S.D., D.A. Drapp, and P. Orlean. 1994. A conditionally lethal yeast mutant blocked at the first step in glycosyl phosphatidylinositol anchor synthesis. *J Biol Chem*. 269:10193-6.

Lisanti, M.P., I.W. Caras, M.A. Davitz, and E. Rodriguez-Boulan. 1989. A glycophospholipid membrane anchor acts as an apical targeting signal in polarized epithelial cells. *J Cell Biol*. 109:2145-56.

Lisanti, M.P., A. Le Bivic, A.R. Saltiel, and E. Rodriguez-Boulan. 1990. Preferred apical distribution of glycosyl-phosphatidylinositol (GPI) anchored proteins: a highly conserved feature of the polarized epithelial cell phenotype. *J Membr Biol*. 113:155-67.

Losev, E., C.A. Reinke, J. Jellen, D.E. Strongin, B.J. Bevis, and B.S. Glick. 2006. Golgi maturation visualized in living yeast. *Nature*. 441:1002-6.

Maeda, Y., Y. Tashima, T. Houjou, M. Fujita, T. Yoko-o, Y. Jigami, R. Taguchi, and T. Kinoshita. 2007. Fatty acid remodeling of GPI-anchored proteins is required for their raft association. *Mol Biol Cell*. 18:1497-506.

Malkus, P., L.A. Graham, T.H. Stevens, and R. Schekman. 2004. Role of Vma21p in assembly and transport of the yeast vacuolar ATPase. *Mol Biol Cell*. 15:5075-91.

Malkus, P., F. Jiang, and R. Schekman. 2002. Concentrative sorting of secretory cargo proteins into COPII-coated vesicles. *J Cell Biol*. 159:915-21.

Marzioch, M., D.C. Henthorn, J.M. Herrmann, R. Wilson, D.Y. Thomas, J.J. Bergeron, R.C. Solari, and A. Rowley. 1999. Erp1p and Erp2p, partners for Emp24p and Erv25p in a yeast p24 complex. *Mol Biol Cell*. 10:1923-38.

Matsuoka, K., L. Orci, M. Amherdt, S.Y. Bednarek, S. Hamamoto, R. Schekman, and T. Yeung. 1998. COPII-coated vesicle formation reconstituted with purified coat proteins and chemically defined liposomes. *Cell*. 93:263-75.

Matsuura-Tokita, K., M. Takeuchi, A. Ichihara, K. Mikuriya, and A. Nakano. 2006. Live imaging of yeast Golgi cisternal maturation. *Nature*. 441:1007-10.

Miller, E.A., T.H. Beilharz, P.N. Malkus, M.C. Lee, S. Hamamoto, L. Orci, and R. Schekman. 2003. Multiple cargo binding sites on the COPII subunit Sec24p ensure capture of diverse membrane proteins into transport vesicles. *Cell*. 114:497-509.

Morsomme, P., C. Prescianotto-Baschong, and H. Riezman. 2003. The ER v-SNAREs are required for GPI-anchored protein sorting from other secretory proteins upon exit from the ER. *J Cell Biol*. 162:403-12.

Morsomme, P., and H. Riezman. 2002. The Rab GTPase Ypt1p and tethering factors couple protein sorting at the ER to vesicle targeting to the Golgi apparatus. *Dev Cell*. 2:307-17.

Mossessova, E., L.C. Bickford, and J. Goldberg. 2003. SNARE selectivity of the COPII coat. *Cell*. 114:483-95.

Muniz, M., P. Morsomme, and H. Riezman. 2001. Protein sorting upon exit from the endoplasmic reticulum. *Cell*. 104:313-20.

Muniz, M., C. Nuoffer, H.P. Hauri, and H. Riezman. 2000. The Emp24 complex recruits a specific cargo molecule into endoplasmic reticulum-derived vesicles. *J Cell Biol*. 148:925-30.

Nagamune, K., T. Nozaki, Y. Maeda, K. Ohishi, T. Fukuma, T. Hara, R.T. Schwarz, C. Sutterlin, R. Brun, H. Riezman, and T. Kinoshita. 2000. Critical roles of glycosylphosphatidylinositol for Trypanosoma brucei. *Proc Natl Acad Sci U S A*. 97:10336-41.

Nagiec, M.M., J.A. Baltisberger, G.B. Wells, R.L. Lester, and R.C. Dickson. 1994. The LCB2 gene of Saccharomyces and the related LCB1 gene encode subunits of serine palmitoyltransferase, the initial enzyme in sphingolipid synthesis. *Proc Natl Acad Sci U S A*. 91:7899-902.

Nakanishi, H., Y. Suda, and A.M. Neiman. 2007. Erv14 family cargo receptors are necessary for ER exit during sporulation in Saccharomyces cerevisiae. *J Cell Sci*. 120:908-16.

Nakano, A., D. Brada, and R. Schekman. 1988. A membrane glycoprotein, Sec12p, required for protein transport from the endoplasmic reticulum to the Golgi apparatus in yeast. *J Cell Biol*. 107:851-63.

Nakano, A., and M. Muramatsu. 1989. A novel GTP-binding protein, Sar1p, is involved in transport from the endoplasmic reticulum to the Golgi apparatus. *J Cell Biol*. 109:2677-91.

Nozaki, M., K. Ohishi, N. Yamada, T. Kinoshita, A. Nagy, and J. Takeda. 1999. Developmental abnormalities of glycosylphosphatidylinositol-anchor-deficient embryos revealed by Cre/loxP system. *Lab Invest*. 79:293-9.

Ohishi, K., N. Inoue, and T. Kinoshita. 2001. PIG-S and PIG-T, essential for GPI anchor attachment to proteins, form a complex with GAA1 and GPI8. *EMBO J*. 20:4088-98.

Orci, L., M. Ravazzola, P. Meda, C. Holcomb, H.P. Moore, L. Hicke, and R. Schekman. 1991. Mammalian Sec23p homologue is restricted to the endoplasmic reticulum transitional cytoplasm. *Proc Natl Acad Sci U S A*. 88:8611-5.

Orlean, P. 1990. Dolichol phosphate mannose synthase is required in vivo for glycosyl phosphatidylinositol membrane anchoring, O mannosylation, and N glycosylation of protein in Saccharomyces cerevisiae. *Mol Cell Biol*. 10:5796-805.

Orlean, P., and A.K. Menon. 2007. Thematic review series: lipid posttranslational modifications. GPI anchoring of protein in yeast and mammalian cells, or: how we learned to stop worrying and love glycophospholipids. *J Lipid Res*. 48:993-1011.

Otte, S., and C. Barlowe. 2002. The Erv41p-Erv46p complex: multiple export signals are required in trans for COPII-dependent transport from the ER. *EMBO J*. 21:6095-104.

Otte, S., and C. Barlowe. 2004. Sorting signals can direct receptor-mediated export of soluble proteins into COPII vesicles. *Nat Cell Biol*. 6:1189-94.

Oxley, D., and A. Bacic. 1999. Structure of the glycosylphosphatidylinositol anchor of an arabinogalactan protein from Pyrus communis suspension-cultured cells. *Proc Natl Acad Sci U S A*. 96:14246-51.

Paladino, S., D. Sarnataro, R. Pillich, S. Tivodar, L. Nitsch, and C. Zurzolo. 2004. Protein oligomerization modulates raft partitioning and apical sorting of GPI-anchored proteins. *J Cell Biol*. 167:699-709.

Paladino, S., D. Sarnataro, S. Tivodar, and C. Zurzolo. 2007. Oligomerization is a specific requirement for apical sorting of glycosyl-phosphatidylinositol-anchored proteins but not for non-raft-associated apical proteins. *Traffic*. 8:251-8.

Peng, R., A. De Antoni, and D. Gallwitz. 2000. Evidence for overlapping and distinct functions in protein transport of coat protein Sec24p family members. *J Biol Chem*. 275:11521-8.

Pittet, M., and A. Conzelmann. 2007. Biosynthesis and function of GPI proteins in the yeast Saccharomyces cerevisiae. *Biochim Biophys Acta*. 1771:405-20.

Powers, J., and C. Barlowe. 2002. Erv14p directs a transmembrane secretory protein into COPII-coated transport vesicles. *Mol Biol Cell*. 13:880-91.

Reggiori, F., E. Canivenc-Gansel, and A. Conzelmann. 1997. Lipid remodeling leads to the introduction and exchange of defined ceramides on GPI proteins in the ER and Golgi of Saccharomyces cerevisiae. *EMBO J*. 16:3506-18.

Saito-Nakano, Y., and A. Nakano. 2000. Sed4p functions as a positive regulator of Sar1p probably through inhibition of the GTPase activation by Sec23p. *Genes Cells*. 5:1039-48.

Sato, K. 2004. COPII coat assembly and selective export from the endoplasmic reticulum. *J Biochem*. 136:755-60.

Sato, K., and A. Nakano. 2002. Emp47p and its close homolog Emp46p have a tyrosine-containing endoplasmic reticulum exit signal and function in glycoprotein secretion in Saccharomyces cerevisiae. *Mol Biol Cell*. 13:2518-32.

Sato, K., and A. Nakano. 2003. Oligomerization of a cargo receptor directs protein sorting into COPII-coated transport vesicles. *Mol Biol Cell*. 14:3055-63.

Sato, K., and A. Nakano. 2004. Reconstitution of coat protein complex II (COPII) vesicle formation from cargo-reconstituted proteoliposomes reveals the potential role of GTP hydrolysis by Sar1p in protein sorting. *J Biol Chem*. 279:1330-5.

Sato, K., and A. Nakano. 2005. Dissection of COPII subunit-cargo assembly and disassembly kinetics during Sar1p-GTP hydrolysis. *Nat Struct Mol Biol*. 12:167-74.

Sato, K., and A. Nakano. 2007. Mechanisms of COPII vesicle formation and protein sorting. *FEBS Lett*. 581:2076-82.

Satoh, T., K. Sato, A. Kanoh, K. Yamashita, Y. Yamada, N. Igarashi, R. Kato, A. Nakano, and S. Wakatsuki. 2006. Structures of the carbohydrate recognition domain of Ca2+-independent cargo receptors Emp46p and Emp47p. *J Biol Chem*. 281:10410-9.

Schuck, S., and K. Simons. 2004. Polarized sorting in epithelial cells: raft clustering and the biogenesis of the apical membrane. *J Cell Sci*. 117:5955-64.

Schuldiner, M., S.R. Collins, N.J. Thompson, V. Denic, A. Bhamidipati, T. Punna, J. Ihmels, B. Andrews, C. Boone, J.F. Greenblatt, J.S. Weissman, and N.J. Krogan. 2005. Exploration of the function and organization of the yeast early secretory pathway through an epistatic miniarray profile. *Cell*. 123:507-19.

Simons, K., and E. Ikonen. 1997. Functional rafts in cell membranes. *Nature*. 387:569-72.

Sipos, G., F. Reggiori, C. Vionnet, and A. Conzelmann. 1997. Alternative lipid remodelling pathways for glycosylphosphatidylinositol membrane anchors in Saccharomyces cerevisiae. *EMBO J*. 16:3494-505.

Stagg, S.M., P. LaPointe, A. Razvi, C. Gurkan, C.S. Potter, B. Carragher, and W.E. Balch. 2008. Structural basis for cargo regulation of COPII coat assembly. *Cell*. 134:474-84.

Stephens, D.J., and R. Pepperkok. 2004. Differential effects of a GTP-restricted mutant of Sar1p on segregation of cargo during export from the endoplasmic reticulum. *J Cell Sci*. 117:3635-44.

Supek, F., D.T. Madden, S. Hamamoto, L. Orci, and R. Schekman. 2002. Sec16p potentiates the action of COPII proteins to bud transport vesicles. *J Cell Biol*. 158:1029-38.

Sutterlin, C., T.L. Doering, F. Schimmoller, S. Schroder, and H. Riezman. 1997a. Specific requirements for the ER to Golgi transport of GPI-anchored proteins in yeast. *J Cell Sci*. 110 (Pt 21):2703-14.

Sutterlin, C., A. Horvath, P. Gerold, R.T. Schwarz, Y. Wang, M. Dreyfuss, and H. Riezman. 1997b. Identification of a species-specific inhibitor of glycosylphosphatidylinositol synthesis. *EMBO J*. 16:6374-83.

Takida, S., Y. Maeda, and T. Kinoshita. 2008. Mammalian GPI-anchored proteins require p24 proteins for their efficient transport from the ER to the plasma membrane. *Biochem J*. 409:555-62.

Tanaka, S., Y. Maeda, Y. Tashima, and T. Kinoshita. 2004. Inositol deacylation of glycosylphosphatidylinositol-anchored proteins is mediated by mammalian PGAP1 and yeast Bst1p. *J Biol Chem*. 279:14256-63.

Taron, B.W., P.A. Colussi, J.M. Wiedman, P. Orlean, and C.H. Taron. 2004. Human Smp3p adds a fourth mannose to yeast and human glycosylphosphatidylinositol precursors in vivo. *J Biol Chem*. 279:36083-92.

Tashima, Y., R. Taguchi, C. Murata, H. Ashida, T. Kinoshita, and Y. Maeda. 2006. PGAP2 is essential for correct processing and stable expression of GPI-anchored proteins. *Mol Biol Cell*. 17:1410-20.

Travers, K.J., C.K. Patil, L. Wodicka, D.J. Lockhart, J.S. Weissman, and P. Walter. 2000. Functional and genomic analyses reveal an essential coordination between the unfolded protein response and ER-associated degradation. *Cell*. 101:249-58.

Umemura, M., M. Fujita, O.T. Yoko, A. Fukamizu, and Y. Jigami. 2007. Saccharomyces cerevisiae CWH43 is involved in the remodeling of the lipid moiety of GPI anchors to ceramides. *Mol Biol Cell*. 18:4304-16.

Valdez-Taubas, J., and H.R. Pelham. 2003. Slow diffusion of proteins in the yeast plasma membrane allows polarity to be maintained by endocytic cycling. *Curr Biol*. 13:1636-40.

Watanabe, R., G.A. Castillon, A. Meury, and H. Riezman. 2008. The presence of an ER exit signal determines the protein sorting upon ER exit in yeast. *Biochem J*.

Watanabe, R., K. Funato, K. Venkataraman, A.H. Futerman, and H. Riezman. 2002. Sphingolipids are required for the stable membrane association of glycosylphosphatidylinositol-anchored proteins in yeast. *J Biol Chem*. 277:49538-44.

Welsh, L.M., A.H. Tong, C. Boone, O.N. Jensen, and S. Otte. 2006. Genetic and molecular interactions of the Erv41p-Erv46p complex involved in transport between the endoplasmic reticulum and Golgi complex. *J Cell Sci*. 119:4730-40.

Yasuda, S., H. Kitagawa, M. Ueno, H. Ishitani, M. Fukasawa, M. Nishijima, S. Kobayashi, and K. Hanada. 2001. A novel inhibitor of ceramide trafficking from the endoplasmic reticulum to the site of sphingomyelin synthesis. *J Biol Chem*. 276:43994-4002.

Yoshihisa, T., C. Barlowe, and R. Schekman. 1993. Requirement for a GTPase-activating protein in vesicle budding from the endoplasmic reticulum. *Science*. 259:1466-8.

Zhang, B., R.J. Kaufman, and D. Ginsburg. 2005. LMAN1 and MCFD2 form a cargo receptor complex and interact with coagulation factor VIII in the early secretory pathway. *J Biol Chem*. 280:25881-6.

Zhang, B., B. McGee, J.S. Yamaoka, H. Guglielmone, K.A. Downes, S. Minoldo, G. Jarchum, F. Peyvandi, N.B. de Bosch, A. Ruiz-Saez, B. Chatelain, M. Olpinski, P. Bockenstedt, W. Sperl, R.J. Kaufman, W.C. Nichols, E.G. Tuddenham, and D. Ginsburg. 2006. Combined deficiency of factor V and factor VIII is due to mutations in either LMAN1 or MCFD2. *Blood*. 107:1903-7.